Solutions manual for
Understanding NMR spectroscopy

James Keeler and Andrew J. Pell

University of Cambridge, Department of Chemistry

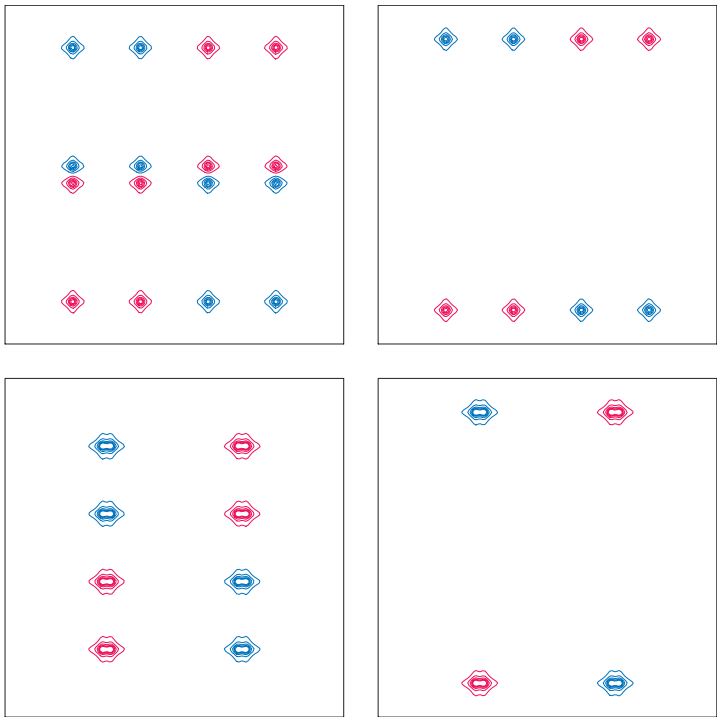

Version 1.0 July 2005

Preface

We hope that this solutions manual will be a useful adjunct to *Understanding NMR Spectroscopy* (Wiley, 2005), and will encourage readers to work through the exercises. The old adage that 'practice makes perfect' certainly applies when it comes to getting to grips with the theory of NMR.

We would be grateful if users of this manual would let us know (by EMAIL to `jhk10@cam.ac.uk`) of any errors they come across. A list of corrections will be maintained on the *spectroscopyNOW* website

`http://www.spectroscopynow.com/nmr` (follow the link 'education')

Cambridge, August 2005

Contents

Chapter 2

Setting the scene

2.1

We need Eq. 2.1 on p. 6:

$$\delta(\text{ppm}) = 10^6 \times \frac{\upsilon - \upsilon_{\text{ref}}}{\upsilon_{\text{ref}}}.$$

For the first peak

$$\delta(\text{ppm}) = 10^6 \times \frac{500.135\,021 - 500.134\,271}{500.134\,271} = \boxed{1.50 \text{ ppm}}.$$

For the second peak the shift is $\boxed{7.30 \text{ ppm}}$.
Using Eq. 2.3 on p. 9

$$\delta(\text{ppm}) = 10^6 \times \frac{\upsilon - \upsilon_{\text{ref}}}{\upsilon_{\text{rx}}},$$

with $\upsilon_{\text{rx}} = 500.135\,271$ MHz gives the two shifts as $\boxed{1.50 \text{ ppm}}$ and $\boxed{7.30 \text{ ppm}}$ i.e. identical values to three significant figures. To all intents and purposes it is perfectly acceptable to use Eq. 2.3.

The separation of the two peaks can be converted to Hz using Eq. 2.2 on p. 7:

$$\text{frequency separation in Hz} = (\delta_1 - \delta_2) \times \upsilon_{\text{ref}}(\text{in MHz}).$$

So the separation is

$$(7.30 - 1.50) \times 400.130\,000 = \boxed{2321 \text{ Hz}}.$$

The conversion to rad s^{-1} is made using Eq. 2.4 on p. 18

$$\omega = 2\pi \times \upsilon = 2\pi \times 2321 = \boxed{14\,583 \text{ rad s}^{-1}}.$$

2.2

For $J_{\text{AB}} = 10$ Hz & $J_{\text{AC}} = 2$ Hz, the line positions are −6, −4, +4, +6 Hz. For $J_{\text{AB}} = 10$ Hz & $J_{\text{AC}} = 12$ Hz, the line positions are −11, −1, +1, +11 Hz; note that compared to the first multiplet the two central lines swap positions. For $J_{\text{AB}} = 10$ Hz & $J_{\text{AC}} = 10$ Hz, the line positions are −10, 0, 0, +10 Hz; in this case, the line associated with the spin states of spins B and C being α and β, and the line in which the spin states are β and α, lie of top of one another giving a 1:2:1 triplet.

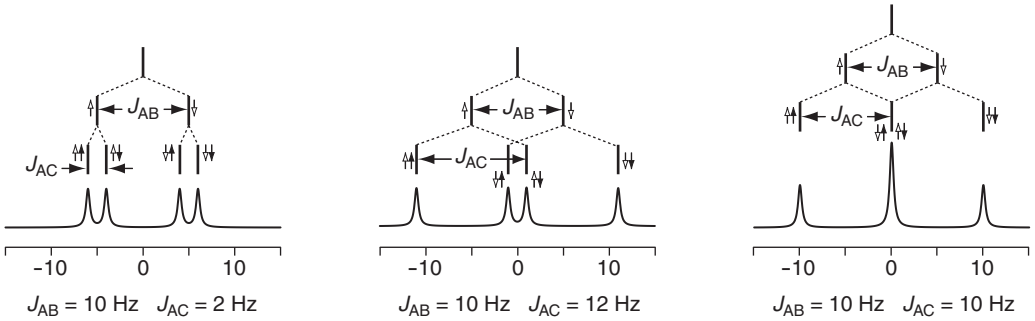

Introducing a third coupling gives a doublet of doublet of doublets. The line positions are ±1.5, ±3.5, ±6.5, ±8.5 Hz. For clarity, only the spin state of the fourth spin, D, are shown by the grey-headed arrows on the last line of the tree.

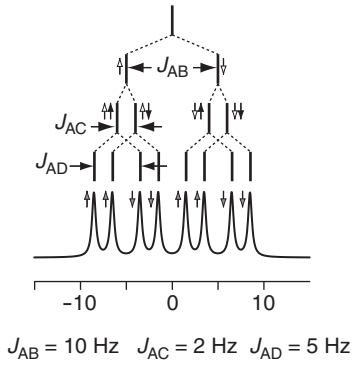

2.3

The frequency, in Hz, is 1/period:

$$\upsilon = \frac{1}{2.5 \times 10^{-9}} = \boxed{4 \times 10^{8}\ \text{Hz}} \text{ or } 400\ \text{MHz}.$$

Converting to rad s^{-1}gives:

$$\omega = 2\pi\upsilon = \boxed{2.51 \times 10^{9}\ \text{rad s}^{-1}}.$$

(a) 90° is one quarter of a rotation so will take $\frac{1}{4} \times 2.5 \times 10^{-9} = \boxed{6.25 \times 10^{-10}\ \text{s}}$.

(b) As 2π radians is a complete rotation, the fraction of a rotation represented by $3\pi/2$ is $(3\pi/2)/(2\pi) = 3/4$, so the time is $0.75 \times 2.5 \times 10^{-9} = \boxed{1.875 \times 10^{-9}\ \text{s}}$.

(c) 720° is two complete rotations, so the time is $2 \times 2.5 \times 10^{-9} = \boxed{5.0 \times 10^{-9}\ \text{s}}$.

To convert from angular frequency to Hz we need Eq. 2.4 on p. 18

$$\upsilon = \frac{\omega}{2\pi} = \frac{7.85 \times 10^4}{2\pi} = \boxed{12\,494 \text{ Hz}}.$$

The period is 1/frequency:

$$T = \frac{1}{\upsilon} = \frac{1}{12\,494} = \boxed{8.00 \times 10^{-5} \text{ s}}.$$

2.4

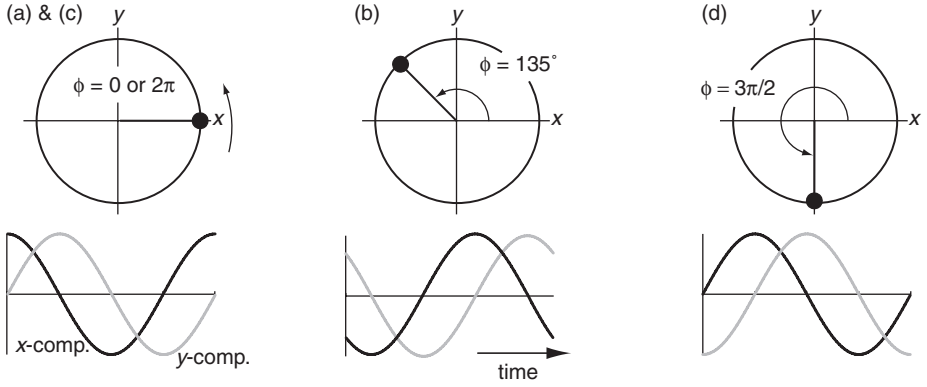

For $\phi = 0$ or 2π radians, the x-component is a cosine wave, and the y-component is a sine wave. For $\phi = 3\pi/2$, the y-component is minus a cosine wave, and the x-component is a sine wave.

2.5

We need the identity

$$\sin(A + B) \equiv \sin A \cos B + \cos A \sin B.$$

Using this we find:

$$\begin{aligned} \sin(\omega t + \pi) &= \sin(\omega t)\cos\pi + \cos(\omega t)\sin\pi \\ &= -\sin(\omega t), \end{aligned}$$

where to go to the second line we have used $\cos\pi = -1$ and $\sin\pi = 0$. So the y-component is indeed $-r\sin(\omega t)$.

Chapter 3

Energy levels and NMR spectra

3.1

The expression for $\hat{H}_{\text{one spin}}$ is given by Eq. 3.2 on p. 31:

$$\hat{H}_{\text{one spin}} = -\gamma B_0 \hat{I}_z.$$

We need to work out the effect that $\hat{H}_{\text{one spin}}$ has on $\psi_{-½}$:

$$\begin{aligned} \hat{H}_{\text{one spin}}\psi_{-½} &= -\gamma B_0 \left[\hat{I}_z \psi_{-½}\right] \\ &= -\gamma B_0 \left[-\tfrac{1}{2}\hbar\psi_{-½}\right] \\ &= \tfrac{1}{2}\hbar\gamma B_0 \psi_{-½}. \end{aligned}$$

To go to the second line we have used Eq. 3.3 on p. 32 i.e. that $\psi_{-½}$ is an eigenfunction of $\hat{I}_z$. The wavefunction has been regenerated, multiplied by a constant; $\psi_{-½}$ is therefore an eigenfunction of $\hat{H}_{\text{one spin}}$ with eigenvalue $\frac{1}{2}\hbar\gamma B_0$.

3.2

The Larmor frequency, in Hz, of a nucleus with zero chemical shift is defined by Eq. 3.8 on p. 35:

$$\begin{aligned} \upsilon_0 &= \frac{-\gamma B_0}{2\pi} \\ &= \frac{-6.7283 \times 10^7 \times 9.4}{2\pi} \\ &= \boxed{-1.01 \times 10^8 \text{ Hz}} \text{ or } -101 \text{ MHz}. \end{aligned}$$

To convert to rad s^{-1}, we need to multiply the frequency in Hz by 2π:

$$\omega_0 = 2\pi\upsilon_0 = 2\pi \times -1.01 \times 10^8 = -6.32 \times 10^8 \text{ rad s}^{-1}.$$

In the case of a non-zero chemical shift, the Larmor frequency, in Hz, is:

$$\begin{aligned} \upsilon_0 &= \frac{-\gamma(1 + 10^{-6}\delta)B_0}{2\pi} \\ &= \frac{-6.7283 \times 10^7 \times (1 + 77 \times 10^{-6}) \times 9.4}{2\pi} \\ &= \boxed{-1.01 \times 10^8 \text{ Hz}}. \end{aligned}$$

This is an identical value to three significant figures. We need to go to considerably more figures to see the difference between these two Larmor frequencies. To seven figures the frequencies are 1.00659×10^8 Hz and 1.00667×10^8 Hz.

3.3

We let $\hat{H}_{\text{one spin}}$ act on the wavefunction $\psi_{+½}$:

$$\begin{aligned}\hat{H}_{\text{one spin}}\psi_{+½} &= \omega_0\hat{I}_z\psi_{+½} \\ &= \tfrac{1}{2}\omega_0\psi_{+½},\end{aligned}$$

where the Hamiltonian has been expressed in angular frequency units. To go to the second line, we have used the fact that $\psi_{+½}$ is an eigenfunction of $\hat{I}_z$ with eigenvalue $+\frac{1}{2}$.

In the same way,

$$\hat{H}_{\text{one spin}}\psi_{-½} = -\tfrac{1}{2}\omega_0\psi_{-½}.$$

Hence, $\psi_{\pm½}$ are eigenfunctions of $\hat{H}_{\text{one spin}}$ with eigenvalues $\pm\frac{1}{2}\omega_0$.

3.4

Following the approach in section 3.5 on p. 37, we let the Hamiltonian act on the product wavefunction:

$$\begin{aligned}\hat{H}_{\text{two spins, no coupl.}}\psi_{\alpha,1}\psi_{\alpha,2} &= \left(\upsilon_{0,1}\hat{I}_{1z} + \upsilon_{0,2}\hat{I}_{2z}\right)\psi_{\alpha,1}\psi_{\alpha,2} \\ &= \upsilon_{0,1}\hat{I}_{1z}\psi_{\alpha,1}\psi_{\alpha,2} + \upsilon_{0,2}\hat{I}_{2z}\psi_{\alpha,1}\psi_{\alpha,2} \\ &= \upsilon_{0,1}\left[\hat{I}_{1z}\psi_{\alpha,1}\right]\psi_{\alpha,2} + \upsilon_{0,2}\psi_{\alpha,1}\left[\hat{I}_{2z}\psi_{\alpha,2}\right].\end{aligned}$$

To go to the third line, we have used the fact that $\hat{I}_{1z}$ acts *only* on $\psi_{\alpha,1}$ and not on $\psi_{\alpha,2}$. Similarly, $\hat{I}_{2z}$ acts only on $\psi_{\alpha,2}$.
Using Eq. 3.11 on p. 37 i.e. that $\psi_{\alpha,1}$ and $\psi_{\alpha,2}$ are eigenfunctions of $\hat{I}_{1z}$ and $\hat{I}_{2z}$, the terms in the square brackets can be rewritten:

$$\begin{aligned}\hat{H}_{\text{two spins, no coupl.}}\psi_{\alpha,1}\psi_{\alpha,2} &= \upsilon_{0,1}\left[\hat{I}_{1z}\psi_{\alpha,1}\right]\psi_{\alpha,2} + \upsilon_{0,2}\psi_{\alpha,1}\left[\hat{I}_{2z}\psi_{\alpha,2}\right] \\ &= \tfrac{1}{2}\upsilon_{0,1}\psi_{\alpha,1}\psi_{\alpha,2} + \tfrac{1}{2}\upsilon_{0,2}\psi_{\alpha,1}\psi_{\alpha,2} \\ &= \left[\tfrac{1}{2}\upsilon_{0,1} + \tfrac{1}{2}\upsilon_{0,2}\right]\psi_{\alpha,1}\psi_{\alpha,2}.\end{aligned}$$

Hence, $\psi_{\alpha,1}\psi_{\alpha,2}$ is an eigenfunction of $\hat{H}_{\text{two spins, no coupl.}}$ with eigenvalue $\frac{1}{2}\upsilon_{0,1} + \frac{1}{2}\upsilon_{0,2}$.

Letting the coupling term act on the product wavefunction:

$$\begin{aligned}J_{12}\hat{I}_{1z}\hat{I}_{2z}\psi_{\alpha,1}\psi_{\alpha,2} &= J_{12}\left[\hat{I}_{1z}\psi_{\alpha,1}\right]\left[\hat{I}_{2z}\psi_{\alpha,2}\right] \\ &= J_{12}\left[\tfrac{1}{2}\psi_{\alpha,1}\right]\left[\tfrac{1}{2}\psi_{\alpha,2}\right] \\ &= \tfrac{1}{4}J_{12}\psi_{\alpha,1}\psi_{\alpha,2}.\end{aligned}$$

$\psi_{\alpha,1}\psi_{\alpha,2}$ is indeed an eigenfunction of the coupling term, with eigenvalue $\frac{1}{4}J_{12}$: this corresponds to the energy.

$\hat{H}_{\text{two spins, no coupl.}}$ and the coupling term share the same eigenfunctions (a result of the fact that the two terms commute). Since the Hamiltonian for two coupled spins can be represented as the sum of these two terms,

$$\hat{H}_{\text{two spins}} = \hat{H}_{\text{two spins, no coupl.}} + 2\pi\, J_{12}\hat{I}_{1z}\hat{I}_{2z},$$

it follows that it must also have the same eigenfunctions. Hence, $\psi_{\alpha,1}\psi_{\alpha,2}$ is an eigenfunction of $\hat{H}_{\text{two spins}}$ with energy eigenvalue $\frac{1}{2}\upsilon_{0,1} + \frac{1}{2}\upsilon_{0,2} + \frac{1}{4}J_{12}$, i.e. the sum of the individual eigenvalues of $\hat{H}_{\text{two spins, no coupl.}}$ and $J_{12}\hat{I}_{1z}\hat{I}_{2z}$.

3.5

Reproducing Table 3.2 on p. 40 for $\upsilon_{0,1} = -100$ Hz, $\upsilon_{0,2} = -200$ Hz and $J_{12} = 5$ Hz:

number	m_1	m_2	spin states	eigenfunction	eigenvalue/Hz
1	$+\frac{1}{2}$	$+\frac{1}{2}$	$\alpha\alpha$	$\psi_{\alpha,1}\psi_{\alpha,2}$	$+\frac{1}{2}\upsilon_{0,1} + \frac{1}{2}\upsilon_{0,2} + \frac{1}{4}J_{12} = -148.75$
2	$+\frac{1}{2}$	$-\frac{1}{2}$	$\alpha\beta$	$\psi_{\alpha,1}\psi_{\beta,2}$	$+\frac{1}{2}\upsilon_{0,1} - \frac{1}{2}\upsilon_{0,2} - \frac{1}{4}J_{12} = 48.75$
3	$-\frac{1}{2}$	$+\frac{1}{2}$	$\beta\alpha$	$\psi_{\beta,1}\psi_{\alpha,2}$	$-\frac{1}{2}\upsilon_{0,1} + \frac{1}{2}\upsilon_{0,2} - \frac{1}{4}J_{12} = -51.25$
4	$-\frac{1}{2}$	$-\frac{1}{2}$	$\beta\beta$	$\psi_{\beta,1}\psi_{\beta,2}$	$-\frac{1}{2}\upsilon_{0,1} - \frac{1}{2}\upsilon_{0,2} + \frac{1}{4}J_{12} = 151.25$

The set of allowed transitions is:

transition	spin states	frequency/Hz
$1 \rightarrow 2$	$\alpha\alpha \rightarrow \alpha\beta$	$E_2 - E_1 = 197.50$
$3 \rightarrow 4$	$\beta\alpha \rightarrow \beta\beta$	$E_4 - E_3 = 202.50$
$1 \rightarrow 3$	$\alpha\alpha \rightarrow \beta\alpha$	$E_3 - E_1 = 97.50$
$2 \rightarrow 4$	$\alpha\beta \rightarrow \beta\beta$	$E_4 - E_2 = 102.50$

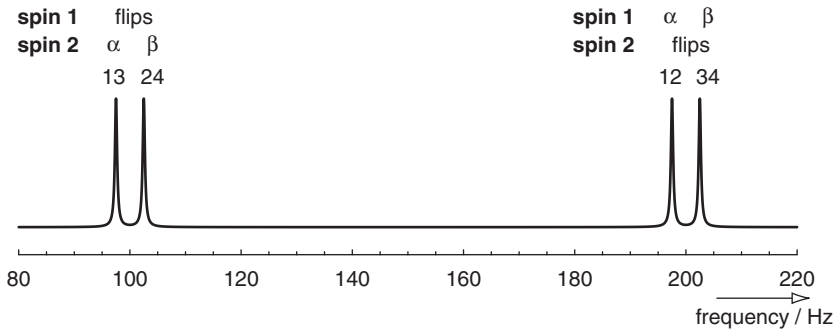

If $J_{12} = -5$ Hz, the table of energies becomes:

number	m_1	m_2	spin states	eigenfunction	eigenvalue/Hz
1	$+\frac{1}{2}$	$+\frac{1}{2}$	$\alpha\alpha$	$\psi_{\alpha,1}\psi_{\alpha,2}$	$+\frac{1}{2}\upsilon_{0,1} + \frac{1}{2}\upsilon_{0,2} + \frac{1}{4}J_{12} = -151.25$
2	$+\frac{1}{2}$	$-\frac{1}{2}$	$\alpha\beta$	$\psi_{\alpha,1}\psi_{\beta,2}$	$+\frac{1}{2}\upsilon_{0,1} - \frac{1}{2}\upsilon_{0,2} - \frac{1}{4}J_{12} = 51.25$
3	$-\frac{1}{2}$	$+\frac{1}{2}$	$\beta\alpha$	$\psi_{\beta,1}\psi_{\alpha,2}$	$-\frac{1}{2}\upsilon_{0,1} + \frac{1}{2}\upsilon_{0,2} - \frac{1}{4}J_{12} = -48.75$
4	$-\frac{1}{2}$	$-\frac{1}{2}$	$\beta\beta$	$\psi_{\beta,1}\psi_{\beta,2}$	$-\frac{1}{2}\upsilon_{0,1} - \frac{1}{2}\upsilon_{0,2} + \frac{1}{4}J_{12} = 148.75$

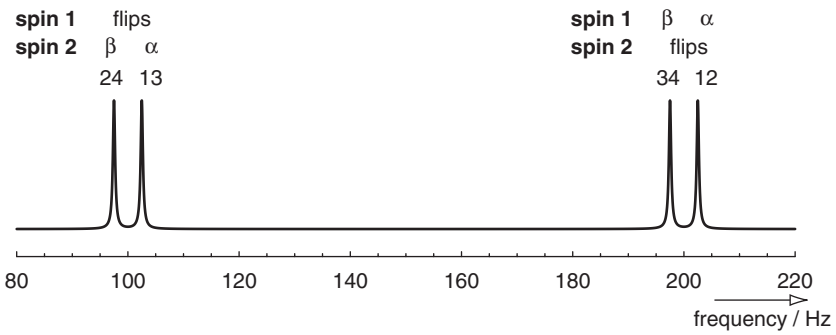

The spectrum in unchanged in appearance. However, the labels of the lines have changed; the spin state of the passive spin for each line of the doublet has swapped over.

3.6

The allowed transitions in which spin two flips are 1–2, 3–4, 5–6 and 7–8. Their frequencies are:

transition	state of spin one	state of spin three	frequency/Hz
1–2	α	α	$-\upsilon_{0,2} - \frac{1}{2}J_{12} - \frac{1}{2}J_{23} = 193$
3–4	β	α	$-\upsilon_{0,2} + \frac{1}{2}J_{12} - \frac{1}{2}J_{23} = 203$
5–6	α	β	$-\upsilon_{0,2} - \frac{1}{2}J_{12} + \frac{1}{2}J_{23} = 197$
7–8	β	β	$-\upsilon_{0,2} + \frac{1}{2}J_{12} + \frac{1}{2}J_{23} = 207$

The multiplet is a doublet of doublets centred on minus the Larmor frequency of spin two.

There are two lines associated with spin three being in the α state, and two with this spin being in the β state. Changing the sign of J_{23} swaps the labels associated with spin three, but leaves those associated with spin one unaffected.

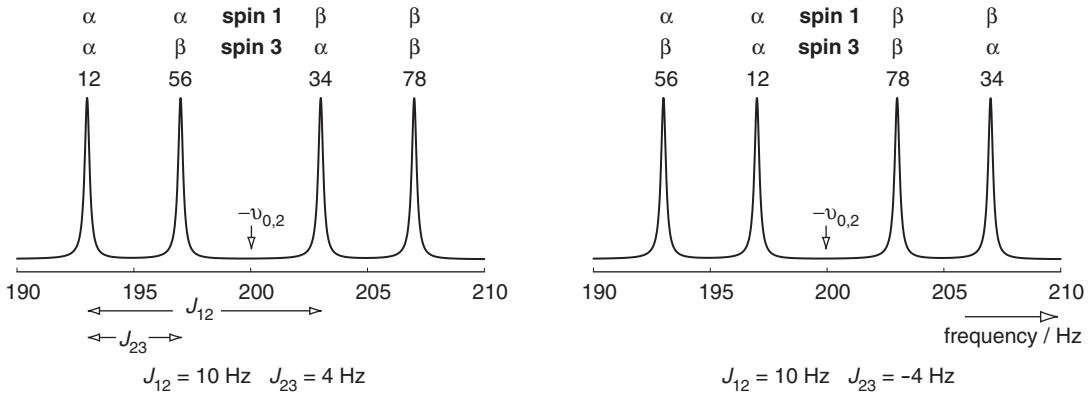

3.7

The six zero-quantum transitions have the following frequencies:

transition	initial state	final state	frequency
2–3	$\alpha\beta\alpha$	$\beta\alpha\alpha$	$-\upsilon_{0,1} + \upsilon_{0,2} - \frac{1}{2}J_{13} + \frac{1}{2}J_{23}$
6–7	$\alpha\beta\beta$	$\beta\alpha\beta$	$-\upsilon_{0,1} + \upsilon_{0,2} + \frac{1}{2}J_{13} - \frac{1}{2}J_{23}$
3–5	$\beta\alpha\alpha$	$\alpha\alpha\beta$	$\upsilon_{0,1} - \upsilon_{0,3} + \frac{1}{2}J_{12} - \frac{1}{2}J_{23}$
4–6	$\beta\beta\alpha$	$\alpha\beta\beta$	$\upsilon_{0,1} - \upsilon_{0,3} - \frac{1}{2}J_{12} + \frac{1}{2}J_{23}$
2–5	$\alpha\beta\alpha$	$\alpha\alpha\beta$	$\upsilon_{0,2} - \upsilon_{0,3} + \frac{1}{2}J_{12} - \frac{1}{2}J_{13}$
4–7	$\beta\beta\alpha$	$\beta\alpha\beta$	$\upsilon_{0,2} - \upsilon_{0,3} - \frac{1}{2}J_{12} + \frac{1}{2}J_{13}$

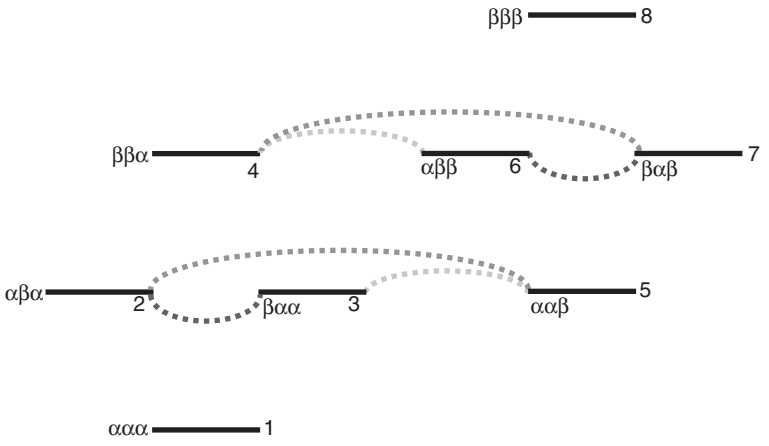

The six transitions can be divided up into three pairs:

- 2–3 and 6–7 in which spins one and two flip, and spin three is passive,
- 3–5 and 4–6 in which spins one and three flip, and spin two is passive,
- 2–5 and 4–7 in which spins two and three flip, and spin one is passive.

Each pair of transitions is centred at the *difference* in the Larmor frequencies of the two spins which flip, and is split by the *difference* in the couplings between the two active spins and the passive spin.

Chapter 4

The vector model

4.1

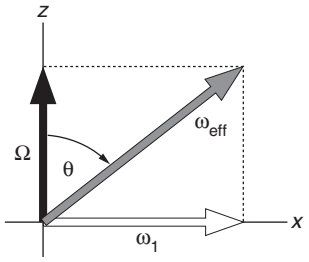

The offset of the peak is 5 ppm. This can be converted to Hz using Eq. 2.2 on p. 7:

$$\frac{\Omega}{2\pi} = 10^{-6}\Delta\delta\,\upsilon_{\text{ref}} = 10^{-6} \times 5 \times 600 \times 10^{6} = 5 \times 600 = \boxed{3000\text{ Hz}} \text{ or } 3\text{ kHz}.$$

From the diagram,

$$\tan\theta = \frac{\omega_1}{\Omega} = \frac{25 \times 10^3 \times 2\pi}{3 \times 10^3 \times 2\pi} = \frac{25}{3} = 8.33,$$

so $\theta = \boxed{83\ ^\circ}$.
For a peak at the edge of the spectrum, the tilt angle is within 7° of that for an on-resonance pulse; the B_1 field is therefore strong enough to give a reasonable approximation to a hard pulse over the full shift range.

For a Larmor frequency of 900 MHz, the peak at the edge of the spectrum has an offset of 4.5 kHz, so the tilt angle is $\boxed{80\ ^\circ}$. The larger offset results in the same B_1 field giving a poorer approximation to a hard pulse.

4.2

From Fig. 4.16 on p. 63, the y-component of the magnetization after a pulse of flip angle β is $M_0 \sin\beta$. The intensity of the signal will, therefore, vary as $\sin\beta$, which is a maximum for $\beta = 90°$.

(a) If $\beta = 180°$, the magnetization is rotated onto the $-z$-axis. As $\sin 180° = 0$, the signal intensity is zero.

(b) If $\beta = 270°$, the magnetization is rotated onto the y-axis. As $\sin 270° = -1$, the signal will have negative intensity of the same magnitude as for $\beta = 90°$.

4.3

From Fig. 4.16 on p. 63, the intensity of the signal is proportional to $\sin\beta$, where the value of the flip angle β is given by Eq. 4.5 on p. 62:

$$\beta = \omega_1 t_\mathrm{p}.$$

The pulse lengths of 5 and 10 μs correspond to flip angles below 90°. Increasing t_p further causes β to increase past 90°, and so the value of $\sin\beta$ (and hence the signal intensity) decreases. The null at 20.5 μs corresponds to $\beta = 180°$.

From the expression for the flip angle, it follows that $\pi = \omega_1 t_{180}$. Therefore,

$$\omega_1 = \frac{\pi}{t_{180}} = \frac{\pi}{20.5 \times 10^{-6}} = 1.5 \times 10^5 \text{ rad s}^{-1} \text{ or } \boxed{2.4 \times 10^4 \text{ Hz}}.$$

Another way to answer this question is to see that since a 180° pulse has a length of 20.5 μs, a complete rotation of 360° takes 41.0 μs. The period of this rotation is thus 41.0 μs, so the frequency is

$$\frac{1}{41.0 \times 10^{-6}} = \boxed{2.4 \times 10^4 \text{ Hz}}.$$

This frequency is $\omega_1/2\pi$, the RF field strength in Hz.

The length of the 90° pulse is simply half that of the 180° pulse:

$$t_{90} = \tfrac{1}{2} \times 20.5 = 10.25\ \mu\text{s}.$$

The further null occurs at a pulse length that is twice the value of t_{180}. This corresponds to a flip angle of 360°, for which the magnetization is rotated back onto the z-axis.

4.4

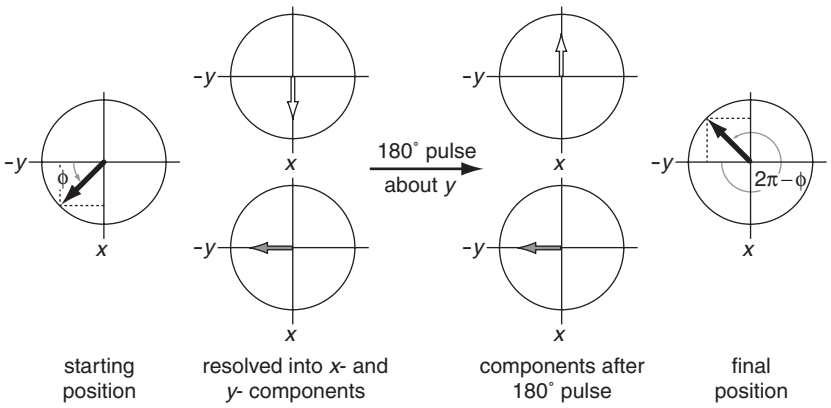

The vector has been reflected in the yz-plane, and has a final phase of $2\pi - \phi$, measured anti-clockwise from the $-y$-axis.

4.5

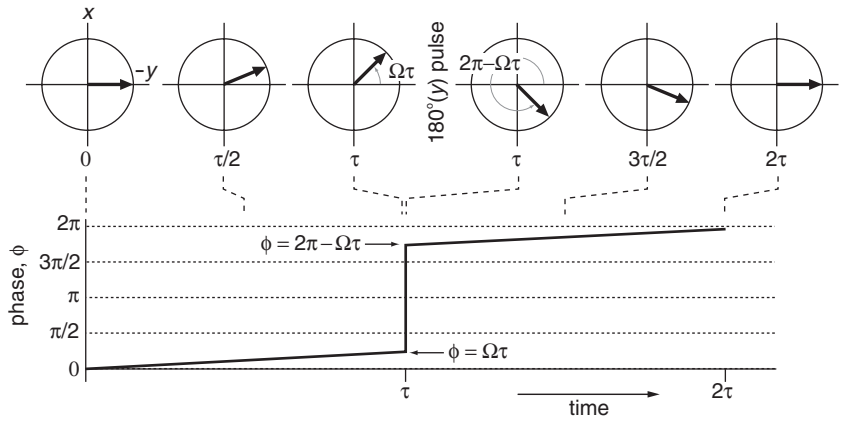

The spin echo sequence $90°(x)-\tau-180°(x)-\tau-$ results in the magnetization appearing along the y-axis. In contrast, the $90°(x)-\tau-180°(y)-\tau-$ sequence results in the magnetization appearing along the $-y$-axis. Shifting the phase of the 180° pulse by 90° thus causes the phase of the magnetization to shift by 180°.

A $180°(-x)$ pulse rotates the magnetization in the opposite sense to a $180°(x)$ pulse, but the net effect is still to reflect the magnetization vectors in the xz-plane. The sequence

$90°(x) - \tau - 180°(-x) - \tau-$ will, therefore, have the same effect as the $90°(x) - \tau - 180°(x) - \tau-$ sequence i.e. the vector appears on the y-axis at the end of the sequence.

4.6

From section 4.11 on p. 71, the criterion for the excitation of a peak to at least 90% of its theoretical maximum is for the offset to be less than 1.6 times the RF field strength. The Larmor frequency of ^{31}P at $B_0 = 9.4$ T is:

$$\upsilon_0 = -\frac{\gamma B_0}{2\pi} = -\frac{1.08 \times 10^8 \times 9.4}{2\pi} = -1.62 \times 10^8 \text{ Hz or } -162 \text{ MHz}.$$

If the transmitter frequency is placed at the centre of the spectrum, the maximum offset is approximately 350 ppm. In Hz, this is an offset of

$$\frac{\Omega}{2\pi} = 350 \times 162 = 5.66 \times 10^4 \text{ Hz or } 56.6 \text{ kHz}.$$

According to our criterion, the RF field strength must be at least $56.6/1.6 = 35.3$ kHz, from which the time for a 360° pulse is simply $1/(35.3 \times 10^3) = 28.28$ μs. Thus, the 90° pulse length is $\frac{1}{4} \times 28.28 = \boxed{7.07\ \mu\text{s}}$.

4.7

The flip angle of a pulse is given by Eq. 4.5 on p. 62:

$$\beta = \omega_1 t_\text{p}$$

So,

$$\omega_1 = \frac{\beta}{t_\text{p}}.$$

For a 90° pulse, $\beta = \pi/2$, so the B_1 field strength in Hz is:

$$\frac{\omega_1}{2\pi} = \frac{(\pi/2)}{2\pi\, t_\text{p}} = \frac{1}{4 \times 10 \times 10^{-6}} = \boxed{2.5 \times 10^4 \text{ Hz}} \text{ or } 25 \text{ kHz}.$$

The offset of ^{13}C from ^{1}H is 300 MHz, which is very much greater than the B_1 field strength. The ^{13}C nuclei are therefore unaffected by the ^{1}H pulses.

4.8

From Eq. 4.4 on p. 61,

$$\omega_{\text{eff}} = \sqrt{\omega_1^2 + \Omega^2}.$$

If we let $\Omega = \kappa\omega_1$, ω_{eff} can be written

$$\omega_{\text{eff}} = \sqrt{\omega_1^2 + \kappa^2\omega_1^2} = \omega_1\sqrt{1+\kappa^2}. \tag{4.1}$$

If t_{p} is the length of a 90° pulse, we have $\omega_1 t_{\text{p}} = \pi/2$ and so

$$\omega_1 = \frac{\pi}{2t_{\text{p}}},$$

and hence substituting this into Eq. 4.1 gives

$$\omega_{\text{eff}} = \frac{\pi}{2t_{\text{p}}}\sqrt{1+\kappa^2}.$$

Therefore the angle of rotation about the effective field, $\omega_{\text{eff}}t_{\text{p}}$, is given by

$$\begin{aligned}\omega_{\text{eff}}t_{\text{p}} &= \frac{\pi}{2t_{\text{p}}}\sqrt{1+\kappa^2} \times t_{\text{p}} \\ &= \frac{\pi}{2}\sqrt{1+\kappa^2}.\end{aligned}$$

The null condition is when there is a complete rotation about the effective field i.e. $\omega_{\text{eff}}t_{\text{p}} = 2\pi$:

$$2\pi = \frac{\pi}{2}\sqrt{1+\kappa^2}.$$

Rearranging this gives

$$4 = \sqrt{1+\kappa^2} \qquad \text{i.e. } \kappa = \boxed{\sqrt{15}} \text{ or } \Omega = \sqrt{15}\,\omega_1,$$

which is in agreement with Fig. 4.28 on p. 73.

The next null appears at $\omega_{\text{eff}}t_{\text{p}} = 4\pi$ i.e. two complete rotations; this corresponds to $\kappa = \boxed{\sqrt{63}}$.

For large offsets, $\kappa \gg 1$, so $\sqrt{1+\kappa^2} \approx \kappa$. The general null condition is $\omega_{\text{eff}}t_{\text{p}} = 2n\pi$, where $n = 1,\ 2,\ 3,\ \ldots$ Combining these two conditions gives

$$2n\pi = \frac{\pi}{2}\sqrt{1+\kappa^2} \approx \frac{\pi}{2}\kappa,$$

for which we find $\kappa = 4n$.

4.9

In section 4.11.3 on p. 75, it was demonstrated that, on applying a hard 180° pulse, the range of offsets over which complete inversion is achieved is much more limited than the range over which a 90° pulse gives significant excitation. Therefore, only peaks with small offsets will be inverted completely. Peaks with large offsets will not exhibit a null on the application of the 180° pulse.

4.10

The initial 90°(x) pulse rotates the magnetization from the z-axis to the $-y$-axis; after this the evolution in the transverse plane is as follows:

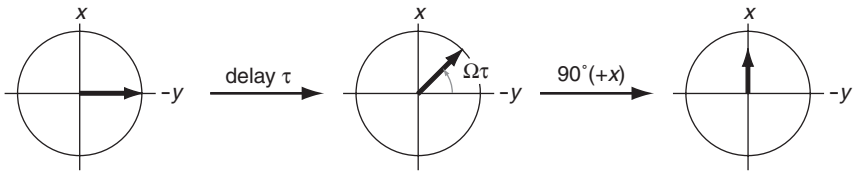

The x-, y- and z-components after each element of the pulse sequence are:

component	after first 90°(x)	after τ	after second 90°(x)
x	0	$M_0 \sin \Omega\tau$	$M_0 \sin \Omega\tau$
y	$-M_0$	$-M_0 \cos \Omega\tau$	0
z	0	0	$-M_0 \cos \Omega\tau$

The final pulse is along the x-axis, and so leaves the x-component of the magnetization unchanged, but rotates the y-component onto the $-z$-axis. The overall result of the sequence is $M_y = 0$ and $M_x = M_0 \sin \Omega\tau$.

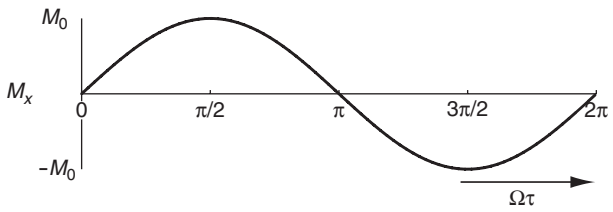

A null occurs when $M_x = 0$, i.e. when $\Omega\tau = n\pi$, where $n = 0,\ 1,\ 2,\ \ldots$

4.11

The initial spin echo sequence refocuses the offset, and aligns the magnetization along the y-axis.

If the final pulse is about the y- or $-y$-axis, then it has no effect on the magnetization as the vector is aligned along the same axis as the B_1 field. The magnetization remains along y.

If the final pulse is about the x-axis, then it rotates the magnetization from the y-axis to the z-axis. Overall, the sequence returns the magnetization to its starting position.

If the final pulse is about the $-x$-axis, then the magnetization is rotated from the y-axis to the $-z$-axis. Overall, the magnetization has been inverted.

4.12

The initial $90°(x)$ pulse rotates the magnetization from the z-axis to the $-y$-axis. For on-resonance peaks, $\Omega = 0$, so the magnetization does not precess during the delay τ. The final $90°(-x)$ then simply undoes the rotation caused by the first pulse. Overall, the magnetization is returned to its starting position.

$\Omega\tau = \pi/2$. During the delay, the magnetization rotates to the x-axis and is therefore not affected by the final $90°(-x)$ pulse. The net result is that the magnetization appears along the x-axis.

$\Omega\tau = \pi$. During the delay, the magnetization rotates onto the y-axis. The final pulse rotates the magnetization onto the $-z$-axis. The equilibrium magnetization is inverted: no observable transverse magnetization is produced.

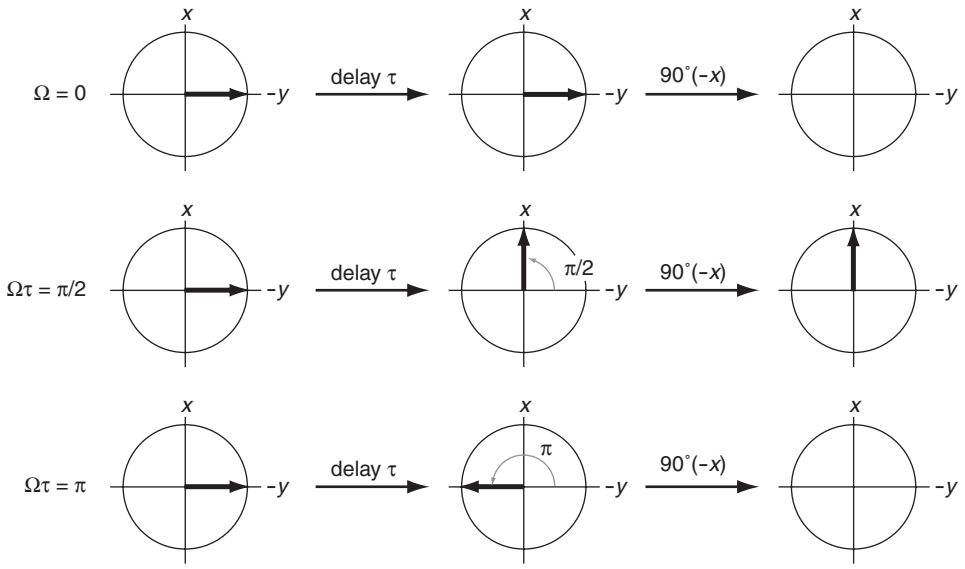

The overall effect of the sequence is to produce x-magnetization which varies as $M_0 \sin(\Omega\tau)$.

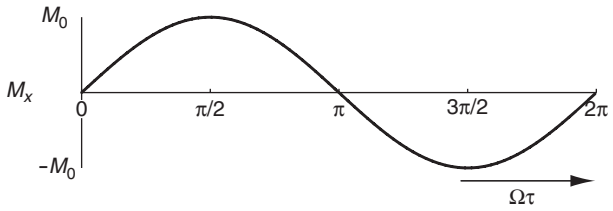

To suppress a strong solvent peak, it is placed on-resonance. The delay τ is then chosen so that $\Omega_{av}\tau = \pi/2$, where Ω_{av} is the average value of the offset of the peaks we wish to excite.

4.13

The initial 90° pulse rotates the equilibrium magnetization to the $-y$-axis; from there the magnetization precesses about the z-axis through an angle of $\Omega\tau$. The 90°(y) pulse rotates the x-component of the magnetization onto the $-z$-axis.

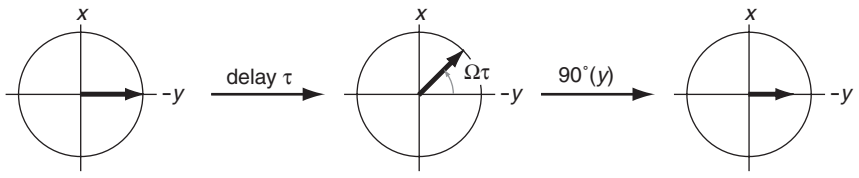

The y-component of the magnetization varies as $-M_0 \cos\Omega\tau$:

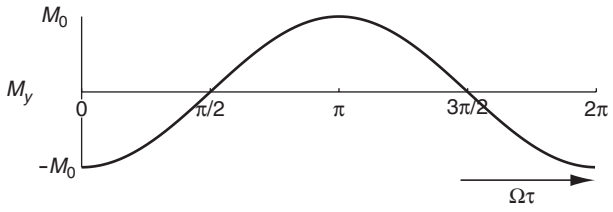

The nulls are located at $\Omega\tau = (2n + 1)\pi/2$, where $n = 0,\ 1,\ 2,\ \ldots$

To suppress the solvent peak, the transmitter frequency is placed in the middle of the peaks of interest, and then τ is chosen so that $\Omega\tau = \pi/2$, where Ω is the offset of the solvent. With such a choice, the solvent will not be excited.

4.14

Line A is on-resonance, so its magnetization does not precess during the delay τ. The pulse sequence is, effectively, a 180°(x) pulse, and so the magnetization is inverted.
For line B, the x-, y- and z-components of the magnetization after each element of the sequence are:

component	after first 90°(x)	after τ	after second 90°(x)
x	0	$M_0 \sin \Omega\tau$	$M_0 \sin \Omega\tau$
y	$-M_0$	$-M_0 \cos \Omega\tau$	0
z	0	0	$-M_0 \cos \Omega\tau$

The final pulse is along the x-axis, so leaves the x-component of the magnetization unchanged. Substituting in the values of Ω and τ we find (note that the offset of 100 Hz has to be converted to rad s^{-1}):

$$\begin{aligned} M_x &= M_0 \sin(2\pi \times 100 \times 5 \times 10^{-3}) = M_0 \sin \pi = 0 \\ M_z &= -M_0 \cos(2\pi \times 100 \times 5 \times 10^{-3}) = -M_0 \cos \pi = M_0. \end{aligned}$$

The magnetization is therefore returned to the z-axis.

The 90° pulse rotates the equilibrium magnetization onto the $-y$-axis. During the delay τ, the vector precesses about z to give the following x- and y-components:

$$M_x = M_0 \sin \Omega\tau \qquad M_y = -M_0 \cos \Omega\tau.$$

For line A, offset 50 Hz:

$$\begin{aligned} M_x &= M_0 \sin(2\pi \times 50 \times 5 \times 10^{-3}) = M_0 \sin(\pi/2) = M_0 \\ M_y &= -M_0 \cos(2\pi \times 50 \times 5 \times 10^{-3}) = -M_0 \cos(\pi/2) = 0. \end{aligned}$$

For line B, offset −50 Hz:

$$\begin{aligned} M_x &= M_0 \sin(2\pi \times -50 \times 5 \times 10^{-3}) = M_0 \sin(-\pi/2) = -M_0 \\ M_y &= -M_0 \cos(2\pi \times -50 \times 5 \times 10^{-3}) = -M_0 \cos(-\pi/2) = 0. \end{aligned}$$

The two magnetization vectors rotate at the same rate in the opposite sense. After a delay of $\tau = 5$ ms, they are both aligned along the x-axis, but pointing in opposite directions.

Chapter 5

Fourier transformation and data processing

5.1

One desirable feature of the dispersion lineshape is that it crosses the frequency axis at the frequency of the transition. This allows for a more accurate measurement of the chemical shift than might be possible for the absorption lineshape, especially in the case of broad lines.

In a spectrum containing many peaks, the following features of the dispersion lineshape make it undesirable:

- It is broader than the absorption lineshape – the long 'dispersive tails' may interfere with nearby, low intensity peaks.
- It is half the height of the absorption lineshape – the SNR is therefore reduced by half.
- The positive part of one peak may be cancelled by the negative part of an adjacent one – in a complex spectrum, the result can be very difficult to interpret.

5.2

Setting $A(\omega) = S_0/2R$, we obtain

$$\frac{S_0}{2R} = \frac{S_0 R}{R^2 + \omega_2}.$$

Cancelling the factor of S_0 from both sides and inverting the quotient, we obtain

$$2R = \frac{R^2 + \omega^2}{R}.$$

Hence,

$$\begin{aligned} \omega^2 &= 2R^2 - R^2 = R^2 \\ \omega &= \boxed{\pm R}. \end{aligned}$$

The width of the line is therefore $\boxed{2R}$ in rad s^{-1}, or $\boxed{R/\pi}$ in Hz.

5.3

$D(\omega)$ can be differentiated using the product rule:

$$\begin{aligned}\frac{\mathrm{d}D(\omega)}{\mathrm{d}\omega} &= \frac{\mathrm{d}}{\mathrm{d}\omega}\left(\frac{-\omega}{R^2+\omega^2}\right)\\ &= \frac{-1}{R^2+\omega^2}+\frac{2\omega^2}{(R^2+\omega^2)^2}\\ &= \frac{-R^2-\omega^2+2\omega^2}{(R^2+\omega^2)^2}\\ &= \frac{\omega^2-R^2}{(R^2+\omega^2)^2}.\end{aligned}$$

At the turning points

$$\frac{\mathrm{d}D(\omega)}{\mathrm{d}\omega}=0,$$

so,

$$\frac{\omega^2-R^2}{(R^2+\omega^2)^2}=0.$$

The denominator is always non-zero, so the equation can be solved by setting the numerator to zero:

$$\begin{aligned}\omega^2-R^2 &= 0\\ \omega &= \boxed{\pm R}.\end{aligned}$$

Substituting these values into $D(\omega)$:

$$D(\pm R)=\mp\frac{R}{2R^2}=\mp\frac{1}{2R}.$$

These values are the maximum and minimum heights in the lineshape.

There are two values of ω at which $D(\omega)$ is half its maximum positive height. At these frequencies, $D(\omega)=1/(4R)$. Hence,

$$\frac{-\omega}{R^2+\omega^2}=\frac{1}{4R}.$$

Inverting the quotients we obtain,

$$\frac{R^2+\omega^2}{\omega}=-4R,$$

so,

$$\omega^2+4R\omega+R^2=0.$$

This is a quadratic equation in ω that can be solved by applying the usual formula:

$$\omega = \tfrac{1}{2}\left(-4R \pm \sqrt{16R^2 - 4R^2}\right) = \boxed{R(-2 \pm \sqrt{3})}.$$

Similarly, $D(\omega) = -1/(4R)$ has two solutions: $\omega = \boxed{R(2 \pm \sqrt{3})}$.

The width, W_{disp}, is the distance between the outer two half-maximum points, as shown in the diagram. Its value is

$$W_{\text{disp}} = R(2 + \sqrt{3}) - R(-2 - \sqrt{3}) = 2(2 + \sqrt{3})R.$$

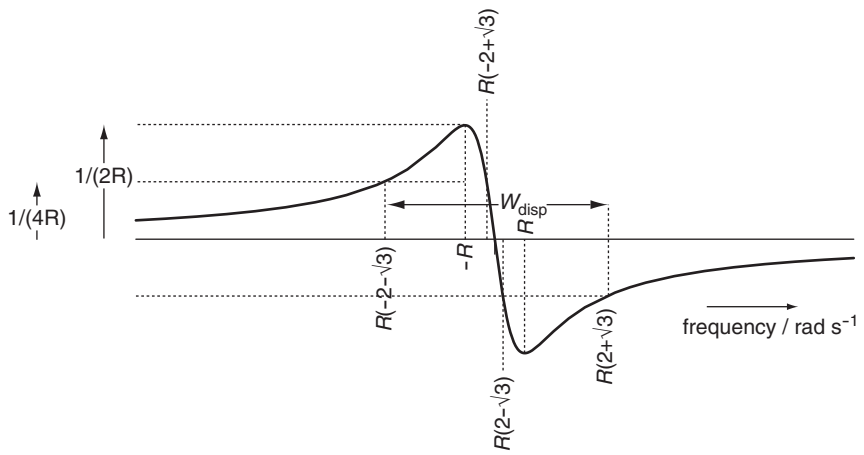

For comparison, the width of the absorption mode is $W_{\text{abs}} = 2R$. Therefore, the ratio $W_{\text{disp}}/W_{\text{abs}} = 2 + \sqrt{3} \approx \boxed{3.7}$. The dispersion lineshape is almost four times wider than the absorption lineshape.

5.4

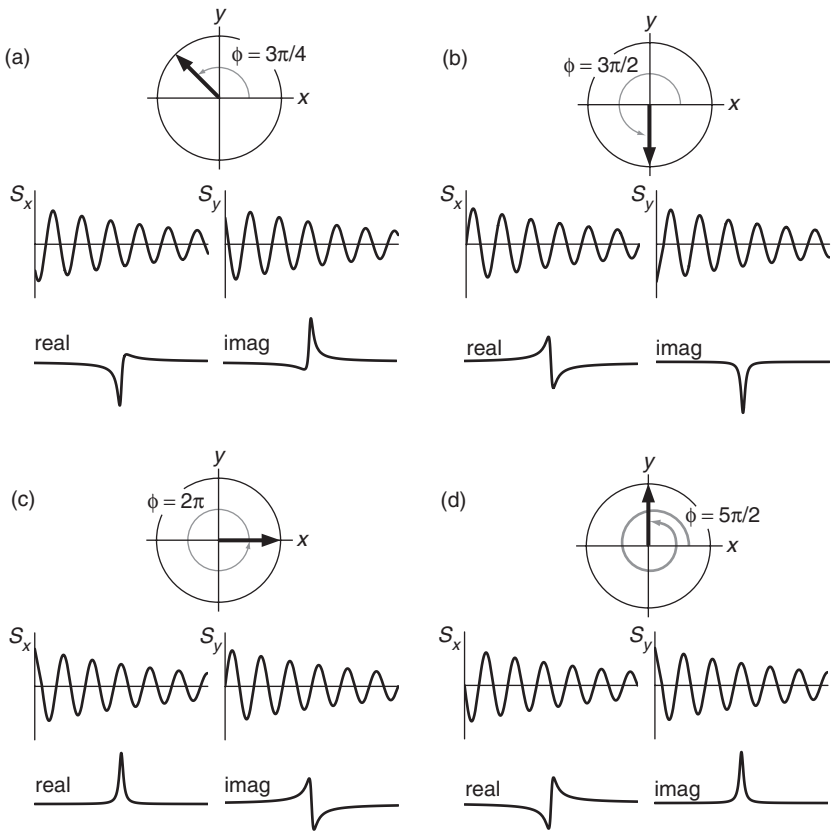

5.5

A 90°(x) pulse rotates the equilibrium magnetization onto the $-y$-axis. The resulting spectrum is phased to absorption, so that magnetization along $-y$ can be said to have a phase $\phi = 0$.
A 90°(y) pulse rotates the equilibrium magnetization onto the x-axis. This corresponds to a phase shift of $\phi = \pi/2$ with respect to the initial experiment.

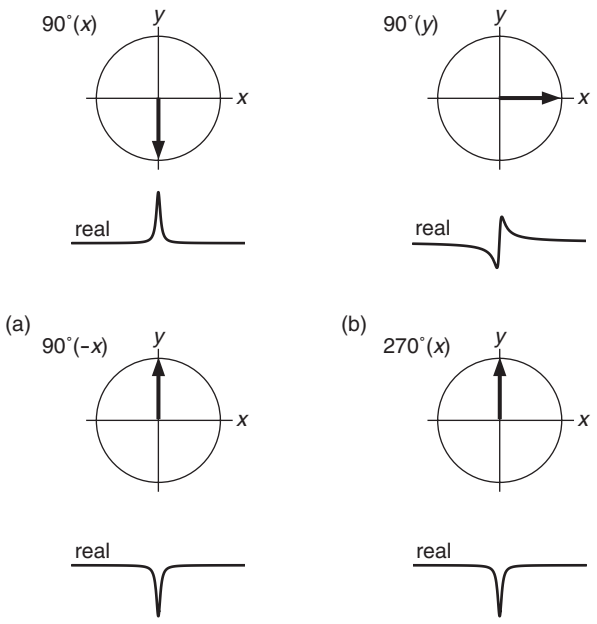

(a) Applying the pulse about $-x$ rotates the magnetization vector onto y. This corresponds to a phase shift of $\phi = \pi$, therefore the spectrum will exhibit a negative absorption lineshape.

(b) A $270°(x)$ pulse is equivalent to a $90°(-x)$ pulse. The spectrum will be the same as in (a).

5.6

The Larmor frequency of ^{31}P at $B_0 = 9.4$ T is:

$$\frac{\omega_0}{2\pi} = -\frac{\gamma B_0}{2\pi} = -\frac{1.08 \times 10^8 \times 9.4}{2\pi} = -1.62 \times 10^8 \text{ Hz or } -162 \text{ MHz.}$$

The phase correction needed at the edge of the spectrum is given by $\Omega_{max} t_p$, where Ω_{max} is the maximum offset. For ^{31}P the maximum offset is 350 ppm, therefore the phase correction is

$$2\pi \times 162 \times 350 \times 20 \times 10^{-6} = \boxed{7.1 \text{ radians}}.$$

This corresponds to $\boxed{407°}$, a significant frequency-dependent phase error.

5.7

The intensity of the noise in the spectrum depends on both the amplitude of the noise in the time-domain, and the acquisition time. So, recording the time-domain signal long after the NMR signal has decayed just continues to measure noise and no signal. The resulting spectrum will consequently have a lower SNR than it would for a shorter acquisition time.

A full discussion on how line broadening can be used to improve the SNR is given in section 5.4.2 on p. 96; the matched filter is discussed in section 5.4.3 on p. 98.

5.8

Shortening the acquisition time discards the time-domain data that contains mostly noise and little signal. Applying a line broadening weighting function does not discard this section of the time-domain, but reduces its amplitude relative to the earlier part of the FID. Thus, both methods reduce the intensity of the noise in the spectrum.

5.9

Enhancing the resolution of the spectrum by the use of a weighting function that combines a rising exponential and a Gaussian is discussed in section 5.4.4 on p. 98.

Zero filling improves the ‘definition’ of the line in the spectrum by increasing the density of data points in the frequency domain. However, it does not improve the fundamental linewidth as no real data is added to the time-domain.

5.10

Plots of the sine bell weighting functions are given in Fig. 5.21 on p. 102.
A sine bell that is phase-shifted by 45° initially increases over time, therefore partly cancelling the decay of the FID; the linewidth of the spectrum will therefore be decreased. The subsequent decay of the sine bell attenuates the noise at the end of the time-domain. The overall effect will be to enhance the resolution, assuming that the original FID has decayed close to zero by the end of the acquisition time.
The sine bell with a phase shift of 90° is purely a decaying function, which will broaden the lines in just the same way as a decaying exponential does.

5.11

The peak due to TMS is likely to be a sharp line. Hence, the corresponding time-domain signal decays slowly, and is therefore more likely to be truncated. The other lines in the spectrum will usually be broader than TMS, so their time-domain signals decay more rapidly and are less likely to be truncated.
Truncation artefacts (‘sinc wiggles’) can be suppressed by applying a decaying weighting function. This will decrease the resolution, and may reduce the SNR.

Chapter 6

The quantum mechanics of one spin

6.1

$$\hat{I}_z\psi_\beta = -\tfrac{1}{2}\psi_\beta \qquad \text{Dirac notation:} \quad \hat{I}_z\,|\beta\rangle = -\tfrac{1}{2}\,|\beta\rangle$$

$$\int \psi_\beta^\star \psi_\alpha \,\mathrm{d}\tau \qquad \text{Dirac notation:} \quad \langle\beta|\alpha\rangle$$

$$\int \psi_\beta^\star \psi_\beta \,\mathrm{d}\tau \qquad \text{Dirac notation:} \quad \langle\beta|\beta\rangle$$

$$\int \psi^\star \hat{Q}\psi \,\mathrm{d}\tau \qquad \text{Dirac notation:} \quad \langle\psi|\hat{Q}|\psi\rangle$$

(a) $\langle\alpha|\alpha\rangle = 1$

(b) $\langle\alpha|\beta\rangle = 0$ or $\langle\beta|\alpha\rangle = 0$

(c) $\hat{I}_z\,|\alpha\rangle = \frac{1}{2}|\alpha\rangle$

(d) $|\psi\rangle = c_\alpha|\alpha\rangle + c_\beta|\beta\rangle$.

6.2

The expectation value of $\hat{I}_y$ is given by:

$$\langle I_y\rangle = \frac{\langle\psi|\hat{I}_y|\psi\rangle}{\langle\psi|\psi\rangle}.$$

If $|\psi\rangle$ is normalized, $\langle\psi|\psi\rangle = 1$, so the expectation value is given by

$$\langle I_y\rangle = \langle\psi|\hat{I}_y|\psi\rangle.$$

Substituting in $|\psi\rangle = c_\alpha|\alpha\rangle + c_\beta|\beta\rangle$, we obtain

$$\begin{aligned}
\langle I_y\rangle &= \left[c_\alpha^\star\langle\alpha| + c_\beta^\star\langle\beta|\right]\hat{I}_y\left[c_\alpha|\alpha\rangle + c_\beta|\beta\rangle\right] \\
&= c_\alpha^\star c_\alpha\langle\alpha|\hat{I}_y|\alpha\rangle + c_\alpha^\star c_\beta\langle\alpha|\hat{I}_y|\beta\rangle + c_\beta^\star c_\alpha\langle\beta|\hat{I}_y|\alpha\rangle + c_\beta^\star c_\beta\langle\beta|\hat{I}_y|\beta\rangle \\
&= \tfrac{1}{2}\mathrm{i}\,c_\alpha^\star c_\alpha\langle\alpha|\beta\rangle - \tfrac{1}{2}\mathrm{i}\,c_\alpha^\star c_\beta\langle\alpha|\alpha\rangle + \tfrac{1}{2}\mathrm{i}\,c_\beta^\star c_\alpha\langle\beta|\beta\rangle - \tfrac{1}{2}\mathrm{i}\,c_\beta^\star c_\beta\langle\beta|\alpha\rangle \\
&= \tfrac{1}{2}\mathrm{i}\,c_\beta^\star c_\alpha - \tfrac{1}{2}\mathrm{i}\,c_\alpha^\star c_\beta\,.
\end{aligned}$$

To go to the third line, we have used Eq. 6.11 on p. 115,

$$\hat{I}_y |\alpha\rangle = \tfrac{1}{2}\mathrm{i}\,|\beta\rangle \qquad \hat{I}_y |\beta\rangle = -\tfrac{1}{2}\mathrm{i}\,|\alpha\rangle,$$

and to go to the last line, we have used the fact that $|\alpha\rangle$ and $|\beta\rangle$ are orthonormal (Eq. 6.5 and Eq. 6.6 on p. 112).

$\langle I_y \rangle$ can be interpreted as the average value of the y-component of angular momentum when measured for a large number of spins, each of which has the same wavefunction $|\psi\rangle$.

6.3

The matrix representation of $\hat{I}_x$ is

$$\begin{aligned} I_x &= \begin{pmatrix} \langle\alpha|\hat{I}_x|\alpha\rangle & \langle\alpha|\hat{I}_x|\beta\rangle \\ \langle\beta|\hat{I}_x|\alpha\rangle & \langle\beta|\hat{I}_x|\beta\rangle \end{pmatrix} \\ &= \begin{pmatrix} \frac{1}{2}\langle\alpha|\beta\rangle & \frac{1}{2}\langle\alpha|\alpha\rangle \\ \frac{1}{2}\langle\beta|\beta\rangle & \frac{1}{2}\langle\beta|\alpha\rangle \end{pmatrix} \\ &= \begin{pmatrix} 0 & \frac{1}{2} \\ \frac{1}{2} & 0 \end{pmatrix}. \end{aligned}$$

To go to the second line, we have used Eq. 6.10 on p. 115,

$$\hat{I}_x|\alpha\rangle = \tfrac{1}{2}|\beta\rangle \qquad \hat{I}_x|\beta\rangle = \tfrac{1}{2}|\alpha\rangle,$$

and to go to the last line we have used the fact that $|\alpha\rangle$ and $|\beta\rangle$ are orthonormal (Eq. 6.5 and Eq. 6.6 on p. 112).

Similarly,

$$\begin{aligned} I_y &= \begin{pmatrix} \langle\alpha|\hat{I}_y|\alpha\rangle & \langle\alpha|\hat{I}_y|\beta\rangle \\ \langle\beta|\hat{I}_y|\alpha\rangle & \langle\beta|\hat{I}_y|\beta\rangle \end{pmatrix} \\ &= \begin{pmatrix} \frac{1}{2}\mathrm{i}\,\langle\alpha|\beta\rangle & -\frac{1}{2}\mathrm{i}\,\langle\alpha|\alpha\rangle \\ \frac{1}{2}\mathrm{i}\,\langle\beta|\beta\rangle & -\frac{1}{2}\mathrm{i}\,\langle\beta|\alpha\rangle \end{pmatrix} \\ &= \begin{pmatrix} 0 & -\frac{1}{2}\mathrm{i} \\ \frac{1}{2}\mathrm{i} & 0 \end{pmatrix}. \end{aligned}$$

6.4

Starting with the expression for $\langle I_y \rangle$, and substituting in $c_\alpha = r_\alpha \exp(\mathrm{i}\,\phi_\alpha)$ and $c_\beta = r_\beta \exp(\mathrm{i}\,\phi_\beta)$ we find:

$$\begin{aligned}
\langle I_y \rangle &= \tfrac{1}{2}\mathrm{i}\, c_\beta^\star c_\alpha - \tfrac{1}{2}\mathrm{i}\, c_\alpha^\star c_\beta \\
&= \tfrac{1}{2}\mathrm{i}\, \left[r_\alpha r_\beta \exp(-\mathrm{i}\,\phi_\beta) \exp(\mathrm{i}\,\phi_\alpha) - r_\alpha r_\beta \exp(-\mathrm{i}\,\phi_\alpha) \exp(\mathrm{i}\,\phi_\beta) \right] \\
&= \tfrac{1}{2}\mathrm{i}\, r_\alpha r_\beta \left[\exp\left(-\mathrm{i}\,(\phi_\beta - \phi_\alpha)\right) - \exp\left(\mathrm{i}\,(\phi_\beta - \phi_\alpha)\right) \right] \\
&= \tfrac{1}{2\mathrm{i}} r_\alpha r_\beta \left[\exp\left(\mathrm{i}\,(\phi_\beta - \phi_\alpha)\right) - \exp\left(-\mathrm{i}\,(\phi_\beta - \phi_\alpha)\right) \right],
\end{aligned}$$

where to go to the last line we have multiplied top and bottom by i.

Applying the identity

$$\exp(\mathrm{i}\theta) - \exp(-\mathrm{i}\theta) \equiv 2\mathrm{i}\sin\theta$$

to the above expression gives

$$\langle I_y \rangle = r_\alpha r_\beta \sin(\phi_\beta - \phi_\alpha).$$

The bulk y-magnetization is then given by

$$\begin{aligned}
M_y &= \gamma \langle I_x \rangle^{(1)} + \gamma \langle I_x \rangle^{(2)} + \ldots \\
&= \gamma r_\alpha^{(1)} r_\beta^{(1)} \sin(\phi_\beta^{(1)} - \phi_\alpha^{(1)}) + \gamma r_\alpha^{(2)} r_\beta^{(2)} \sin(\phi_\beta^{(2)} - \phi_\alpha^{(2)}) + \ldots \\
&= \gamma N \overline{r_\alpha r_\beta \sin(\phi_\beta - \phi_\alpha)}.
\end{aligned}$$

At equilibrium, the phases ϕ are randomly distributed, and so $\sin(\phi_\beta - \phi_\alpha)$ is randomly distributed between ± 1. As a result, the equilibrium y-magnetization is zero.

6.5

Starting from Eq. 6.31 on p. 124 and premultiplying by $\langle\beta|$, we obtain:

$$\begin{aligned}
\frac{\mathrm{d}c_\alpha(t)}{\mathrm{d}t}|\alpha\rangle + \frac{\mathrm{d}c_\beta(t)}{\mathrm{d}t}|\beta\rangle &= -\tfrac{1}{2}\mathrm{i}\,\Omega c_\alpha(t)|\alpha\rangle + \tfrac{1}{2}\mathrm{i}\,\Omega c_\beta(t)|\beta\rangle \\
\langle\beta|\frac{\mathrm{d}c_\alpha(t)}{\mathrm{d}t}|\alpha\rangle + \langle\beta|\frac{\mathrm{d}c_\beta(t)}{\mathrm{d}t}|\beta\rangle &= \langle\beta|\left[-\tfrac{1}{2}\mathrm{i}\,\Omega c_\alpha(t)\right]|\alpha\rangle + \langle\beta|\left[\tfrac{1}{2}\mathrm{i}\,\Omega c_\beta(t)\right]|\beta\rangle.
\end{aligned}$$

The derivatives of c_α and c_β, and the quantities in square brackets, are numbers, so the above expression can be rearranged to give

$$\begin{aligned}
\frac{\mathrm{d}c_\alpha(t)}{\mathrm{d}t}\langle\beta|\alpha\rangle + \frac{\mathrm{d}c_\beta(t)}{\mathrm{d}t}\langle\beta|\beta\rangle &= -\tfrac{1}{2}\mathrm{i}\,\Omega c_\alpha(t)\langle\beta|\alpha\rangle + \tfrac{1}{2}\mathrm{i}\,\Omega c_\beta(t)\langle\beta|\beta\rangle \\
\frac{\mathrm{d}c_\beta(t)}{\mathrm{d}t} &= \tfrac{1}{2}\mathrm{i}\,\Omega c_\beta(t).
\end{aligned}$$

To go to the last line, we have used the orthonormality property of $|\alpha\rangle$ and $|\beta\rangle$.

Substituting Eq. 6.58 into the left-hand side of Eq. 6.57 gives:

$$\begin{aligned}\frac{\mathrm{d}c_\beta(t)}{\mathrm{d}t} &= \frac{\mathrm{d}}{\mathrm{d}t}\left[c_\beta(0)\exp\left(\tfrac{1}{2}\mathrm{i}\,\Omega t\right)\right] \\ &= \tfrac{1}{2}\mathrm{i}\,\Omega c_\beta(0)\exp\left(\tfrac{1}{2}\mathrm{i}\,\Omega t\right) \\ &= \tfrac{1}{2}\mathrm{i}\,\Omega c_\beta(t).\end{aligned}$$

Eq. 6.58 is indeed the solution.

6.6

The expectation value of $\hat{I}_y$ is

$$\langle I_y\rangle = \tfrac{1}{2}\mathrm{i}\,c_\beta^\star c_\alpha - \tfrac{1}{2}\mathrm{i}\,c_\alpha^\star c_\beta\,.$$

Substituting in the expressions for how c_α and c_β vary under free evolution (Eq. 6.34 on p. 125) gives:

$$\begin{aligned}\langle I_y\rangle(t) &= \tfrac{1}{2}\mathrm{i}\left[c_\beta^\star(0)\exp\left(-\tfrac{1}{2}\mathrm{i}\,\Omega t\right)\right]\left[c_\alpha(0)\exp\left(-\tfrac{1}{2}\mathrm{i}\,\Omega t\right)\right] - \tfrac{1}{2}\mathrm{i}\left[c_\alpha^\star(0)\exp\left(\tfrac{1}{2}\mathrm{i}\,\Omega t\right)\right]\left[c_\beta(0)\exp\left(\tfrac{1}{2}\mathrm{i}\,\Omega t\right)\right] \\ &= \tfrac{1}{2}\mathrm{i}\,c_\beta^\star(0)c_\alpha(0)\exp\left(-\mathrm{i}\,\Omega t\right) - \tfrac{1}{2}\mathrm{i}\,c_\alpha^\star(0)c_\beta(0)\exp\left(\mathrm{i}\,\Omega t\right) \\ &= \tfrac{1}{2}\mathrm{i}\,c_\beta^\star(0)c_\alpha(0)\left[\cos(\Omega t) - \mathrm{i}\,\sin(\Omega t)\right] - \tfrac{1}{2}\mathrm{i}\,c_\alpha^\star(0)c_\beta(0)\left[\cos(\Omega t) + \mathrm{i}\,\sin(\Omega t)\right] \\ &= \cos(\Omega t)\left[\tfrac{1}{2}\mathrm{i}\,c_\beta^\star(0)c_\alpha(0) - \tfrac{1}{2}\mathrm{i}\,c_\alpha^\star(0)c_\beta(0)\right] + \sin(\Omega t)\left[\tfrac{1}{2}c_\alpha^\star(0)c_\beta(0) + \tfrac{1}{2}c_\beta^\star(0)c_\alpha(0)\right] \\ &= \cos(\Omega t)\langle I_y\rangle(0) + \sin(\Omega t)\langle I_x\rangle(0).\end{aligned}$$

To go to the third line, the identities

$$\exp(\mathrm{i}\theta) \equiv \cos\theta + \mathrm{i}\sin\theta \qquad \exp(-\mathrm{i}\theta) \equiv \cos\theta - \mathrm{i}\sin\theta$$

were used, and to go to the last line, the expressions for $\langle I_x\rangle$ and $\langle I_y\rangle$ in terms of c_α and c_β were used (Eqs 6.12 and 6.13 on p. 115).

This result is summarized in the diagram below. The grey arrow shows the initial position, and the black arrow shows the position after time t.

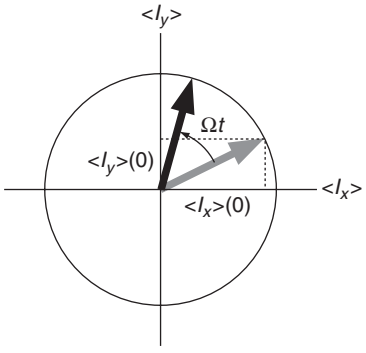

6.7

The matrix representation of the density operator is given by:

$$\rho = \begin{pmatrix} \overline{\langle\alpha|\hat{\rho}|\alpha\rangle} & \overline{\langle\alpha|\hat{\rho}|\beta\rangle} \\ \overline{\langle\beta|\hat{\rho}|\alpha\rangle} & \overline{\langle\beta|\hat{\rho}|\beta\rangle} \end{pmatrix} \equiv \begin{pmatrix} \rho_{11} & \rho_{12} \\ \rho_{21} & \rho_{22} \end{pmatrix}.$$

We can now calculate the ρ_{11} element (for clarity, the overbars indicating the ensemble averaging have been omitted until the last line):

$$\begin{aligned} \rho_{11} &= \langle\alpha|\hat{\rho}|\alpha\rangle \\ &= \langle\alpha|\psi\rangle\langle\psi|\alpha\rangle \\ &= \langle\alpha|\left[c_\alpha|\alpha\rangle + c_\beta|\beta\rangle\right]\left[c_\alpha^\star\langle\alpha| + c_\beta^\star\langle\beta|\right]|\alpha\rangle \\ &= \left[c_\alpha\langle\alpha|\alpha\rangle + c_\beta\langle\alpha|\beta\rangle\right]\left[c_\alpha^\star\langle\alpha|\alpha\rangle + c_\beta^\star\langle\beta|\alpha\rangle\right] \\ &= \overline{c_\alpha c_\alpha^\star}. \end{aligned}$$

To go to the second line, the definition of $\hat{\rho}$ was inserted, and on the third line $|\psi\rangle$ was expressed as a superposition of $|\alpha\rangle$ and $|\beta\rangle$.
The other elements can be calculated in a similar way to give:

$$\rho_{12} = \overline{c_\alpha c_\beta^\star} \qquad \rho_{21} = \overline{c_\beta c_\alpha^\star} \qquad \rho_{22} = \overline{c_\beta c_\beta^\star}.$$

Hence,

$$\rho = \begin{pmatrix} \overline{c_\alpha c_\alpha^\star} & \overline{c_\alpha c_\beta^\star} \\ \overline{c_\beta c_\alpha^\star} & \overline{c_\beta c_\beta^\star} \end{pmatrix}.$$

Chapter 7

Product operators

7.1

- $\exp(-\mathrm{i}\,\theta\hat{I}_x)\hat{I}_y\exp(\mathrm{i}\,\theta\hat{I}_x)$ represents a rotation of $\hat{I}_y$ about x through angle θ. From Fig. 7.4 (a) on p. 152, $\hat{I}_y$ is transformed into $\hat{I}_z$. Hence,

$$\hat{I}_y \xrightarrow{\theta\hat{I}_x} \cos\theta\,\hat{I}_y + \sin\theta\,\hat{I}_z.$$

  This is consistent with the identity on line one of Table 7.1 on p. 146.

- $\exp(-\mathrm{i}\,\theta\hat{S}_y)\hat{S}_z\exp(\mathrm{i}\,\theta\hat{S}_y)$. From (b) of Fig. 7.4 on p. 152, $\hat{S}_z$ is transformed into $\hat{S}_x$ by a rotation about y:

$$\hat{S}_z \xrightarrow{\theta\hat{S}_y} \cos\theta\,\hat{S}_z + \sin\theta\,\hat{S}_x.$$

- $\exp(-\mathrm{i}\,\theta\hat{I}_x)\hat{I}_x\exp(\mathrm{i}\,\theta\hat{I}_x)$. Rotating $\hat{I}_x$ about the x-axis has no effect:

$$\hat{I}_x \xrightarrow{\theta\hat{I}_x} \hat{I}_x.$$

- $\exp(-\mathrm{i}\,\theta\hat{I}_z)(-\hat{I}_y)\exp(\mathrm{i}\,\theta\hat{I}_z)$. Fig. 7.4 (c) shows the effect of a rotation about z on $-\hat{I}_y$: the result is a transformation to $\hat{I}_x$. Hence,

$$-\hat{I}_y \xrightarrow{\theta\hat{I}_z} -\cos\theta\,\hat{I}_y + \sin\theta\,\hat{I}_x.$$

- $\exp(-\mathrm{i}\,(\theta/2)\hat{I}_y)\hat{I}_x\exp(\mathrm{i}\,(\theta/2)\hat{I}_y)$. This represents the rotation of $\hat{I}_x$ about y through angle $\theta/2$. From Fig. 7.4 (b), $\hat{I}_x$ is transformed to $-\hat{I}_z$. Hence,

$$\hat{I}_x \xrightarrow{(\theta/2)\hat{I}_y} \cos(\theta/2)\,\hat{I}_x - \sin(\theta/2)\,\hat{I}_z.$$

- $\exp(\mathrm{i}\,\theta\hat{I}_z)(-\hat{I}_z)\exp(-\mathrm{i}\,\theta\hat{I}_z)$. Careful inspection of the arguments of the exponentials reveals that this represents a z-rotation through angle $-\theta$ i.e. the rotation is in a clockwise sense. In this case, it does not matter as $-\hat{I}_z$ is unaffected by a rotation about the z-axis:

$$-\hat{I}_z \xrightarrow{-\theta\hat{I}_z} -\hat{I}_z.$$

7.2

The 90°(x) pulse rotates the equilibrium magnetization (represented by $\hat{I}_z$) onto the $-y$-axis:

$$\begin{aligned}\hat{I}_z &\xrightarrow{(\pi/2)\hat{I}_x} \cos(\pi/2)\,\hat{I}_z - \sin(\pi/2)\,\hat{I}_y \\ &= -\hat{I}_y.\end{aligned}$$

This transverse term evolves under the offset during the delay τ to give

$$-\hat{I}_y \xrightarrow{\Omega\tau\hat{I}_z} -\cos(\Omega\tau)\,\hat{I}_y + \sin(\Omega\tau)\,\hat{I}_x,$$

where (c) of Fig. 7.4 on p. 152 has been used.
The 180°(y) pulse does not affect the $\hat{I}_y$ term, but inverts the $\hat{I}_x$ term:

$$\begin{aligned}-\cos(\Omega\tau)\,\hat{I}_y + \sin(\Omega\tau)\,\hat{I}_x \xrightarrow{\pi\hat{I}_y} &-\cos(\Omega\tau)\,\hat{I}_y + \cos\pi\sin(\Omega\tau)\,\hat{I}_x - \sin\pi\sin(\Omega\tau)\,\hat{I}_z \\ &= -\cos(\Omega\tau)\,\hat{I}_y - \sin(\Omega\tau)\,\hat{I}_x.\end{aligned}$$

Now we consider the evolution during the second delay. Taking each term separately, we obtain

$$\begin{aligned}-\cos(\Omega\tau)\,\hat{I}_y &\xrightarrow{\Omega\tau\hat{I}_z} -\cos(\Omega\tau)\cos(\Omega\tau)\,\hat{I}_y + \sin(\Omega\tau)\cos(\Omega\tau)\,\hat{I}_x, \\ -\sin(\Omega\tau)\,\hat{I}_x &\xrightarrow{\Omega\tau\hat{I}_z} -\cos(\Omega\tau)\sin(\Omega\tau)\,\hat{I}_x - \sin(\Omega\tau)\sin(\Omega\tau)\,\hat{I}_y.\end{aligned}$$

Combining these terms gives the final result as

$$-\left[\cos^2(\Omega\tau) + \sin^2(\Omega\tau)\right]\hat{I}_y = -\hat{I}_y,$$

where the terms in $\hat{I}_x$ cancel, and the identity $\cos^2\theta + \sin^2\theta \equiv 1$ has been used. At the end of the sequence, the magnetization has been refocused onto the $-y$-axis, irrespective of the offset.

7.3

$$\begin{aligned}\hat{I}_y &\xrightarrow{(\pi/2)\hat{I}_y} \hat{I}_y \\ \hat{I}_y &\xrightarrow{-(\pi/2)\hat{I}_y} \hat{I}_y \\ \hat{S}_y &\xrightarrow{\pi\hat{S}_y} \hat{S}_y.\end{aligned}$$

In all three cases, the pulse is applied about the same axis along which the magnetization is aligned, therefore the magnetization is unaffected.

In the following cases, we refer to Fig. 7.4 on p. 152 to determine how the operator is transformed by the rotation.

$$\begin{aligned}\hat{I}_x &\xrightarrow{-\pi\hat{I}_y} \cos(-\pi)\hat{I}_x - \sin(-\pi)\hat{I}_z \\ &= -\hat{I}_x.\end{aligned}$$

In this case the magnetization is simply inverted.
The difference between the next two examples is the sense of the 90° rotation.

$$\begin{aligned}\hat{I}_z &\xrightarrow{(\pi/2)\hat{I}_y} \cos(\pi/2)\,\hat{I}_z + \sin(\pi/2)\,\hat{I}_x \\ &= \hat{I}_x.\end{aligned}$$

$$\begin{aligned}\hat{I}_z &\xrightarrow{-(\pi/2)\hat{I}_y} \cos(-\pi/2)\,\hat{I}_z + \sin(-\pi/2)\,\hat{I}_x \\ &= -\hat{I}_x.\end{aligned}$$

The next two are simply inversions:

$$\begin{aligned}\hat{S}_z &\xrightarrow{\pi\hat{S}_y} \cos\pi\,\hat{S}_z + \sin\pi\,\hat{S}_x \\ &= -\hat{S}_z.\end{aligned}$$

$$\begin{aligned}\hat{I}_z &\xrightarrow{-\pi\hat{I}_y} \cos(-\pi)\,\hat{I}_z + \sin(-\pi)\,\hat{I}_x \\ &= -\hat{I}_z.\end{aligned}$$

7.4

The 90°(x) pulse rotates the equilibrium magnetization $\hat{I}_z$ to $-\hat{I}_y$. Free evolution is a rotation about z, so the state of the system after the delay τ is

$$-\cos(\Omega\tau)\,\hat{I}_y + \sin(\Omega\tau)\,\hat{I}_x.$$

The 90°(y) pulse does not affect the $\hat{I}_y$ term, but rotates $\hat{I}_x$ to $-\hat{I}_z$. The final result is

$$-\cos(\Omega\tau)\,\hat{I}_y - \sin(\Omega\tau)\,\hat{I}_z.$$

The pulse sequence has therefore produced transverse magnetization along y, whose amplitude varies as $-\cos(\Omega\tau)$. This becomes zero if $\cos(\Omega\tau) = 0$. Hence, there is a null at $\Omega\tau = \pi/2$, which corresponds to an offset of $\Omega = \pi/(2\tau)$ in rad s^{-1}, or $1/(4\tau)$ in Hz.
There is a maximum in the excitation when $\cos(\Omega\tau) = \pm 1$. This occurs at offsets satisfying $\Omega\tau = n\pi$ where $n = 0, 1, 2, \ldots$ i.e. $\Omega = (n\pi)/\tau$ or $n/(2\tau)$ in Hz.

7.5

Figure 7.6 (b) on p. 156 shows that, as a result of evolution of the scalar coupling, the in-phase term $-\hat{I}_{1y}$ is partly transformed into the anti-phase term $2\hat{I}_{1x}\hat{I}_{2z}$; the angle of rotation is $\pi J_{12}\tau$. This is represented as:

$$-\hat{I}_{1y} \xrightarrow{2\pi J_{12}\tau \hat{I}_{1z}\hat{I}_{2z}} -\cos(\pi J_{12}\tau)\,\hat{I}_{1y} + \sin(\pi J_{12}\tau)\,2\hat{I}_{1x}\hat{I}_{2z}.$$

Using the same figure, we see that $-2\hat{I}_{1x}\hat{I}_{2z}$ is partly transformed to $-\hat{I}_{1y}$:

$$-2\hat{I}_{1x}\hat{I}_{2z} \xrightarrow{2\pi J_{12}\tau \hat{I}_{1z}\hat{I}_{2z}} -\cos(\pi J_{12}\tau)\,2\hat{I}_{1x}\hat{I}_{2z} - \sin(\pi J_{12}\tau)\,\hat{I}_{1y}.$$

Similarly,

$$\begin{aligned}
\hat{S}_x &\xrightarrow{2\pi J_{IS}(\tau/2)\hat{I}_z\hat{S}_z} \cos(\pi J_{IS}\tau/2)\,\hat{S}_x + \sin(\pi J_{IS}\tau/2)\,2\hat{I}_z\hat{S}_y.\\
\hat{I}_{2y} &\xrightarrow{2\pi J_{12}\tau \hat{I}_{1z}\hat{I}_{2z}} \cos(\pi J_{12}\tau)\,\hat{I}_{2y} - \sin(\pi J_{12}\tau)\,2\hat{I}_{1z}\hat{I}_{2x}.\\
2\hat{I}_{1z}\hat{I}_{2y} &\xrightarrow{2\pi J_{12}\tau \hat{I}_{1z}\hat{I}_{2z}} \cos(\pi J_{12}\tau)\,2\hat{I}_{1z}\hat{I}_{2y} - \sin(\pi J_{12}\tau)\,\hat{I}_{2x}.\\
\hat{I}_{2z} &\xrightarrow{2\pi J_{12}\tau \hat{I}_{1z}\hat{I}_{2z}} \hat{I}_{2z}.
\end{aligned}$$

In the last example we see that z-magnetization is not affected by evolution under coupling simply because the Hamiltonian for coupling only contains $\hat{I}_z$ operators.

7.6

The evolution is determined by the Hamiltonian given in Eq. 7.14 on p. 154:

$$\hat{H}_{\text{two spins}} = \Omega_1\hat{I}_{1z} + \Omega_2\hat{I}_{2z} + 2\pi J_{12}\hat{I}_{1z}\hat{I}_{2z}.$$

We will now work out the effect in turn of the three terms in the Hamiltonian. The first is a rotation about z:

$$\hat{I}_{1y} \xrightarrow{\Omega_1 t\hat{I}_{1z}} \cos(\Omega_1 t)\,\hat{I}_{1y} - \sin(\Omega_1 t)\,\hat{I}_{1x}.$$

The second term, $\Omega_2\hat{I}_{2z}$, does not need to be considered as spin-two operators have no effect on spin-one operators. Finally, we consider the effect of evolution under scalar coupling:

$$\begin{aligned}
\cos(\Omega_1 t)\,\hat{I}_{1y} - \sin(\Omega_1 t)\,\hat{I}_{1x} &\xrightarrow{2\pi J_{12}t\hat{I}_{1z}\hat{I}_{2z}}\\
&\underbrace{\cos(\pi J_{12}t)\cos(\Omega_1 t)\,\hat{I}_{1y}}_{y\text{-magnetization}} - \sin(\pi J_{12}t)\cos(\Omega_1 t)\,2\hat{I}_{1x}\hat{I}_{2z}\\
&\underbrace{-\cos(\pi J_{12}t)\sin(\Omega_1 t)\,\hat{I}_{1x}}_{x\text{-magnetization}} - \sin(\pi J_{12}t)\sin(\Omega_1 t)\,2\hat{I}_{1y}\hat{I}_{2z}.
\end{aligned}$$

The NMR signal is given by:

$$\begin{aligned} S(t) &= M_x + \mathrm{i}M_y \\ &= -\cos(\pi J_{12}t)\sin(\Omega_1 t) + \mathrm{i}\cos(\pi J_{12}t)\cos(\Omega_1 t) \\ &= \mathrm{i}\cos(\pi J_{12}t)\,[\cos(\Omega_1 t) + \mathrm{i}\sin(\Omega_1 t)] \\ &= \mathrm{i}\cos(\pi J_{12}t)\exp(\mathrm{i}\,\Omega_1 t) \\ &= \tfrac{1}{2}\mathrm{i}\,[\exp(\mathrm{i}\,\pi J_{12}t) + \exp(-\mathrm{i}\,\pi J_{12}t)]\exp(\mathrm{i}\,\Omega_1 t) \\ &= \tfrac{1}{2}\mathrm{i}\exp\left(\mathrm{i}[\Omega_1 + \pi J_{12}]t\right) + \tfrac{1}{2}\mathrm{i}\exp\left(\mathrm{i}[\Omega_1 - \pi J_{12}]t\right). \end{aligned}$$

To go to the fourth line, we have used the identity $\cos\theta + \mathrm{i}\sin\theta \equiv \exp(\mathrm{i}\,\theta)$, and to go to the fifth line, we have used $\cos\theta \equiv \frac{1}{2}[\exp(\mathrm{i}\,\theta) + \exp(-\mathrm{i}\,\theta)]$. Finally, to go to the sixth line we have multiplied out the square brackets. Fourier transformation of this signal gives a positive line at $\Omega_1 + \pi J_{12}$, and a second positive line at $\Omega_1 - \pi J_{12}$ i.e. an in-phase doublet on spin one. The factor of i corresponds to a phase shift of 90°, so the imaginary part of the spectrum contains the absorption mode lineshape.

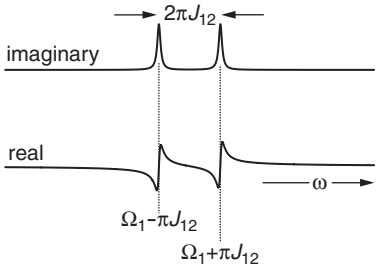

A similar line of argument gives the observable signal arising from $2\hat{I}_{1y}\hat{I}_{2z}$ as

$$S(t) = \tfrac{1}{2}\mathrm{i}\exp\left(\mathrm{i}[\Omega_1 + \pi J_{12}]t\right) - \tfrac{1}{2}\mathrm{i}\exp\left(\mathrm{i}[\Omega_1 - \pi J_{12}]t\right).$$

The corresponding spectrum is an anti-phase doublet on spin one. Again, the factor of i means that the absorption mode lines will appear in the imaginary part of the spectrum.

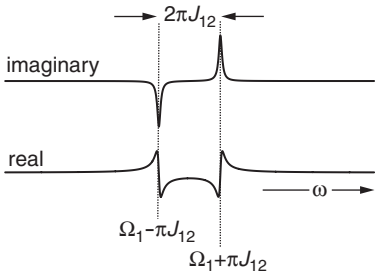

7.7

$\hat{I}_{1y}$ represents in-phase magnetization on spin one, aligned along the y-axis. The resulting spectrum will be an in-phase doublet centred on the offset of spin one, both peaks of which are in the absorption mode.

$\hat{I}_{2x}$ represents in-phase magnetization on spin two. However, it is aligned along the x-axis, so has a phase of $3\pi/2$ relative to the y-axis. The spectrum therefore comprises an in-phase doublet that is centred on the offset of spin two, with both peaks in the dispersion mode.

$2\hat{I}_{1y}\hat{I}_{2z}$ represents magnetization on spin one that is anti-phase with respect to spin two, and aligned along y. The spectrum is therefore an anti-phase doublet in the absorption mode.

$2\hat{I}_{1z}\hat{I}_{2x}$ represents anti-phase magnetization on spin two. It is aligned along x, so the lineshape will be dispersive. Therefore, the spectrum is an anti-phase spin-two doublet with the dispersion lineshape.

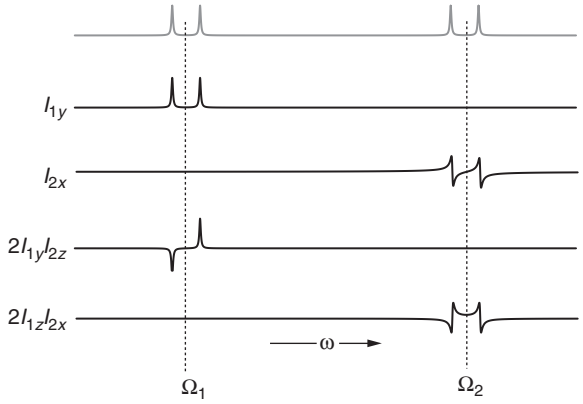

7.8

In-phase magnetization $\hat{I}_{1x}$ is rotated in the xz-plane towards $-\hat{I}_{1z}$ by the application of the y-pulse of duration t_p.

$$\hat{I}_{1x} \xrightarrow{\omega_1 t_\mathrm{p} \hat{I}_{1y}} \cos(\omega_1 t_\mathrm{p})\,\hat{I}_{1x} - \sin(\omega_1 t_\mathrm{p})\,\hat{I}_{1z}$$

A 180° pulse about y applied only to spin two changes the sign of the anti-phase magnetization on spin one.

$$\begin{aligned} 2\hat{I}_{1x}\hat{I}_{2z} \xrightarrow{-\pi \hat{I}_{2y}} & \cos(-\pi)\,2\hat{I}_{1x}\hat{I}_{2z} + \sin(-\pi)\,2\hat{I}_{1x}\hat{I}_{2x} \\ & = -2\hat{I}_{1x}\hat{I}_{2z} \end{aligned}$$

In-phase magnetization on spin one is allowed to evolve under coupling for time t, thus generating anti-phase magnetization on the same spin.

$$-\hat{I}_{1x} \xrightarrow{2\pi J_{12} t \hat{I}_{1z}\hat{I}_{2z}} -\cos(\pi J_{12} t)\,\hat{I}_{1x} - \sin(\pi J_{12} t)\,2\hat{I}_{1y}\hat{I}_{2z}$$

Letting each term act sequentially, we obtain

$$2\hat{I}_{1x}\hat{I}_{2z} \xrightarrow{(\pi/2)\hat{I}_{1y}} -2\hat{I}_{1z}\hat{I}_{2z} \xrightarrow{(\pi/2)\hat{I}_{2y}} -2\hat{I}_{1z}\hat{I}_{2x}.$$

Note that the spin-one operators do not act on spin-two operators and *vice versa*. The net result is that the non-selective 90°(y) pulse has caused a coherence transfer from spin one to spin two.

Transverse, in-phase magnetization on the S spin evolves under offset for time t. The offset term for the I spin has no effect on the $\hat{S}_x$.

$$\hat{S}_x \xrightarrow{\Omega_I t \hat{I}_z} \hat{S}_x \xrightarrow{\Omega_S t \hat{S}_z} \cos(\Omega_S t)\,\hat{S}_x + \sin(\Omega_S t)\,\hat{S}_y$$

Anti-phase magnetization on spin two evolves under coupling to generate in-phase magnetization on the same spin.

$$-2\hat{I}_{1z}\hat{I}_{2y} \xrightarrow{2\pi J_{12} t \hat{I}_{1z}\hat{I}_{2z}} -\cos(\pi J_{12} t)\,2\hat{I}_{1z}\hat{I}_{2y} + \sin(\pi J_{12} t)\,\hat{I}_{2x}$$

7.9

The Hamiltonian for free evolution is given by Eq. 7.14 on p. 154:

$$\hat{H}_{\text{two spins}} = \Omega_1 \hat{I}_{1z} + \Omega_2 \hat{I}_{2z} + 2\pi J_{12} \hat{I}_{1z}\hat{I}_{2z}.$$

The spin echo refocuses the evolution due to offset, so we only need to consider the evolution of $2\hat{I}_{1x}\hat{I}_{2z}$ under coupling, which gives

$$2\hat{I}_{1x}\hat{I}_{2z} \xrightarrow{2\pi J_{12}\tau \hat{I}_{1z}\hat{I}_{2z}} \cos(\pi J_{12}\tau)\,2\hat{I}_{1x}\hat{I}_{2z} + \sin(\pi J_{12}\tau)\,\hat{I}_{1y}.$$

The π pulse about the x-axis acts on both spins, leaving $\hat{I}_{1x}$ unaffected, but inverting $\hat{I}_{2z}$ and $\hat{I}_{1y}$:

$$\cos(\pi J_{12}\tau)\,2\hat{I}_{1x}\hat{I}_{2z} + \sin(\pi J_{12}\tau)\,\hat{I}_{1y} \xrightarrow{\pi(\hat{I}_{1x}+\hat{I}_{2x})} -\cos(\pi J_{12}\tau)\,2\hat{I}_{1x}\hat{I}_{2z} - \sin(\pi J_{12}\tau)\,\hat{I}_{1y}.$$

Finally, evolution under coupling during the second delay gives

$$\begin{aligned}
&-\cos(\pi J_{12}\tau)\,2\hat{I}_{1x}\hat{I}_{2z} - \sin(\pi J_{12}\tau)\,\hat{I}_{1y} \xrightarrow{2\pi J_{12}\tau \hat{I}_{1z}\hat{I}_{2z}} \\
&\quad -\cos^2(\pi J_{12}\tau)\,\hat{I}_{1x}\hat{I}_{2z} - \sin(\pi J_{12}\tau)\cos(\pi J_{12}\tau)\,\hat{I}_{1y} - \cos(\pi J_{12}\tau)\sin(\pi J_{12}\tau)\,\hat{I}_{1y} + \sin^2(\pi J_{12}\tau)\,2\hat{I}_{1x}\hat{I}_{2z} \\
&\quad = -\left[\cos^2(\pi J_{12}\tau) - \sin^2(\pi J_{12}\tau)\right] 2\hat{I}_{1x}\hat{I}_{2z} - \left[2\cos(\pi J_{12}\tau)\sin(\pi J_{12}\tau)\right]\,\hat{I}_{1y} \\
&\quad = -\cos(2\pi J_{12}\tau)\,2\hat{I}_{1x}\hat{I}_{2z} - \sin(2\pi J_{12}\tau)\,\hat{I}_{1y}.
\end{aligned}$$

To go to the last line, we have used the identities $\cos^2\theta - \sin^2\theta \equiv \cos 2\theta$ and $2\cos\theta\sin\theta \equiv \sin 2\theta$.

By a similar method we can show:

$$2\hat{I}_{1y}\hat{I}_{2z} \xrightarrow{\tau-\pi_x-\tau} \cos(2\pi J_{12}\tau)\,2\hat{I}_{1y}\hat{I}_{2z} - \sin(2\pi J_{12}\tau)\,\hat{I}_{1x}.$$

The effect of the $\tau - \pi_y - \tau$ spin echo on spin-one and spin-two terms is shown in the table below:

	final state	
initial state	$\times\cos(2\pi J_{12}\tau)$	$\times\sin(2\pi J_{12}\tau)$
$\hat{I}_{1x}$	$-\hat{I}_{1x}$	$-2\hat{I}_{1y}\hat{I}_{2z}$
$\hat{I}_{1y}$	$\hat{I}_{1y}$	$-2\hat{I}_{1x}\hat{I}_{2z}$
$2\hat{I}_{1x}\hat{I}_{2z}$	$2\hat{I}_{1x}\hat{I}_{2z}$	$\hat{I}_{1y}$
$2\hat{I}_{1y}\hat{I}_{2z}$	$-2\hat{I}_{1y}\hat{I}_{2z}$	$\hat{I}_{1x}$
$\hat{I}_{2x}$	$-\hat{I}_{2x}$	$-2\hat{I}_{1z}\hat{I}_{2y}$
$\hat{I}_{2y}$	$\hat{I}_{2y}$	$-2\hat{I}_{1z}\hat{I}_{2x}$
$2\hat{I}_{1z}\hat{I}_{2x}$	$2\hat{I}_{1z}\hat{I}_{2x}$	$\hat{I}_{2y}$
$2\hat{I}_{1z}\hat{I}_{2y}$	$-2\hat{I}_{1z}\hat{I}_{2y}$	$\hat{I}_{2x}$

The results for the in- and anti-phase operators on spin two can be obtained from those for spin one simply by swapping the labels 1 and 2.

Likewise for the $\tau - \pi_x - \tau$ spin echo:

	final state	
initial state	$\times\cos(2\pi J_{12}\tau)$	$\times\sin(2\pi J_{12}\tau)$
$\hat{I}_{2x}$	$\hat{I}_{2x}$	$\hat{I}_{1z}\hat{I}_{2y}$
$\hat{I}_{2y}$	$-\hat{I}_{2y}$	$2\hat{I}_{1z}\hat{I}_{2x}$
$2\hat{I}_{1z}\hat{I}_{2x}$	$-2\hat{I}_{1z}\hat{I}_{2x}$	$-\hat{I}_{2y}$
$2\hat{I}_{1z}\hat{I}_{2y}$	$2\hat{I}_{1z}\hat{I}_{2y}$	$-\hat{I}_{2x}$

7.10

A spin echo in a homonuclear two-spin system is equivalent to:

(a) evolution of the coupling for time 2τ,

(b) a $180°(x)$ pulse.

Applying this to the first example, we obtain

$$\hat{I}_{2y} \xrightarrow{\tau-\pi_x-\tau} -\cos(2\pi J_{12}\tau)\,\hat{I}_{2y} + \sin(2\pi J_{12}\tau)\,2\hat{I}_{1z}\hat{I}_{2x}.$$

For complete transformation to $2\hat{I}_{1z}\hat{I}_{2x}$, we need $\sin(2\pi J_{12}\tau) = 1$ and $\cos(2\pi J_{12}\tau) = 0$. These occur when $2\pi J_{12}\tau = \pi/2$, i.e. $\tau = 1/(4J_{12})$.

$$\hat{I}_{1x} \xrightarrow{\tau-\pi_x-\tau} \cos(2\pi J_{12}\tau)\hat{I}_{1x} + \sin(2\pi J_{12}\tau)2\hat{I}_{1y}\hat{I}_{2z}.$$

Setting $2\pi J_{12}\tau = \pi/4$ gives $\cos(2\pi J_{12}\tau) = \sin(2\pi J_{12}\tau) = 1/\sqrt{2}$. The required delay is therefore $\tau = 1/(8J_{12})$.
To achieve conversion to $-\hat{I}_{1x}$, we need $\cos(2\pi J_{12}\tau) = -1$ and $\sin(2\pi J_{12}\tau) = 0$ i.e. $\tau = 1/(2J_{12})$.

$$2\hat{I}_{1z}\hat{I}_{2x} \xrightarrow{\tau-\pi_x-\tau} -\cos(2\pi J_{12}\tau)2\hat{I}_{1z}\hat{I}_{2x} - \sin(2\pi J_{12}\tau)\hat{I}_{2y}.$$

Setting the delay to $\tau = 1/(4J_{12})$ gives complete conversion to in-phase magnetization.

7.11

The pulse sequence is given in Fig. 7.14 on p. 168:

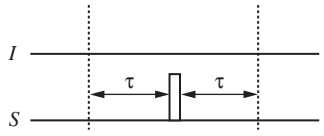

The 180°(x) pulse is applied to only the S spin, so the evolution of the offset of the S spin will be refocused. We need to consider the evolution of the coupling. Starting with $\hat{S}_x$, the state of the system after the first delay is

$$\cos(\pi J_{12}\tau)\,\hat{S}_x + \sin(\pi J_{12}\tau)\,2\hat{I}_z\hat{S}_y.$$

The 180°(x) pulse is applied only to the S spin, and so does not affect $\hat{I}_z$ or $\hat{S}_x$. However, the term in $\hat{S}_y$ changes sign to give:

$$\cos(\pi J_{12}\tau)\,\hat{S}_x - \sin(\pi J_{12}\tau)\,2\hat{I}_z\hat{S}_y.$$

Evolution of the coupling during the second delay gives

$$\left[\cos^2(\pi J_{12}\tau) + \sin^2(\pi J_{12}\tau)\right]\hat{S}_x + [\sin(\pi J_{12}\tau)\cos(\pi J_{12}\tau) - \cos(\pi J_{12}\tau)\sin(\pi J_{12}\tau)]\,2\hat{I}_z\hat{S}_y = \hat{S}_x,$$

where the anti-phase terms cancel, and the identity $\cos^2\theta + \sin^2\theta \equiv 1$ has been used. The evolution of the coupling has therefore been refocused.

Repeating the calculation for the anti-phase term, we see that $2\hat{I}_z\hat{S}_x$ is unaffected by the spin echo sequence. Again, the coupling is refocused.

Both operators are unchanged, which is the same effect that a $180°(x)$ pulse to the S spin would have:

$$\hat{S}_x \xrightarrow{\pi\hat{S}_x} \hat{S}_x$$
$$2\hat{I}_z\hat{S}_x \xrightarrow{\pi\hat{S}_x} 2\hat{I}_z\hat{S}_x.$$

Likewise, the operators $\hat{I}_x$ and $2\hat{I}_x\hat{S}_z$ will have their evolution under coupling refocused. However, as the $180°(x)$ pulse is not applied to the I spin, the offset will not be refocused, but will evolve for the duration of the spin echo (time 2τ).

7.12

The pulse sequence for the INEPT experiment is reproduced below from Fig. 7.15 on p. 172:

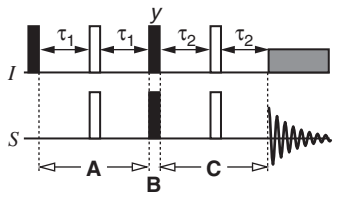

At the end of period **A** it was shown in section 7.10.2 on p. 172 that the state of the spin system is

$$k_I \cos(2\pi J_{IS}\tau_1)\,\hat{I}_y - k_I \sin(2\pi J_{IS}\tau_1)\,\hat{I}_x\hat{S}_z.$$

The purpose of the two 90° pulses in period **B** is to transfer the anti-phase magnetization (the second term) from the I spin to the S spin. This requires the pulse acting on the I spin to cause the transformation $\hat{I}_x \rightarrow \hat{I}_z$, which requires a rotation about the y-axis.

If the initial 90° pulse is about the $-x$-axis, it rotates the equilibrium $k_I\hat{I}_z$ to $k_I\hat{I}_y$. At the end of the spin echo in period **A**, the system is in the following state:

$$-k_I \cos(2\pi J_{IS}\tau_1)\,\hat{I}_y + k_I \sin(2\pi J_{IS}\tau_1)\,2\hat{I}_x\hat{S}_z.$$

As before, the $\hat{I}_y$ term is not affected by the $90°(y)$ pulse on the I spin, and can be discarded. The two pulses affect the ant-phase term as follows:

$$k_I \sin(2\pi J_{IS}\tau_1)\,2\hat{I}_x\hat{S}_z \xrightarrow{(\pi/2)\hat{I}_y} -k_I \sin(2\pi J_{IS}\tau_1)\,2\hat{I}_z\hat{S}_z \xrightarrow{(\pi/2)\hat{S}_x} k_I \sin(2\pi J_{IS}\tau_1)\,2\hat{I}_z\hat{S}_y.$$

This term evolves under coupling during the spin echo in **C** to give:

$$k_I \cos(2\pi J_{IS}\tau_2)\sin(2\pi J_{IS}\tau_1)\,2\hat{I}_z\hat{S}_y - k_I \sin(2\pi J_{IS}\tau_2)\sin(2\pi J_{IS}\tau_1)\,\hat{S}_x,$$

the observable term of which is the one in $\hat{S}_x$.
The $90°(x)$ pulse acting on the S spin during **B** also rotates equilibrium $k_S\hat{S}_z$ to $-k_I\hat{S}_y$, which evolves during the spin echo in **C** to give:

$$-k_S \cos(2\pi J_{IS}\tau_2)\,\hat{S}_y + k_S \sin(2\pi J_{IS}\tau_2)\,2\hat{I}_z\hat{S}_x.$$

This also has an observable term in $\hat{S}_y$. Hence, the two observable terms are combined to give:

$$-k_S \cos(2\pi J_{IS}\tau_2)\,\hat{S}_y - k_I \sin(2\pi J_{IS}\tau_2)\sin(2\pi J_{IS}\tau_1)\,\hat{S}_x.$$

The first term is unaffected by changing the phase of the I spin 90° pulse from x to $-x$, whereas the second term changes sign.

7.13

- By definition, $\hat{I}_+$ has coherence order +1.
- $\hat{I}_z$ is unaffected by a z-rotation, so has coherence order zero.
- $\hat{I}_-$ has coherence order −1, again by definition.
- Using the definitions of $\hat{I}_{1+}$ and $\hat{I}_{1-}$ (Eq. 7.28 on p. 178) as applied to spin one:

  $$\begin{aligned}\hat{I}_{1+} &\equiv \hat{I}_{1x} + \mathrm{i}\,\hat{I}_{1y}\\ \hat{I}_{1-} &\equiv \hat{I}_{1x} - \mathrm{i}\,\hat{I}_{1y},\end{aligned}$$

  we can write $\hat{I}_{1x}$ as:

  $$\hat{I}_{1x} \equiv \tfrac{1}{2}\left(\hat{I}_{1+} + \hat{I}_{1-}\right).$$

  Therefore, $\hat{I}_{1x}$ is an equal mixture of coherence orders +1 and −1.
- Similarly, $\hat{I}_{2y}$ can be written as

  $$\hat{I}_{2y} \equiv \tfrac{1}{2\mathrm{i}}\left(\hat{I}_{2+} - \hat{I}_{2-}\right).$$

  Hence, $2\hat{I}_{1z}\hat{I}_{2y}$ can be written as

  $$2\hat{I}_{1z}\hat{I}_{2y} \equiv 2 \times \tfrac{1}{2\mathrm{i}}\hat{I}_{1z}\left(\hat{I}_{2+} - \hat{I}_{2-}\right),$$

  which is an equal mixture of coherence orders +1 and −1, found by summing the coherence orders of spins one and two (spin one has coherence order zero).
- Since both $\hat{I}_{1z}$ and $\hat{I}_{2z}$ have coherence order zero, so does $2\hat{I}_{1z}\hat{I}_{2z}$.
- $2\hat{I}_{1+}\hat{I}_{2-}$ has coherence order zero since the coherence order of spin one is +1 and that of spin two is −1.
- $2\hat{I}_{1x}\hat{I}_{2y}$ can be written as:

  $$\begin{aligned}2\hat{I}_{1x}\hat{I}_{2y} &\equiv 2 \times \tfrac{1}{2}\left(\hat{I}_{1+} + \hat{I}_{1-}\right) \times \tfrac{1}{2\mathrm{i}}\left(\hat{I}_{2+} - \hat{I}_{2-}\right)\\ &\equiv \tfrac{1}{2\mathrm{i}}\left(\hat{I}_{1+}\hat{I}_{2+} - \hat{I}_{1-}\hat{I}_{2-} - \hat{I}_{1+}\hat{I}_{2-} + \hat{I}_{1-}\hat{I}_{2+}\right).\end{aligned}$$

  $2\hat{I}_{1x}\hat{I}_{2y}$ is therefore an equal mixture of coherence orders +2 and −2, double-quantum coherence, and coherence order 0, zero-quantum coherence.

7.14

Using the definitions of $\hat{I}_{i\pm}$ given by Eq. 7.28 on p. 178, we can write $2\hat{I}_{1x}\hat{I}_{2y}$ as:

$$\begin{aligned} 2\hat{I}_{1x}\hat{I}_{2y} &\equiv 2 \times \tfrac{1}{2}\left(\hat{I}_{1+} + \hat{I}_{1-}\right) \times \tfrac{1}{2\mathrm{i}}\left(\hat{I}_{2+} - \hat{I}_{2-}\right) \\ &\equiv \underbrace{\tfrac{1}{2\mathrm{i}}\left(\hat{I}_{1+}\hat{I}_{2+} - \hat{I}_{1-}\hat{I}_{2-}\right)}_{\text{double-quantum part}} + \underbrace{\tfrac{1}{2\mathrm{i}}\left(\hat{I}_{1-}\hat{I}_{2+} - \hat{I}_{1+}\hat{I}_{2-}\right)}_{\text{zero-quantum part}}. \end{aligned}$$

The other relationships in the table can be verified in the same way.

7.15

The first $90°(x)$ pulse rotates the equilibrium $\hat{I}_{1z}$ to $-\hat{I}_{1y}$. During the spin echo sequence, the offset is refocused, but the coupling evolves throughout. The state of the spin system at the end of the spin echo is

$$\cos(2\pi J_{12}\tau)\,\hat{I}_{1y} - \sin(2\pi J_{12}\tau)\,2\hat{I}_{1x}\hat{I}_{2z}.$$

The final pulse acts to give

$$\cos(2\pi J_{12}\tau)\,\hat{I}_{1z} + \sin(2\pi J_{12}\tau)\,2\hat{I}_{1x}\hat{I}_{2y}.$$

Using the definitions of $\hat{\mathrm{DQ}}_y$ and $\hat{\mathrm{ZQ}}_y$ given in the last table of section 7.12.1 on p. 178, we see that we can rewrite the second term as

$$\tfrac{1}{2}\sin(2\pi J_{12}\tau)\left(\hat{\mathrm{DQ}}_y - \hat{\mathrm{ZQ}}_y\right),$$

which is a mixture of double- and zero-quantum coherence.

The amplitude of this multiple quantum term is a maximum when $\sin(2\pi J_{12}\tau) = 1$, which occurs when $\tau = 1/(4J_{12})$.

Starting with equilibrium magnetization on spin two, $\hat{I}_{2z}$, the terms present after the final pulse are

$$\cos(2\pi J_{12}\tau)\,\hat{I}_{2z} + \sin(2\pi J_{12}\tau)\,2\hat{I}_{1y}\hat{I}_{2x};$$

we have taken the terms from the previous calculation and swapped the labels 1 and 2. Again, from the definitions of $\hat{\mathrm{DQ}}_y$ and $\hat{\mathrm{ZQ}}_y$ in section 7.12.1 on p. 178, we can write the multiple quantum term as

$$\tfrac{1}{2}\sin(2\pi J_{12}\tau)\left(\hat{\mathrm{DQ}}_y + \hat{\mathrm{ZQ}}_y\right).$$

Therefore, adding this term to the one originating from $\hat{I}_{1z}$, we obtain;

$$\tfrac{1}{2}\sin(2\pi J_{12}\tau)\left(\hat{\mathrm{DQ}}_y - \hat{\mathrm{ZQ}}_y\right) + \tfrac{1}{2}\sin(2\pi J_{12}\tau)\left(\hat{\mathrm{DQ}}_y + \hat{\mathrm{ZQ}}_y\right) = \sin(2\pi J_{12}\tau)\,\hat{\mathrm{DQ}}_y,$$

which is pure double-quantum coherence. It is a rather unusual feature of this sequence that, in a two-spin system, it generates pure double-quantum coherence.

7.16

From the table on p. 180, $\hat{ZQ}_x$ is equal to $\left(2\hat{I}_{1x}\hat{I}_{2x} + 2\hat{I}_{1y}\hat{I}_{2y}\right)$. Zero-quantum coherence between spins one and two does not evolve under the coupling between these two spins, so we need only consider the evolution under offset. Considering first the $2\hat{I}_{1x}\hat{I}_{2x}$ term:

$$2\hat{I}_{1x}\hat{I}_{2x} \xrightarrow{\Omega_1 t\hat{I}_{1z}+\Omega_2 t\hat{I}_{2z}} 2\left[\cos(\Omega_1 t)\,\hat{I}_{1x} + \sin(\Omega_1 t)\,\hat{I}_{1y}\right]\left[\cos(\Omega_2 t)\,\hat{I}_{2x} + \sin(\Omega_2 t)\,\hat{I}_{2y}\right].$$

We will now look at the $2\hat{I}_{1y}\hat{I}_{2y}$ term;

$$2\hat{I}_{1y}\hat{I}_{2y} \xrightarrow{\Omega_1 t\,\hat{I}_{1z}+\Omega_2 t\,\hat{I}_{2z}} 2\left[\cos(\Omega_1 t)\,\hat{I}_{1y} - \sin(\Omega_1 t)\hat{I}_{1x}\right]\left[\cos(\Omega_2 t)\,\hat{I}_{2y} - \sin(\Omega_2 t)\,\hat{I}_{2x}\right].$$

Collecting these terms together, we obtain:

$$\begin{aligned}&[\cos(\Omega_1 t)\cos(\Omega_2 t) + \sin(\Omega_1 t)\sin(\Omega_2 t)]\,(2\hat{I}_{1x}\hat{I}_{2x} + 2\hat{I}_{1y}\hat{I}_{2y})\\ +\,&[\sin(\Omega_1 t)\cos(\Omega_2 t) - \cos(\Omega_1 t)\sin(\Omega_2 t)]\,(2\hat{I}_{1y}\hat{I}_{2x} - 2\hat{I}_{1x}\hat{I}_{2y}).\end{aligned}$$

Using the identities:

$$\begin{aligned}\cos(A-B) &= \cos A\cos B + \sin A\sin B\\ \sin(A-B) &= \sin A\cos B - \cos A\sin B,\end{aligned}$$

and the definitions of $\hat{ZQ}_x$ and $\hat{ZQ}_y$:

$$\hat{ZQ}_x \equiv (2\hat{I}_{1x}\hat{I}_{2x} + 2\hat{I}_{1y}\hat{I}_{2y}) \qquad \hat{ZQ}_y \equiv (2\hat{I}_{1y}\hat{I}_{2x} - 2\hat{I}_{1x}\hat{I}_{2y}),$$

we obtain

$$\cos\left([\Omega_1 - \Omega_2]t\right)\,\hat{ZQ}_x + \sin\left([\Omega_1 - \Omega_2]t\right)\,\hat{ZQ}_y.$$

Chapter 8

Two-dimensional NMR

8.1

In each example, the preparation period is highlighted with a grey box, and the mixing period with a grey box with a dashed border.

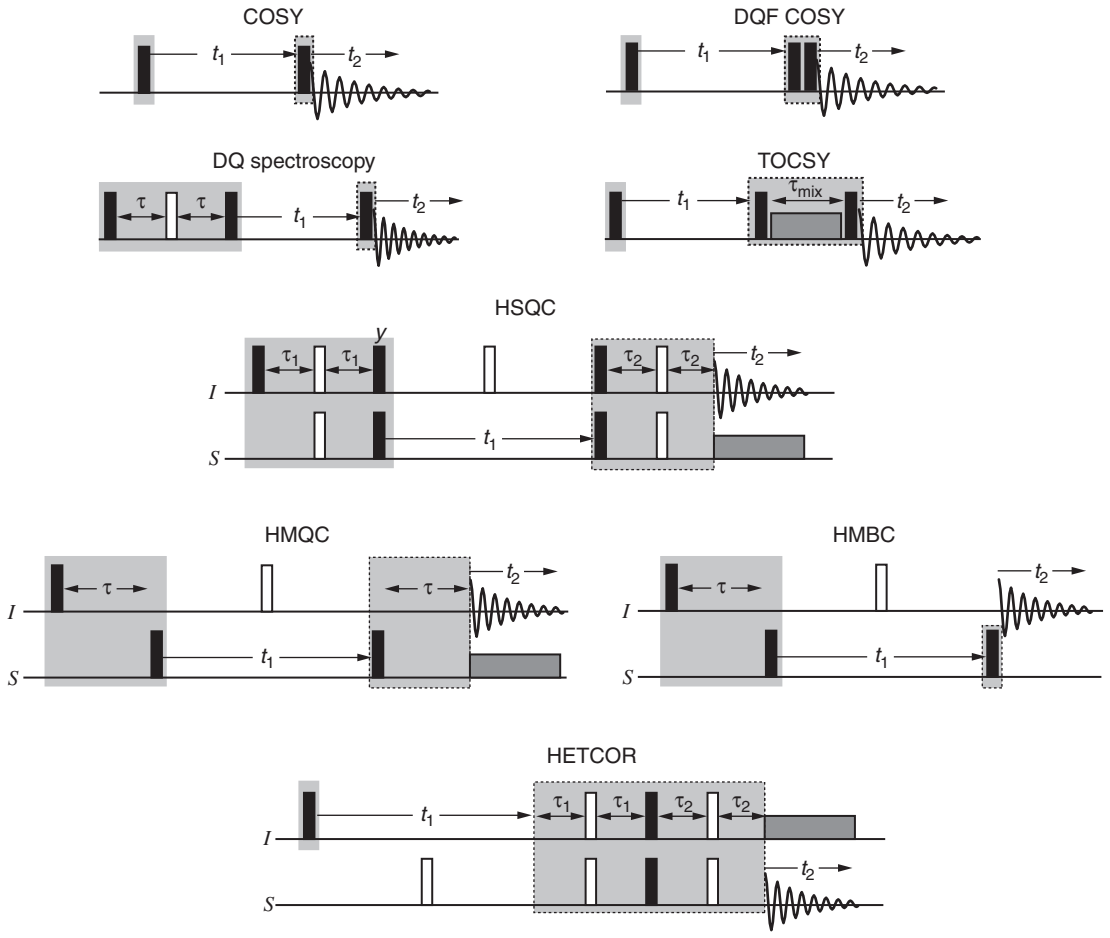

8.2

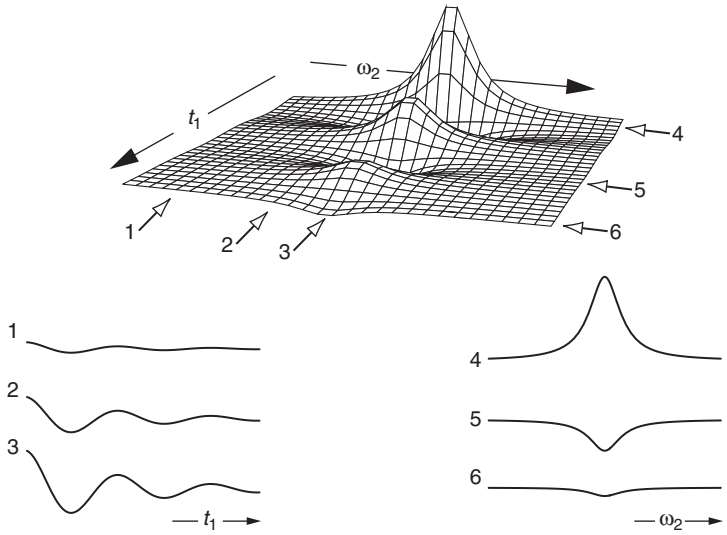

1, 2 and 3 are cross-sections of the damped cosine wave, whose amplitude provides the modulation in t_1. The period is the same for each wave, and the amplitude increases as we approach the centre of the peak in ω_2.
4, 5 and 6 are cross-sections through the ω_2 dimension. The amplitude and sign of the peak is modulated by a damped cosine wave in t_1.

8.3

The COSY pulse sequence is given in Fig. 8.8 on p. 195.

Starting with equilibrium magnetization on spin two, the state of the system at $t_2 = 0$ can be determined from terms [1]–[4] on p. 195 by swapping the spin labels 1 and 2. The result is:

$$-\cos(\pi J_{12}t_1)\cos(\Omega_2 t_1)\,\hat{I}_{2z} \quad [1]$$

$$-\sin(\pi J_{12}t_1)\cos(\Omega_2 t_1)\,2\hat{I}_{1y}\hat{I}_{2x} \quad [2]$$

$$+\cos(\pi J_{12}t_1)\sin(\Omega_2 t_1)\,\hat{I}_{2x} \quad [3]$$

$$-\sin(\pi J_{12}t_1)\sin(\Omega_2 t_1)\,2\hat{I}_{1y}\hat{I}_{2z}. \quad [4]$$

The observable terms are [3] and [4]. The operator in term [3] is $\hat{I}_{2x}$, which will give rise to a doublet on spin two in the ω_2 dimension. It is modulated in t_1 by $\sin(\Omega_2 t_1)$ i.e. at the offset of spin two. Thus, [3] produces a diagonal-peak multiplet.

The operator in term [4] is $2\hat{I}_{1y}\hat{I}_{2z}$; this gives rise to an anti-phase doublet centred at the offset of spin one in the ω_2 dimension. It is also modulated in t_1 by $\sin(\Omega_2 t_1)$. Therefore, it produces a cross-peak multiplet.

It was shown in section 7.5.2 on p. 158 that the evolution of $2\hat{I}_{1y}\hat{I}_{2z}$ during t_2 gives rise to the following time domain signal:

$$\tfrac{1}{2}\mathrm{i}\exp(\mathrm{i}[\Omega_1 + \pi J_{12}]t_2) - \tfrac{1}{2}\mathrm{i}\exp(\mathrm{i}[\Omega_1 - \pi J_{12}]t_2).$$

Imposing an exponential decay on this signal and Fourier transforming, we obtain the following spectrum

$$\tfrac{1}{2}\mathrm{i}\left[A_2(\Omega_1 + \pi J_{12}) + \mathrm{i}D_2(\Omega_1 + \pi J_{12})\right] - \tfrac{1}{2}\mathrm{i}\left[A_2(\Omega_1 - \pi J_{12}) + \mathrm{i}D_2(\Omega_1 - \pi J_{12})\right].$$

To ensure that the absorption mode lineshape appears in the real part of the spectrum, we multiply the expression above by a $-90°$ phase correction factor i.e. by $\exp(-\mathrm{i}\,\pi/2)$. Noting that $\exp(-\mathrm{i}\,\pi/2) \equiv -\mathrm{i}$, we obtain:

$$\tfrac{1}{2}\left[A_2(\Omega_1 + \pi J_{12}) + \mathrm{i}D_2(\Omega_1 + \pi J_{12})\right] - \tfrac{1}{2}\left[A_2(\Omega_1 - \pi J_{12}) + \mathrm{i}D_2(\Omega_1 - \pi J_{12})\right].$$

Clearly this is an anti-phase doublet on spin one.
The t_1 modulation of term [4] has the form $-\sin(\pi J_{12}t_1)\sin(\Omega_2 t_1)$. Applying the identity

$$\sin A \sin B \equiv \tfrac{1}{2}\left[\cos(A - B) - \cos(A + B)\right],$$

gives

$$\tfrac{1}{2}\left[\cos(\Omega_2 + \pi J_{12})t_1 - \cos(\Omega_2 - \pi J_{12})t_1\right].$$

Imposing an exponential decay and taking the cosine Fourier transform yields the spectrum

$$\tfrac{1}{2}\left[A_1(\Omega_2 + \pi J_{12}) - A_1(\Omega_2 - \pi J_{12})\right].$$

This is clearly an anti-phase doublet on spin two.
Multiplying the ω_1 and ω_2 spectra together, and taking the real part, gives the following four lines which form the cross-peak multiplet. Note that they form an anti-phase square array.

$$\begin{aligned}
&+ \tfrac{1}{4}A_1(\Omega_2 + \pi J_{12})A_2(\Omega_1 + \pi J_{12}) - \tfrac{1}{4}A_1(\Omega_2 + \pi J_{12})A_2(\Omega_1 - \pi J_{12}) \\
&- \tfrac{1}{4}A_1(\Omega_2 - \pi J_{12})A_2(\Omega_1 + \pi J_{12}) + \tfrac{1}{4}A_1(\Omega_2 - \pi J_{12})A_2(\Omega_1 - \pi J_{12}).
\end{aligned}$$

The operator in the diagonal peak term [3] is $\hat{I}_{2x}$. Evolution of this operator during t_2 gives the following time domain signal:

$$\tfrac{1}{2}\exp(\mathrm{i}[\Omega_2 + \pi J_{12}]t_2) + \tfrac{1}{2}\exp(\mathrm{i}[\Omega_2 - \pi J_{12}]t_2).$$

Imposing an exponential decay to this, and Fourier transforming gives the spectrum

$$\tfrac{1}{2}\left[A_2(\Omega_2 + \pi J_{12}) + \mathrm{i}D_2(\Omega_2 + \pi J_{12})\right] + \tfrac{1}{2}\left[A_2(\Omega_2 - \pi J_{12}) + \mathrm{i}D_2(\Omega_2 - \pi J_{12})\right].$$

This is an in-phase doublet on spin two.
The t_1 modulation is:

$$\cos(\pi J_{12}t_1)\sin(\Omega_2 t_1) \equiv \tfrac{1}{2}\left[\sin(\Omega_2 + \pi J_{12})t_1 + \sin(\Omega_2 - \pi J_{12})t_1\right],$$

where we have used the identity

$$\sin A \sin B \equiv \tfrac{1}{2}\left[\sin(A+B) + \sin(A-B)\right].$$

Assuming an exponential decay and applying a sine Fourier transform gives the spectrum:

$$\tfrac{1}{2}\left[A_1(\Omega_2 + \pi J_{12}) + A_1(\Omega_2 - \pi J_{12})\right].$$

This is an in-phase doublet on spin two.
Multiplying together the ω_1 and ω_2 parts of the spectrum and taking the real part yields the following four components of the diagonal-peak multiplet. Note that they all have the same sign.

$$+ \tfrac{1}{4}A_1(\Omega_2 + \pi J_{12})A_2(\Omega_2 + \pi J_{12}) + \tfrac{1}{4}A_1(\Omega_2 + \pi J_{12})A_2(\Omega_2 - \pi J_{12})$$
$$+ \tfrac{1}{4}A_1(\Omega_2 - \pi J_{12})A_2(\Omega_2 + \pi J_{12}) + \tfrac{1}{4}A_1(\Omega_2 - \pi J_{12})A_2(\Omega_2 - \pi J_{12}).$$

8.4

The DQF COSY pulse sequence is given in Fig. 8.15 on p. 205.

Starting with equilibrium magnetization on spin two, $\hat{I}_{2z}$, the state of the spin system after the second pulse is exactly the same as for the COSY experiment at $t_2 = 0$ as calculated in Exercise 8.3. Of the four terms present, the only one that contains double-quantum coherence is [2]:

$$-\sin(\pi J_{12} t_1)\cos(\Omega_2 t_1)\, 2\hat{I}_{1y}\hat{I}_{2x}.$$

In section 7.12.1 on p. 178, it was shown that $2\hat{I}_{1y}\hat{I}_{2x}$ is a mixture of double- and zero-quantum coherence. The double-quantum operator $\mathrm{D\hat{Q}}_y$, and the zero-quantum operator $\mathrm{Z\hat{Q}}_y$, are defined as:

$$\mathrm{D\hat{Q}}_y \equiv 2\hat{I}_{1x}\hat{I}_{2y} + 2\hat{I}_{1y}\hat{I}_{2x} \qquad \mathrm{Z\hat{Q}}_y \equiv 2\hat{I}_{1y}\hat{I}_{2x} - 2\hat{I}_{1x}\hat{I}_{2y}.$$

Hence,

$$2\hat{I}_{1y}\hat{I}_{2x} = \tfrac{1}{2}\left(\mathrm{D\hat{Q}}_y + \mathrm{Z\hat{Q}}_y\right).$$

The double-quantum part that is retained is therefore:

$$-\tfrac{1}{2}\sin(\pi J_{12} t_1)\cos(\Omega_2 t_1)\,\mathrm{D\hat{Q}}_y = -\tfrac{1}{2}\sin(\pi J_{12} t_1)\cos(\Omega_2 t_1)\left(2\hat{I}_{1x}\hat{I}_{2y} + 2\hat{I}_{1y}\hat{I}_{2x}\right).$$

The third 90° pulse acts to give:

$$-\tfrac{1}{2}\sin(\pi J_{12} t_1)\cos(\Omega_2 t_1)\left(2\hat{I}_{1x}\hat{I}_{2z} + 2\hat{I}_{1z}\hat{I}_{2x}\right).$$

$2\hat{I}_{1x}\hat{I}_{2z}$ and $2\hat{I}_{1z}\hat{I}_{2x}$ represent anti-phase magnetization on spins one and two, respectively. Both are modulated in t_1 at Ω_2, so the first term therefore gives the cross-peak multiplet, and the second the diagonal-peak multiplet.

Expanding the t_1 modulation, we obtain

$$-\tfrac{1}{2}\sin(\pi J_{12}t_1)\cos(\Omega_2 t_1) \equiv -\tfrac{1}{4}\left[\sin(\Omega_2 + \pi J_{12})t_1 - \sin(\Omega_2 - \pi J_{12})t_1\right],$$

which is an anti-phase doublet on spin two. Hence, both the cross- and diagonal-peak multiplets are anti-phase in both dimensions. Furthermore, both terms have the same t_1 modulation, and both appear along the x-axis at the start of acquisition, so the spectrum can be phased so that all the peaks appear in the double absorption mode.

8.5

The pulse sequence is given in Fig. 8.19 on p. 209.

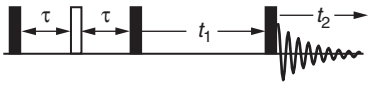

The first 90° pulse rotates equilibrium $\hat{I}_{1z}$ to $-\hat{I}_{1y}$, which then evolves under coupling during the spin echo (the offset is refocused) to give

$$\cos(2\pi J_{12}\tau)\,\hat{I}_{1y} - \sin(2\pi J_{12}\tau)\,2\hat{I}_{1x}\hat{I}_{2z}.$$

This is rotated by the second 90° pulse to give

$$\cos(2\pi J_{12}\tau)\,\hat{I}_{1z} + \sin(2\pi J_{12}\tau)\,2\hat{I}_{1x}\hat{I}_{2y}.$$

We select just zero-quantum coherence at this point. From the table on p. 180, the zero-quantum part of $2\hat{I}_{1x}\hat{I}_{2y}$ is $-\frac{1}{2}\hat{\mathrm{ZQ}}_y$, so at the start of t_1 we have:

$$-\tfrac{1}{2}\sin(2\pi J_{12}\tau)\,\hat{\mathrm{ZQ}}_y.$$

This evolves during t_1 according to the rules in section 7.12.3 on p. 180:

$$-\tfrac{1}{2}\sin(2\pi J_{12}\tau)\,\hat{\mathrm{ZQ}}_y \xrightarrow{\Omega_1 t_1 \hat{I}_{1z} + \Omega_2 t_1 \hat{I}_{2z}} -\tfrac{1}{2}\cos([\Omega_1 - \Omega_2]t_1)\sin(2\pi J_{12}\tau)\,\hat{\mathrm{ZQ}}_y + \tfrac{1}{2}\sin([\Omega_1 - \Omega_2]t_1)\sin(2\pi J_{12}\tau)\,\hat{\mathrm{ZQ}}_x,$$

where

$$\hat{\mathrm{ZQ}}_x \equiv 2\hat{I}_{1x}\hat{I}_{2x} + 2\hat{I}_{1y}\hat{I}_{2y} \qquad \hat{\mathrm{ZQ}}_y \equiv 2\hat{I}_{1y}\hat{I}_{2x} - 2\hat{I}_{1x}\hat{I}_{2y}.$$

Note that the zero-quantum coherence between spins one and two does not evolve due to the coupling between these two spins.
The final pulse rotates the zero-quantum terms to give

$$-\tfrac{1}{2}\sin(2\pi J_{12}\tau)\cos([\Omega_1 - \Omega_2]t_1)\left(2\hat{I}_{1z}\hat{I}_{2x} - 2\hat{I}_{1x}\hat{I}_{2z}\right) + \tfrac{1}{2}\sin(2\pi J_{12}\tau)\sin([\Omega_1 - \Omega_2]t_1)\left(2\hat{I}_{1x}\hat{I}_{2x} + 2\hat{I}_{1z}\hat{I}_{2z}\right),$$

the observable terms of which are:

$$\tfrac{1}{2}\sin(2\pi J_{12}\tau)\cos([\Omega_1 - \Omega_2]t_1)\left(2\hat{I}_{1x}\hat{I}_{2z} - 2\hat{I}_{1z}\hat{I}_{2x}\right).$$

The spectrum has the same form as the double-quantum spectrum shown in Fig. 8.20 on p. 210 with the following differences:

- In ω_2 the anti-phase doublet on spin two, which arises from the $2\hat{I}_{1z}\hat{I}_{2x}$ term, appears with the opposite sign.
- The frequency of the peaks in ω_1 is $(\Omega_1 - \Omega_2)$ i.e. the zero-quantum frequency.

The information that can be gained from this spectrum is the same as for the double-quantum spectrum.

8.6

From section 8.8 on p. 214, the terms present after the first spin echo are

$$\cos(2\pi J_{IS}\tau_1)\hat{I}_y - \sin(2\pi J_{IS}\tau_1)2\hat{I}_x\hat{S}_z.$$

The subsequent 90° pulses are required to transfer the anti-phase magnetization (the second term) to the S spin, so that it can evolve under the offset of the S spin during t_1. This requires the I spin pulse to rotate $\hat{I}_x$ to $\hat{I}_z$, which is only possible if the pulse is about y.

Applying the I spin pulse about $-y$ gives:

$$-\sin(2\pi J_{IS}\tau_1)\,2\hat{I}_x\hat{S}_z \xrightarrow{(-\pi/2)\hat{I}_y} -\sin(2\pi J_{IS}\tau_1)\,2\hat{I}_z\hat{S}_z \xrightarrow{(\pi/2)\hat{S}_x} \sin(2\pi J_{IS}\tau_1)\,2\hat{I}_z\hat{S}_y.$$

The $2\hat{I}_z\hat{S}_y$ term, present at the start of t_1, simply changes sign when the I spin pulse is changed in phase from $+y$ to $-y$.

8.7

The pulse sequence is given in Fig. 8.23(a).

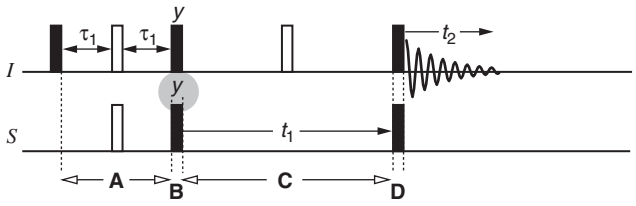

The state of the spin system after the spin echo (**A**) is, from section 8.8 on p. 214:

$$\cos(2\pi J_{IS}\tau_1)\,\hat{I}_y - \sin(2\pi J_{IS}\tau_1)\,2\hat{I}_x\hat{S}_z.$$

The pulses during period **B** have the following effect on the anti-phase term:

$$-\sin(2\pi J_{IS}\tau_1)2\hat{I}_x\hat{S}_z \xrightarrow{(\pi/2)(\hat{I}_y+\hat{S}_y)} \sin(2\pi J_{IS}\tau_1)\,2\hat{I}_z\hat{S}_x.$$

Period **C** is a spin echo, during which the coupling is refocused, but the offset of the S spin evolves for time t_1. At the end of this period, the terms are:

$$-\cos(\Omega_S t_1)\sin(2\pi J_{IS}\tau_1)\,2\hat{I}_z\hat{S}_x - \sin(\Omega_S t_1)\sin(2\pi J_{IS}\tau_1)\,2\hat{I}_z\hat{S}_y.$$

The final two pulses (period **D**) produce the following state at $t_2 = 0$:

$$\cos(\Omega_S t_1)\sin(2\pi J_{IS}\tau_1)\,2\hat{I}_y\hat{S}_x + \sin(\Omega_S t_1)\sin(2\pi J_{IS}\tau_1)\,2\hat{I}_y\hat{S}_z.$$

The observable signal is due to the $2\hat{I}_y\hat{S}_z$ term, and is now modulated in t_1 according to $\sin(\Omega_S t_1)$. So, shifting the phase of the first 90° pulse to the S spin from x to y does indeed alter the modulation in t_1 from cosine to sine.

8.8

The pulse sequence is given in Fig. 8.25 (a) on p. 218. We will now modify it so that the first 90° S spin pulse is about $-x$.

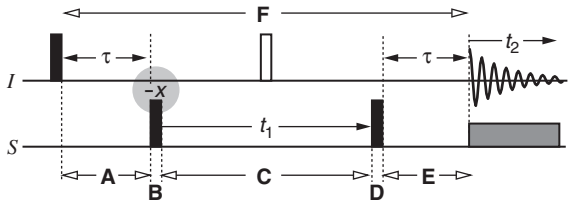

As argued in section 8.9 on p. 217, the offset of the I spin is refocused over the whole of period **F**. The first pulse creates $-\hat{I}_y$, which evolves during period **A** under coupling to give

$$-\cos(\pi J_{IS}\tau)\,\hat{I}_y + \sin(\pi J_{IS}\tau)\,2\hat{I}_x\hat{S}_z.$$

Taking just the second term (the first does not produce any useful peaks), and applying to it the first S spin pulse (with phase $-x$) gives:

$$\sin(\pi J_{IS}\tau)\,2\hat{I}_x\hat{S}_y,$$

which is of opposite sign to the corresponding term in section 8.9 on p. 217. This sign change propagates throughout the rest of the calculation so that the observable term

$$\sin^2(\pi J_{IS}\tau)\cos(\Omega_S t_1)\hat{I}_y,$$

also has the opposite sign. The same result is produced on changing the phase of the second 90° S spin pulse to $-x$.

I spins that are not coupled to S spins do not give rise to anti-phase magnetization, and so are not affected by the S spin pulses. This I spin magnetization is therefore unaffected by altering the phase of the first S spin pulse. So, recording two spectra, the first with the first S spin pulse about x, and the second with it about $-x$, and then subtracting one from the other will retain the wanted signal and eliminate the unwanted signal.

8.9

It was shown in section 8.9 on p. 217 that the observable term at the start of acquisition is

$$-\sin^2(\pi J_{IS}\tau)\cos(\Omega_S t_1)\,\hat{I}_y.$$

The amplitude of the signal is given by $\sin^2(\pi J_{IS}\tau)$, which has a maximum value of 1. This occurs when the argument of the sine is an odd multiple of $\pi/2$ i.e. when $\pi J_{IS}\tau = n\pi/2,\ n = 1,\ 3,\ 5,\ldots$ Hence, $\tau = n/(2J_{IS}),\ n = 1,\ 3,\ 5,\ldots$

$\sin^2(\pi J_{IS}\tau) = 0$ when $\pi J_{IS}\tau = n\pi/2,\ n = 0,\ 2,\ 4,\ldots$ i.e. is an even multiple of $\pi/2$. Hence the amplitude will be zero when $\tau = n/(2J_{IS}),\ n = 0,\ 2,\ 4,\ldots$

8.10

The HSQC pulse sequence, without decoupling during acquisition, is shown in Fig. 8.23 (b) on p. 215.

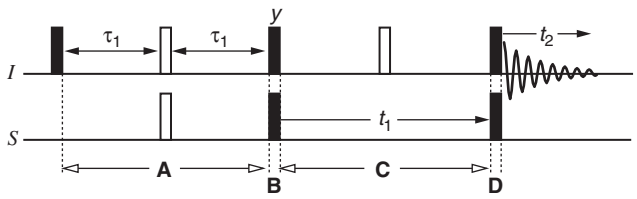

At the start of acquisition, the observable terms are:

$$-\cos(2\pi J_{IS}\tau_2)\sin(2\pi J_{IS}\tau_1)\cos(\Omega_S t_1)\,2\hat{I}_y\hat{S}_z$$
$$+\sin(2\pi J_{IS}\tau_2)\sin(2\pi J_{IS}\tau_1)\cos(\Omega_S t_1)\,\hat{I}_x.$$

The modifications for detecting long-range correlation are essentially the same as those discussed for the HMQC experiment in section 8.9 on p. 217. They are:

- Increase the length of the delay τ_1 so that $\sin(2\pi J_{IS}\tau_1)$ is significant for typical values of the long-range coupling constants.
- Acquire immediately after the final transfer pulses **D**, thus avoiding loss of signal due to relaxation during the final spin echo **E**, as in sequence (b) of Fig. 8.23.
- Acquire without broadband decoupling, as the wanted term is anti-phase with respect to J_{IS}.

8.11

The diagonal peak is

$$A_{1\to1}\cos(\pi J_{IS}t_1)\cos(\Omega_1 t_1)\hat{I}_{1y}.$$

It was shown in section 7.5.1 on p. 157 that evolution of $\hat{I}_{1y}$ during t_2 gives the following time-domain signal:

$$\tfrac{1}{2}\mathrm{i}\exp(\mathrm{i}[\Omega_1+\pi J_{12}]t_2)+\tfrac{1}{2}\mathrm{i}\exp(\mathrm{i}[\Omega_1-\pi J_{12}]t_2).$$

Imposing an exponential decay and Fourier transforming yields the following spectrum:

$$\tfrac{1}{2}\mathrm{i}\left[A_2(\Omega_1+\pi J_{12})+\mathrm{i}D_2(\Omega_1+\pi J_{12})\right]+\tfrac{1}{2}\mathrm{i}\left[A_2(\Omega_1-\pi J_{12})+\mathrm{i}D_2(\Omega_1-\pi J_{12})\right].$$

Applying a $-90°$ phase correction and taking the real part, we obtain an in-phase doublet on spin one:

$$\tfrac{1}{2}A_2(\Omega_1+\pi J_{12})+\tfrac{1}{2}A_2(\Omega_1-\pi J_{12}).$$

The modulation with respect to t_1 is $A_{1\to1}\cos(\pi J_{IS}t_1)\cos(\Omega_1 t_1)$, which can be expanded using the identity

$$\cos A\cos B\equiv\tfrac{1}{2}\left[\cos(A+B)+\cos(A-B)\right],$$

to give

$$\tfrac{1}{2}A_{1\to1}\left[\cos(\Omega_1+\pi J_{IS})t_2+\cos(\Omega_1-\pi J_{IS})t_2\right].$$

Imposing an exponential decay, and then taking the cosine Fourier transform gives:

$$\tfrac{1}{2}A_{1\to1}\left[A_1(\Omega_1+\pi J_{12})+A_1(\Omega_1-\pi J_{12})\right],$$

which is an in-phase doublet in ω_1.
Multiplying the spectra in the ω_1 and ω_2 dimensions together gives the following four peaks for the diagonal-peak multiplet:

$$\begin{aligned}&+\tfrac{1}{4}A_{1\to1}A_1(\Omega_1+\pi J_{12})A_2(\Omega_1+\pi J_{12})+\tfrac{1}{4}A_{1\to1}A_1(\Omega_1+\pi J_{12})A_2(\Omega_1-\pi J_{12})\\&+\tfrac{1}{4}A_{1\to1}A_1(\Omega_1-\pi J_{12})A_2(\Omega_1+\pi J_{12})+\tfrac{1}{4}A_{1\to1}A_1(\Omega_1-\pi J_{12})A_2(\Omega_1-\pi J_{12}).\end{aligned}$$

All the peaks are positive and in the absorption mode.

The cross peak term

$$A_{1\to2}\cos(\pi J_{IS}t_1)\cos(\Omega_1 t_1)\hat{I}_{2y}$$

has the same modulation in t_1 as the diagonal peak, and in t_2 the operator is $\hat{I}_{2y}$, rather than $\hat{I}_{1y}$, so in ω_2 the doublet appears at Ω_2. We can simply write down the four peaks which contribute to the cross-peak multiplet as:

$$\begin{aligned}&+\tfrac{1}{4}A_{1\to2}A_1(\Omega_1+\pi J_{12})A_2(\Omega_2+\pi J_{12})+\tfrac{1}{4}A_{1\to2}A_1(\Omega_1+\pi J_{12})A_2(\Omega_2-\pi J_{12})\\&+\tfrac{1}{4}A_{1\to2}A_1(\Omega_1-\pi J_{12})A_2(\Omega_2+\pi J_{12})+\tfrac{1}{4}A_{1\to2}A_1(\Omega_1-\pi J_{12})A_2(\Omega_2-\pi J_{12}).\end{aligned}$$

Again, these are in the absorption mode, and are all positive.

8.12

The phase-twist lineshape is

$$S(\omega_1, \omega_2) = \underbrace{[A_1(\Omega_A)A_2(\Omega_B) - D_1(\Omega_A)D_2(\Omega_B)]}_{\text{real}} + \mathrm{i}\,\underbrace{[A_1(\Omega_A)D_2(\Omega_B) + D_1(\Omega_A)A_2(\Omega_B)]}_{\text{imaginary}}.$$

The plot shows the imaginary part.

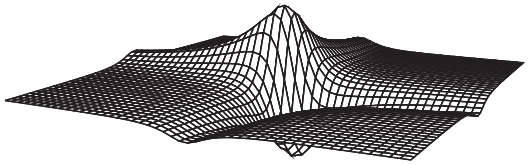

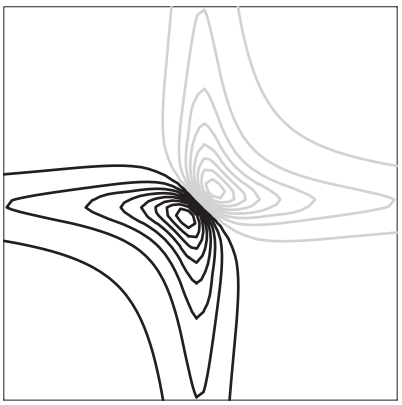

8.13

The observable signal, acquired with broadband decoupling, is

$$\sin(2\pi J_{IS}\tau_2)\cos(\Omega_S t_1)\sin(2\pi J_{IS}\tau_1)\,\hat{I}_x.$$

(a) Applying the SHR method to the HSQC sequence requires the acquisition of two time-domain signals: one with $\cos(\Omega_S t_1)$ modulation in t_1, the second with $\sin(\Omega_S t_1)$ modulation in t_1. It was shown in section 8.13.1 on p. 232 that the modulation can be changed from cosine to sine by shifting the phase of the first 90° S spin pulse by 90°.

(b) For TPPI, each time t_1 is incremented, the phase of the first 90° pulse on the S spin must be incremented by 90°.

8.14

In order to obtain a sine modulated data set from

$$\cos([\Omega_1 + \Omega_2]t_1 + 2\phi),$$

we need to set $2\phi = -\pi/2$ i.e. $\phi = -\pi/4$. To show this explicitly, we expand the argument of the cosine using the identity

$$\cos(A - B) \equiv \cos A \cos B + \sin A \sin B,$$

hence

$$\begin{aligned} \cos([\Omega_1 + \Omega_2]t_1 - \pi/2) &\equiv \cos([\Omega_1 + \Omega_2]t_1)\cos(\pi/2) + \sin([\Omega_1 + \Omega_2]t_1)\sin(\pi/2) \\ &\equiv \sin([\Omega_1 + \Omega_2]t_1), \end{aligned}$$

where we have used $\cos(\pi/2) = 0$ and $\sin(\pi/2) = 1$. So, shifting the phase by $-\pi/4$ alters the modulation from cosine to sine. Thus, to implement TPPI, each time we increment t_1 the phases of the pulses preceding t_1 are incremented by $-45°$.

Chapter 9

Relaxation and the NOE

9.1

The equilibrium populations of the α and β levels are given by Eq. 9.6 on p. 264:

$$n_\alpha^0 = \tfrac{1}{2}N\exp(-E_\alpha/k_\mathrm{B}T) \qquad n_\beta^0 = \tfrac{1}{2}N\exp(-E_\beta/k_\mathrm{B}T),$$

where

$$E_\alpha = -\tfrac{1}{2}\hbar\gamma B_0 \qquad E_\beta = +\tfrac{1}{2}\hbar\gamma B_0.$$

Evaluating the energies yields:

$$\begin{aligned} E_\alpha &= -\tfrac{1}{2}\times 1.055\times 10^{-34}\times 2.675\times 10^{8}\times 9.4 = -1.326\times 10^{-25}\ \mathrm{J}, \\ E_\beta &= +1.326\times 10^{-25}\ \mathrm{J}. \end{aligned}$$

Hence, at 298 K, the populations are:

$$\begin{aligned} n_\alpha^0 &= \tfrac{1}{2}\times 10^{13}\times\exp(1.326\times 10^{-25}/(1.381\times 10^{-23}\times 298)) \\ &= \boxed{5.00016\times 10^{12}}, \\ n_\beta^0 &= \tfrac{1}{2}\times 10^{13}\times\exp(-1.326\times 10^{-25}/(1.381\times 10^{-23}\times 298)) \\ &= \boxed{4.99984\times 10^{12}}. \end{aligned}$$

On account of the very small energy gap, these populations are very similar, although as expected $n_\alpha^0 > n_\beta^0$.

The energy of the system is given by

$$\begin{aligned} E &= n_\alpha E_\alpha + n_\beta E_\beta \\ &= \tfrac{1}{2}\hbar\gamma B_0\left(n_\beta - n_\alpha\right). \end{aligned}$$

Initially, $n_\alpha = n_\beta$, so $E_\mathrm{initial} = 0$. At equilibrium,

$$\begin{aligned} E_\mathrm{equ.} &= 1.326\times 10^{-25}\times(4.99984\times 10^{12} - 5.00016\times 10^{12}) \\ &= -4.243\times 10^{-17}\ \mathrm{J}. \end{aligned}$$

The total change in energy is therefore

$$\Delta E = E_\mathrm{equ.} - E_\mathrm{initial} = \boxed{-4.243\times 10^{-17}\ \mathrm{J}}.$$

The thermal energy of N molecules is of the order

$$Nk_{\mathrm{B}}T = 10^{13} \times 1.381 \times 10^{-23} \times 298 = \boxed{4.115 \times 10^{-8}\ \mathrm{J}},$$

which is nine orders of magnitude greater than the value of ΔE calculated above. This reinforces the point that the energy of interaction between the spins and the magnetic field is minuscule compared to the thermal energy.

9.2

The reduced spectral density function is given by Eq. 9.4 on p. 262

$$j(\omega) = \frac{2\tau_{\mathrm{c}}}{1 + \omega^2\tau_{\mathrm{c}}^2}.$$

For a fixed frequency ω, the maximum value of $j(\omega)$ occurs at a value of τ_{c} given by

$$\frac{\mathrm{d}\, j(\omega)}{\mathrm{d}\tau_{\mathrm{c}}} = 0.$$

Using the product rule, we obtain:

$$\begin{aligned}
\frac{\mathrm{d}}{\mathrm{d}\tau_{\mathrm{c}}} j(\omega) &= \frac{2}{1 + \omega^2\tau_{\mathrm{c}}^2} - \frac{4\omega^2\tau_{\mathrm{c}}^2}{\left(1 + \omega^2\tau_{\mathrm{c}}^2\right)^2} \\
&= \frac{2 + 2\omega^2\tau_{\mathrm{c}}^2 - 4\omega^2\tau_{\mathrm{c}}^2}{\left(1 + \omega^2\tau_{\mathrm{c}}^2\right)^2} \\
&= \frac{2\left(1 - \omega^2\tau_{\mathrm{c}}^2\right)}{\left(1 + \omega^2\tau_{\mathrm{c}}^2\right)^2}.
\end{aligned}$$

The denominator is always non-zero, so the above expression can be solved by setting the numerator to zero:

$$\begin{aligned}
2\left(1 - \omega^2\tau_{\mathrm{c}}^2\right) &= 0 \\
\tau_{\mathrm{c}} &= \frac{1}{\omega}
\end{aligned}$$

Since the rate constant for longitudinal relaxation depends on $j(\omega_0)$, the above result indicates that this rate constant has its maximum value when $\tau_{\mathrm{c}} = 1/\omega_0$.

9.3

At equilibrium, the lower state (α) must have a greater population than the upper state (β), as predicted by the Boltzmann distribution (assuming that the gyromagnetic ratio is positive). Suppose we start with equal populations of the α and β states. The only way in which the population of the α state can increase relative to that of the β state is for the *rate* of transitions from β to α to exceed the *rate* from α to β. As the populations are equal, this implies that the *rate constant* for the transition from β to α must be greater than that for the transition from α to β.

9.4

In the inversion–recovery experiment, the peak height $S(\tau)$ is given by

$$S(\tau) = S(0)\left[2\exp(-R_z\tau) - 1\right],$$

where $S(0)$ is the peak height at time zero. Rearranging this, we get:

$$\ln\left(\frac{S(\tau) + S(0)}{2S(0)}\right) = -R_z\tau,$$

from which we can see that a plot of $\ln[(S(\tau) + S(0))/(2S(0))]$ against τ will be a straight line of gradient $-R_z = -1/T_1$.

τ / s	0.0	0.1	0.5	0.9	1.3	1.7	2.1	2.9
$S(\tau)$	−129.7	−93.4	7.6	62.6	93.4	109.5	118.9	126.4
$\ln[(S(\tau) + S(0))/(2S(0))]$	0.000	−0.151	−0.754	−1.353	−1.968	−2.554	−3.179	−4.370

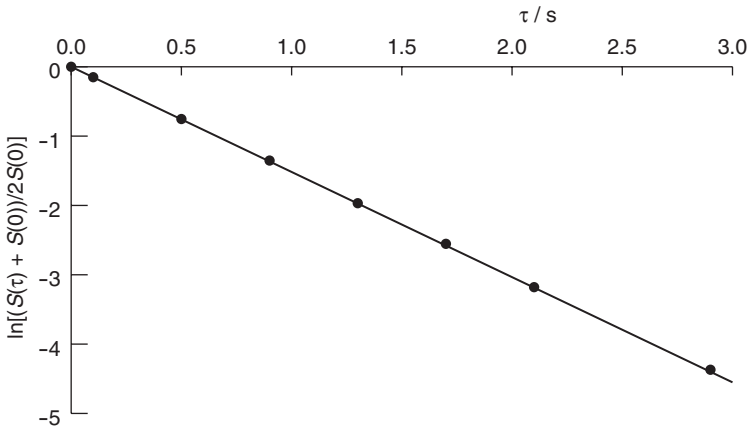

The gradient is $-1.508\ \text{s}^{-1}$, so $R_z = 1.508\ \text{s}^{-1}$ and $T_1 = \boxed{0.663\ \text{s}}$.

9.5

In section 9.5.2 on p. 271, it was shown that an estimate for T_1 is given by $\tau_{\text{null}}/\ln 2$. The values of T_1 are therefore:

τ_{null} / s	0.5	0.6	0.8
T_1 / s	0.72	0.87	1.15

The fact that the solvent was still inverted after a delay of 1.5 s shows that it has a T_1 value that is greater than $1.5/\ln 2 = 2.16$ s i.e. the solvent relaxes at a slower rate than the other spins.

9.6

The z-magnetization relaxes according to Eq. 9.15 on p. 269:

$$M_z(t) = \left(M_z(0) - M_z^0\right)\exp(-R_z t) + M_z^0.$$

Setting $M_z(0) = 0$ and $t = \tau$, we obtain

$$M_z(\tau) = M_z^0\left[1 - \exp(-R_z\tau)\right].$$

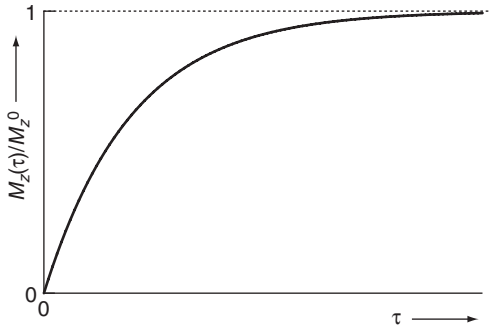

The peak height $S(\tau)$ is proportional to the z-magnetization present just before the 90° pulse. Thus, $S(\tau)$ can be written as

$$S(\tau) = c\left[1 - \exp(-R_z\tau)\right].$$

Letting $\tau \to \infty$, $S_\infty = c$; this will be the height of the peak in a simple 90°–acquire experiment. Substituting this into the above equation gives

$$S(\tau) = S_\infty\left[1 - \exp(-R_z\tau)\right].$$

Rearranging this yields:

$$\begin{aligned}
S(\tau) &= S_\infty\left[1 - \exp(-R_z\tau)\right] \\
\frac{S(\tau)}{S_\infty} &= 1 - \exp(-R_z\tau) \\
\frac{S_\infty - S(\tau)}{S_\infty} &= \exp(-R_z\tau) \\
\ln\left(\frac{S_\infty - S(\tau)}{S_\infty}\right) &= -R_z\tau,
\end{aligned}$$

where we have taken the natural logarithm to go to the last line. Hence, a plot of $\ln[(S_\infty - S(\tau))/S_\infty]$ against τ gives a straight line of gradient $-R_z$.

9.7

Assuming that the rate is proportional to the deviation from the equilibrium population, we can write the rate of change of the population of level 1 (using the labelling in Fig. 9.17 on p. 273) as

$$\frac{\mathrm{d}n_1}{\mathrm{d}t} = \underbrace{-W_1^{(2,\alpha)}\left(n_1 - n_1^0\right) - W_1^{(1,\alpha)}\left(n_1 - n_1^0\right) - W_2\left(n_1 - n_1^0\right)}_{\text{loss from level 1}}$$
$$\underbrace{+W_1^{(2,\alpha)}\left(n_2 - n_2^0\right)}_{\text{gain from level 2}}\underbrace{+W_1^{(1,\alpha)}\left(n_3 - n_3^0\right)}_{\text{gain from level 3}}\underbrace{+W_2\left(n_4 - n_4^0\right)}_{\text{gain from level 4}}.$$

Similarly, the rates of change of the populations of the other levels are:

$$\frac{\mathrm{d}n_2}{\mathrm{d}t} = \underbrace{-W_1^{(2,\alpha)}\left(n_2 - n_2^0\right) - W_0\left(n_2 - n_2^0\right) - W_1^{(1,\beta)}\left(n_2 - n_2^0\right)}_{\text{loss from level 2}}$$
$$\underbrace{+W_1^{(2,\alpha)}\left(n_1 - n_1^0\right)}_{\text{gain from level 1}}\underbrace{+W_0\left(n_3 - n_3^0\right)}_{\text{gain from level 3}}\underbrace{+W_1^{(1,\beta)}\left(n_4 - n_4^0\right)}_{\text{gain from level 4}}.$$

$$\frac{\mathrm{d}n_3}{\mathrm{d}t} = \underbrace{-W_1^{(1,\alpha)}\left(n_3 - n_3^0\right) - W_0\left(n_3 - n_3^0\right) - W_1^{(2,\beta)}\left(n_3 - n_3^0\right)}_{\text{loss from level 3}}$$
$$\underbrace{+W_1^{(1,\alpha)}\left(n_1 - n_1^0\right)}_{\text{gain from level 1}}\underbrace{+W_0\left(n_2 - n_2^0\right)}_{\text{gain from level 2}}\underbrace{+W_1^{(2,\beta)}\left(n_4 - n_4^0\right)}_{\text{gain from level 4}}.$$

$$\frac{\mathrm{d}n_4}{\mathrm{d}t} = \underbrace{-W_2\left(n_4 - n_4^0\right) - W_1^{(1,\beta)}\left(n_4 - n_4^0\right) - W_1^{(2,\beta)}\left(n_4 - n_4^0\right)}_{\text{loss from level 4}}$$
$$\underbrace{+W_2\left(n_1 - n_1^0\right)}_{\text{gain from level 1}}\underbrace{+W_1^{(1,\beta)}\left(n_2 - n_2^0\right)}_{\text{gain from level 2}}\underbrace{+W_1^{(2,\beta)}\left(n_3 - n_3^0\right)}_{\text{gain from level 3}}.$$

9.8

(a) The expression for b is (from section 9.6.3 on p. 277)

$$b = \frac{\mu_0\gamma_\mathrm{H}^2\hbar}{4\pi r^3} = \frac{4\pi \times 10^{-7} \times (2.675 \times 10^8)^2 \times 1.055 \times 10^{-34}}{4\pi \times (1.8 \times 10^{-10})^3} = 1.294 \times 10^5\ \mathrm{s}^{-1}.$$

Hence, $b^2 = \boxed{1.675 \times 10^{10}\ \mathrm{s}^{-2}}$.

(b) The expressions for the transition rate constants are given in section 9.6.3 on p. 277:

$$W_1^{(1)} = \tfrac{3}{40} b^2 j(\omega_{0,1}) \qquad W_1^{(2)} = \tfrac{3}{40} b^2 j(\omega_{0,2})$$
$$W_2 = \tfrac{3}{10} b^2 j(\omega_{0,1} + \omega_{0,2}) \qquad W_0 = \tfrac{1}{20} b^2 j(\omega_{0,1} - \omega_{0,2}).$$

In the fast motion limit, $j(\omega) = 2\tau_c$ for all frequencies ω, so the rate constants have the following numerical values:

$$\begin{aligned}
W_1^{(1)} = \tfrac{3}{20} b^2 \tau_c &= \tfrac{3}{20} \times 1.675 \times 10^{10} \times 20 \times 10^{-12} = \boxed{0.0503 \text{ s}^{-1}}, \\
W_1^{(2)} = \tfrac{3}{20} b^2 \tau_c &= \tfrac{3}{20} \times 1.675 \times 10^{10} \times 20 \times 10^{-12} = \boxed{0.0503 \text{ s}^{-1}}, \\
W_2 = \tfrac{3}{5} b^2 \tau_c &= \tfrac{3}{5} \times 1.675 \times 10^{10} \times 20 \times 10^{-12} = \boxed{0.201 \text{ s}^{-1}}, \\
W_0 = \tfrac{1}{10} b^2 \tau_c &= \tfrac{1}{10} \times 1.675 \times 10^{10} \times 20 \times 10^{-12} = \boxed{0.0335 \text{ s}^{-1}}.
\end{aligned}$$

From Eq. 9.19 on p. 277:

$$\begin{aligned}
R_z^{(1)} &= 2W_1^{(1)} + W_2 + W_0 = (2 \times 0.0503) + 0.201 + 0.0335 = \boxed{0.335 \text{ s}^{-1}}, \\
R_z^{(2)} &= 2W_1^{(2)} + W_2 + W_0 = (2 \times 0.0503) + 0.201 + 0.0335 = \boxed{0.335 \text{ s}^{-1}}, \\
\sigma_{12} &= W_2 - W_0 = 0.201 - 0.0335 = \boxed{0.168 \text{ s}^{-1}}.
\end{aligned}$$

(c) Substituting $j(\omega) = 2\tau_c$ for all values of ω in Eq. 9.20 on p. 278, we obtain:

$$\begin{aligned}
R_z^{(1)} &= b^2 \left[\tfrac{3}{20} j(\omega_{0,1}) + \tfrac{3}{10} j(\omega_{0,1} + \omega_{0,2}) + \tfrac{1}{20} j(\omega_{0,1} - \omega_{0,2}) \right] \\
&= b^2 \tau_c \\
&= 1.675 \times 10^{10} \times 20 \times 10^{-12} \\
&= \boxed{0.335 \text{ s}^{-1}}.
\end{aligned}$$

Similarly, $R_z^{(2)} = \boxed{0.335 \text{ s}^{-1}}$, and $\sigma_{12} = \boxed{0.168 \text{ s}^{-1}}$.

(d) The value of $R_{xy}^{(1)}$ can be calculated from the expression in section 9.8.3 on p. 295:

$$\begin{aligned}
R_{xy}^{(1)} &= b^2 \left[\tfrac{1}{10} j(0) + \tfrac{3}{20} j(\omega_{0,2}) + \tfrac{3}{40} j(\omega_{0,1}) + \tfrac{3}{20} j(\omega_{0,1} + \omega_{0,2}) + \tfrac{1}{40} j(\omega_{0,1} - \omega_{0,2}) \right] \\
&= b^2 \tau_c \\
&= 1.675 \times 10^{10} \times 20 \times 10^{-12} \\
&= \boxed{0.335 \text{ s}^{-1}}.
\end{aligned}$$

To go to the second line, we set $j(\omega) = 2\tau_c$. Similarly, $R_{xy}^{(2)} = \boxed{0.335 \text{ s}^{-1}}$.

(e) As expected in the fast motion limit, the rate constants for the self-relaxation of both longitudinal and transverse magnetization have the same value. The rate constant for the cross-relaxation of longitudinal magnetization has half the value of the self-relaxation rate constant and is positive, again as expected.

(f) The Larmor frequency is:

$$\omega_0 = 2\pi \times 500 \times 10^6 = 3.140 \times 10^9 \text{ rad s}^{-1}.$$

From the expression for the reduced spectral density,

$$j(\omega) = \frac{2\tau_c}{1 + \omega^2\tau_c^2},$$

we can calculate the values of $j(\omega_0)$, $j(2\omega_0)$ and $j(0)$:

$$\begin{aligned} j(\omega_0) &= \frac{2\tau_c}{1 + \omega_0^2\tau_c^2} = \frac{2 \times 500 \times 10^{-12}}{1 + (3.140 \times 10^9 \times 500 \times 10^{-12})^2} = 2.88 \times 10^{-10} \text{ s}, \\ j(2\omega_0) &= 9.20 \times 10^{-11} \text{ s}, \\ j(0) &= 1.00 \times 10^{-9} \text{ s}. \end{aligned}$$

The values of $R_z^{(1)}$, $R_z^{(2)}$ and σ_{12} can be calculated by substituting $\omega_{0,1} = \omega_{0,2} = \omega_0$ into Eq. 9.20 on p. 278, giving $R_z^{(1)} = R_z^{(2)} = \boxed{2.025 \text{ s}^{-1}}$, and $\sigma_{12} = \boxed{-0.375 \text{ s}^{-1}}$. Similarly, from section 9.8.3 on p. 295, $R_{xy}^{(1)} = R_{xy}^{(2)} = \boxed{3.41 \text{ s}^{-1}}$.

(g) As $\omega_0\tau_c = 1.6$, we are now outside the fast motion limit, and beyond the zero-crossing point where $\sigma_{12} = 0$. As a result, σ_{12} is negative and the rate constant for transverse relaxation exceeds that for longitudinal relaxation. We are not very far beyond $\omega_0\tau_c = 1$, so the rate of longitudinal relaxation is significantly faster than for $\tau_c = 20$ ps.

9.9

For a ^{13}C–^{1}H pair, the value of b is:

$$\begin{aligned} b = \frac{\mu_0\gamma_C\gamma_H\hbar}{4\pi r^3} &= \frac{4\pi \times 10^{-7} \times 6.728 \times 10^7 \times 2.675 \times 10^8 \times 1.055 \times 10^{-34}}{4\pi \times (1.1 \times 10^{-10})^3} \\ &= 1.427 \times 10^5 \text{ s}^{-1}. \end{aligned}$$

Hence, $b^2 = 2.035 \times 10^{10}$ s^{-2}.
In the fast motion limit ($\tau_c = 20$ ps), the values of the rate constants can be calculated from those in the previous question by multiplying by the ratio of the b^2 values. Note that we can only do this because $j(\omega)$ is independent of τ_c in this limit. So,

$$\begin{aligned} R_z^{(1)}\left(^{13}\text{C}–^{1}\text{H}\right) &= \left(\frac{b_{\text{C–H}}^2}{b_{\text{H–H}}^2}\right) R_z^{(1)}\left(^{1}\text{H}–^{1}\text{H}\right) \\ &= \frac{2.035 \times 10^{10}}{1.675 \times 10^{10}} \times 0.335 \\ &= \boxed{0.407 \text{ s}^{-1}}. \end{aligned}$$

Similarly, $R_z^{(2)} = \boxed{0.407 \text{ s}^{-1}}$, $\sigma_{12} = \boxed{0.204 \text{ s}^{-1}}$, and $R_{xy}^{(1)} = R_{xy}^{(2)} = \boxed{0.407 \text{ s}^{-1}}$. All these values are greater than for the ^{1}H–^{1}H pair due to the smaller separation between the ^{13}C and ^{1}H. γ_C is a quarter the value of γ_H, so for the same distance we would expect the relaxation to be sixteen times slower. However, the rate constant goes as $1/r^6$, which changes by a factor of 19.2 on going from $r = 1.8$ Å to $r = 1.1$ Å.

9.10

The necessary equations are given in section 9.10.2 on p. 304. At $B_0 = 4.7$ T, c^2 is given by:

$$\begin{aligned} c^2 &= [\gamma B_0 (\sigma_{\parallel} - \sigma_{\perp})]^2 \\ &= \left[6.728 \times 10^7 \times 4.7 \times 100 \times 10^{-6}\right]^2 \\ &= \boxed{1.00 \times 10^9 \text{ s}^{-2}}, \end{aligned}$$

where we have used the gyromagnetic ratio of ^{13}C. In the fast motion limit, $j(\omega) = 2\tau_c$ for all values of ω, so the rate constants are:

$$\begin{aligned} R_z &= c^2 \tfrac{1}{15} j(\omega_0) \\ &= c^2 \tfrac{2}{15} \tau_c \\ &= 1.00 \times 10^9 \times \tfrac{2}{15} \times 20 \times 10^{-12} \\ &= \boxed{0.00267 \text{ s}^{-1}}, \end{aligned}$$

$$\begin{aligned} R_{xy} &= c^2 \left[\tfrac{2}{45} j(0) + \tfrac{1}{30} j(\omega_0)\right] \\ &= c^2 \tfrac{7}{45} \tau_c \\ &= 1.00 \times 10^9 \times \tfrac{7}{45} \times 20 \times 10^{-12} \\ &= \boxed{0.00311 \text{ s}^{-1}}. \end{aligned}$$

At $B_0 = 11.74$ T, the rate constants are greater by a factor of $(11.74/4, 7)^2$:

$$\begin{aligned} c^2 &= \frac{11.74^2}{4.7^2} \times 1.00 \times 10^9 = \boxed{6.24 \times 10^9 \text{ s}^{-2}}, \\ R_z &= \frac{11.74^2}{4.7^2} \times 0.00267 = \boxed{0.0167 \text{ s}^{-1}}, \\ R_{xy} &= \frac{11.74^2}{4.7^2} \times 0.00311 = \boxed{0.0194 \text{ s}^{-1}}. \end{aligned}$$

The values of the CSA relaxation rate constants at $B_0 = 11.74$ T are an order of magnitude smaller than those for dipolar relaxation of ^{13}C due to an attached ^{1}H. However, as the CSA contribution goes as B_0^2 it will become more significant at higher fields.

9.11

The formulae are as for the previous question. For $B_0 = 4.7$ T,

$$\begin{aligned} c^2 &= [\gamma B_0 (\sigma_{\parallel} - \sigma_{\perp})]^2 \\ &= \left[2.675 \times 10^8 \times 4.7 \times 10 \times 10^{-6}\right]^2 \\ &= \boxed{1.581 \times 10^8 \text{ s}^{-2}}. \end{aligned}$$

Hence,

$$\begin{aligned} R_z &= c^2 \tfrac{1}{15} j(\omega_0) \\ &= c^2 \tfrac{2}{15} \tau_c \\ &= 1.581 \times 10^8 \times \tfrac{2}{15} \times 20 \times 10^{-12} \\ &= \boxed{0.00042 \text{ s}^{-1}}, \end{aligned}$$

$$\begin{aligned} R_{xy} &= c^2 \left[\tfrac{2}{45} j(0) + \tfrac{1}{30} j(\omega_0) \right] \\ &= c^2 \tfrac{7}{45} \tau_c \\ &= 1.581 \times 10^8 \times \tfrac{7}{45} \times 20 \times 10^{-12} \\ &= \boxed{0.00049 \text{ s}^{-1}}. \end{aligned}$$

At $B_0 = 11.74$ T, the values are greater by a factor of $(11.74/4.7)^2$: $c^2 = \boxed{9.864 \times 10^8 \text{ s}^{-1}}$, $R_z = \boxed{0.00263 \text{ s}^{-1}}$, and $R_{xy} = \boxed{0.00307 \text{ s}^{-1}}$.

At $B_0 = 23.5$ T, $c^2 = \boxed{3.953 \times 10^9 \text{ s}^{-1}}$, $R_z = \boxed{0.01054 \text{ s}^{-1}}$, and $R_{xy} = \boxed{0.01230 \text{ s}^{-1}}$.
Even at a field of $B_0 = 23.5$ T, the rate constants are still an order of magnitude smaller than the dipolar relaxation rate constants at $B_0 = 11.74$ T.

9.12

We are going to apply the initial rate limit, in which we assume that, on the right hand side of Eq. 9.21 on p. 279,

$$\frac{\mathrm{d}I_{1z}}{\mathrm{d}t} = -R_z^{(1)} \left(I_{1z} - I_{1z}^0 \right) - \sigma_{12} \left(I_{2z} - I_{2z}^0 \right),$$

I_{1z} and I_{2z} have their initial values:

$$\begin{aligned} \left(\frac{\mathrm{d}I_{1z}}{\mathrm{d}t} \right)_{\text{init}} &= -R_z^{(1)} \left(I_{1z}(0) - I_{1z}^0 \right) - \sigma_{12} \left(I_{2z}(0) - I_{2z}^0 \right) \\ &= -R_z^{(1)} \left(I_{1z}^0 - I_{1z}^0 \right) - \sigma_{12} \left(0 - I_{2z}^0 \right) \\ &= \sigma_{12} I_{2z}^0. \end{aligned}$$

Integrating this, we obtain:

$$\begin{aligned} \int \mathrm{d}I_{1z}(t) &= \int \sigma_{12} I_{2z}^0 \, \mathrm{d}t \\ I_{1z}(t) &= \sigma_{12} I_{2z}^0 t + \text{const.} \end{aligned}$$

We know that at time $t = 0$, $I_{1z}(0) = I_{1z}^0$, so the constant of integration is I_{1z}^0. At $t = \tau$:

$$I_{1z}(\tau) = \sigma_{12} I_{2z}^0 \tau + I_{1z}^0.$$

Now we will look at the z-magnetization on spin two in the initial rate limit. Starting from

$$\frac{\mathrm{d}I_{2z}}{\mathrm{d}t} = -R_z^{(2)}\left(I_{2z} - I_{2z}^0\right) - \sigma_{12}\left(I_{1z} - I_{1z}^0\right),$$

we obtain:

$$\begin{aligned}\left(\frac{\mathrm{d}I_{2z}}{\mathrm{d}t}\right)_{\text{init}} &= -R_z^{(2)}\left(I_{2z}(0) - I_{2z}^0\right) - \sigma_{12}\left(I_{1z}(0) - I_{1z}^0\right) \\ &= -R_z^{(2)}\left(0 - I_{2z}^0\right) - \sigma_{12}\left(I_{1z}^0 - I_{1z}^0\right) \\ &= R_z^{(2)} I_{2z}^0.\end{aligned}$$

Integrating this, and noting that $I_{2z}(0) = 0$, we get, at $t = \tau$:

$$I_{2z}^0(\tau) = R_z^{(2)} I_{2z}^0 \tau.$$

The height of the peak due to spin one is proportional to I_{1z}, and the height of that due to spin two is proportional to I_{2z}. Furthermore, both spins are of the same type, so $I_{1z}^0 = I_{2z}^0$. The peak heights for the irradiated, reference and difference spectra are:

spectrum	$S_1(\tau)$	$S_2(\tau)$
irradiated: (a)	$c\,(\sigma_{12}\tau + 1)$	$cR_z^{(2)}\tau$
reference: (b)	c	c
NOE difference: (a) − (b)	$c\,\sigma_{12}\tau$	$c\left(R_z^{(2)}\tau - 1\right)$

Note that $|\sigma_{12}|\,\tau \ll 1$ and $R_z^{(2)}\tau \ll 1$ in the initial rate limit.

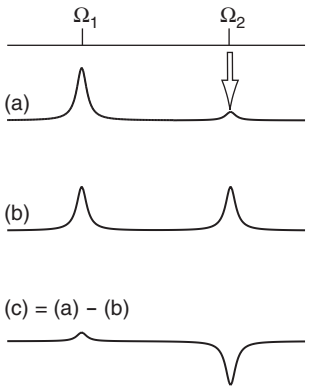

The NOE enhancement is given by:

$$\begin{aligned}\eta &= \frac{\text{peak height in irradiated spectrum} - \text{peak height in reference spectrum}}{\text{peak height in reference spectrum}} \\ &= \frac{c\,(\sigma_{12}\tau + 1) - c}{c} \\ &= \sigma_{12}\tau.\end{aligned}$$

9.13

The NOE difference spectrum is convenient as it only shows the target resonance, and the resonances which are receiving an NOE enhancement.

9.14

(a) The observation that the NOE enhancement depends only upon the cross-relaxation rate constant is a property of the initial rate limit i.e. the assumption that the target peak is still fully inverted after the delay τ. We are effectively ignoring self relaxation during this delay.

(b) At longer times, the inverted spin begins to relax back to equilibrium. This reduces the z-magnetization on that spin and so slows the growth of the NOE: hence the dependence on the self-relaxation rate constant of that spin. The spin receiving the enhancement can also relax, resulting in the NOE enhancement being lost: hence the dependence on its self relaxation rate constant.

(c) Spin one is held saturated throughout the experiment, so its relaxation is of no importance. Cross relaxation gives the rate of transfer of magnetization from spin one to spin two, while self relaxation of spin two leads to a loss of this transferred magnetization. Therefore, there is competition between these two processes, which is reflected in the observation that the enhancement depends upon the ratio of the rate constants for cross and self relaxation.

9.15

In the initial rate limit, the enhancement in a transient NOE experiment depends only upon the cross-relaxation rate constant for the transfer of magnetization between the inverted spin and the spin receiving the enhancement. In this example, σ_{AB} and σ_{BC} will be approximately equal, so when H_B is inverted, the enhancement of H_A and H_C will be the same.
On inverting H_A, the enhancement at H_B still depends only on σ_{AB}, so will be the same as for H_A and H_C when H_B is irradiated. H_C is too far from H_A to receive an enhancement.

In a steady state experiment, the enhancement depends upon the ratio of the cross-relaxation rate constant to the self-relaxation rate constant of the spin receiving the enhancement. R_z^A and R_z^C are equal to each other, so saturation of H_B will give equal enhancements on H_A and H_C.
Irradiation of H_A gives a smaller enhancement on H_B as the self relaxation of this spin is faster than for H_A or H_C. This is because H_B has two nearby protons which relax it, whereas H_A and H_C only have one nearby proton.

9.16

The NOESY pulse sequence is given in Fig. 9.24 on p. 287.

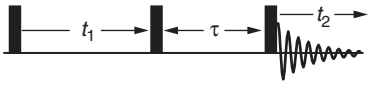

We will start with equilibrium magnetization on spin one, and assume that spins one and two are not coupled. If the phase of the first 90° pulse is $-x$, it rotates equilibrium $\hat{I}_{1z}$ to $\hat{I}_{1y}$. This evolves under the offset during t_1 to give:

$$\hat{I}_{1y} \xrightarrow{\Omega_1 t_1 \hat{I}_{1z} + \Omega_2 t_1 \hat{I}_{2z}} \cos(\Omega_1 t_1)\hat{I}_{1y} - \sin(\Omega_1 t_1)\hat{I}_{1x}.$$

The second 90° pulse acts on the above terms to give:

$$\cos(\Omega_1 t_1)\hat{I}_{1y} - \sin(\Omega_1 t_1)\hat{I}_{1x} \xrightarrow{(\pi/2)(\hat{I}_{1x} + \hat{I}_{2x})} \cos(\Omega_1 t_1)\hat{I}_{1z} - \sin(\Omega_1 t_1)\hat{I}_{1x}.$$

There are also similar terms due to spin two. We select only longitudinal terms after this pulse, so at $\tau = 0$, the z-magnetization on each spin is:

$$I_{1z} = \cos(\Omega_1 t_1)\, I_{1z}^0 \;\text{ and }\; I_{2z} = \cos(\Omega_2 t_1)\, I_{2z}^0.$$

The Solomon equations are (from Eq. 9.26 on p. 287):

$$\begin{aligned}
\frac{\mathrm{d}I_{1z}(t)}{\mathrm{d}t} &= -R_z\left(I_{1z}(t) - I_z^0\right) - \sigma\left(I_{2z}(t) - I_z^0\right) \\
\frac{\mathrm{d}I_{2z}(t)}{\mathrm{d}t} &= -\sigma\left(I_{1z}(t) - I_z^0\right) - R_z\left(I_{2z}(t) - I_z^0\right),
\end{aligned}$$

where we have assumed that $I_{1z}^0 = I_{2z}^0 = I_z^0$. Using the initial rate approximation with the following initial conditions:

$$I_{1z}(0) = \cos(\Omega_1 t_1)\, I_z^0 \;\text{ and }\; I_{2z}(0) = \cos(\Omega_2 t_1)\, I_z^0,$$

we obtain:

$$\begin{aligned}
\left(\frac{\mathrm{d}I_{1z}(t)}{\mathrm{d}t}\right)_{\text{init}} &= -R_z\left[\cos(\Omega_1 t_1) - 1\right] I_z^0 - \sigma\left[\cos(\Omega_2 t_1) - 1\right] I_z^0 \\
\left(\frac{\mathrm{d}I_{2z}(t)}{\mathrm{d}t}\right)_{\text{init}} &= -\sigma\left[\cos(\Omega_1 t_1) - 1\right] I_z^0 - R_z\left[\cos(\Omega_2 t_1) - 1\right] I_z^0.
\end{aligned}$$

Integrating these, and using the initial conditions to determine the values of the constants of integration, we obtain:

$$\begin{aligned}
\frac{I_{1z}(\tau)}{I_z^0} &= \underbrace{\cos(\Omega_1 t_1)\,(1 - R_z\tau)}_{\text{diagonal peak}} - \underbrace{\cos(\Omega_2 t_1)\sigma\tau}_{\text{cross peak}} + \underbrace{(R_z + \sigma)\,\tau}_{\text{axial peak}}, \\
\frac{I_{2z}(\tau)}{I_z^0} &= \underbrace{\cos(\Omega_2 t_1)\,(1 - R_z\tau)}_{\text{diagonal peak}} - \underbrace{\cos(\Omega_1 t_1)\sigma\tau}_{\text{cross peak}} + \underbrace{(R_z + \sigma)\,\tau}_{\text{axial peak}}.
\end{aligned}$$

Comparing these with Eq. 9.28 and Eq. 9.29 on p. 288, we see that the terms which give the diagonal and cross peaks have changed sign, while the axial peak terms have not. The axial peaks can therefore be suppressed by difference spectroscopy: we record two spectra with the phase of the first pulse set to $+x$ and $-x$ in turn, then we subtract one spectrum from the other. The cross and diagonal peaks reinforce, and the axial peaks cancel.

9.17

The Larmor frequency in rad s^{-1} is

$$\omega_0 = 2\pi \times 500 \times 10^6 = 3.142 \times 10^9 \text{ rad s}^{-1}.$$

The value of $\omega_0\tau_c$ is 0.03, which is much less than 1. Therefore, we are working in the fast motion limit, where $j(\omega) = 2\tau_c$ for all frequencies. The rate constant for longitudinal relaxation is given by Eq. 9.31 on p. 293:

$$R_z = \gamma^2 \overline{B_{loc}^2} j(\omega_0),$$

where $R_z = 1/T_1$. Substituting in this, and using the fast motion limit expression for $j(\omega_0)$, we obtain:

$$\begin{aligned}
\frac{1}{T_1} &= 2\gamma^2\tau_c\overline{B_{loc}^2} \\
\overline{B_{loc}^2} &= \frac{1}{2T_1\gamma^2\tau_c} \\
&= \frac{1}{2 \times 1 \times (2.675 \times 10^8)^2 \times 10 \times 10^{-12}} \\
&= \boxed{6.99 \times 10^{-7} \text{ T}^2}.
\end{aligned}$$

This corresponds to a root mean square field of 8.4×10^{-4} T, which is 10^{-4} times smaller than B_0. The local fields are indeed very weak.

9.18

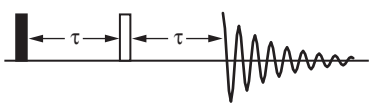

Any effects of inhomogeneous broadening are refocused by the spin echo, so the amplitude of the transverse magnetization present at the start of acquisition depends only upon R_{xy} and the time 2τ. The peak height is therefore given by:

$$\begin{aligned}
S(\tau) &= S_0 \exp(-2R_{xy}\tau) \\
\frac{S(\tau)}{S_0} &= \exp(-2R_{xy}\tau).
\end{aligned}$$

Taking logarithms of both sides gives us

$$\ln\left(\frac{S(\tau)}{S_0}\right) = -2R_{xy}\tau,$$

so a plot of $\ln(S(\tau)/S_0)$ against τ is a straight line of gradient $-2R_{xy}$.

τ / s	0	0.1	0.2	0.3	0.4	0.5	0.6	0.7
$S(\tau)$	65	39.4	23.9	14.5	8.8	5.34	3.24	1.96
$\ln(S(\tau)/S_0)$	0	−0.501	−1.001	−1.500	−2.000	−2.499	−2.999	−3.501

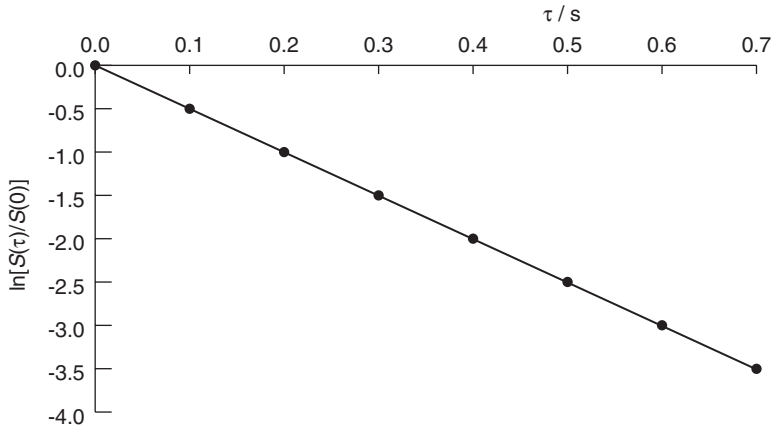

The gradient is $-5.00\ \text{s}^{-1}$, giving $R_{xy} = \boxed{2.50\ \text{s}^{-1}}$, or $T_2 = 0.4$ s.

Chapter 10

Advanced topics in two-dimensional NMR

10.1

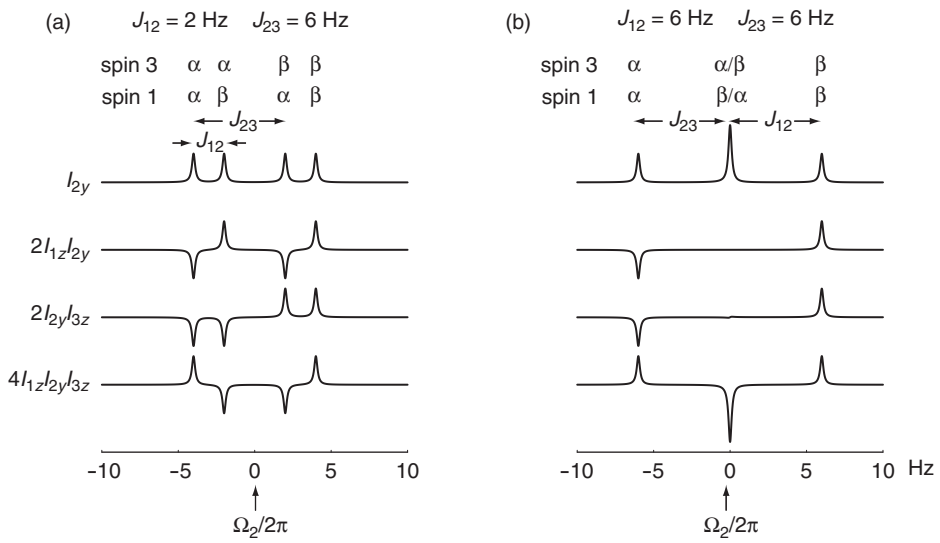

(a) Assuming that the offset of spin two is 0 Hz, the line positions are −4, −2, 2 and 4 Hz.

(b) Assuming that the offset of spin two is 0 Hz, the line positions are −6, 0, 0 and 6 Hz; we have a doublet of doublets, with the central two lines falling on top of one another, giving a triplet.

10.2

We do not need to consider the 1–3 coupling as this does not affect the evolution of a spin-two operator. First, let us consider the evolution due to the 1–2 coupling:

$$\hat{I}_{2y} \xrightarrow{2\pi J_{12} t \hat{I}_{1z}\hat{I}_{2z}} \cos(\pi J_{12} t)\,\hat{I}_{2y} - \sin(\pi J_{12} t)\,2\hat{I}_{1z}\hat{I}_{2x}.$$

We will now consider the effect of the 2–3 coupling separately on each of the terms on the right. For the term in $\hat{I}_{2y}$ the evolution is straightforward:

$$\cos(\pi J_{12} t)\,\hat{I}_{2y} \xrightarrow{2\pi J_{23} t \hat{I}_{2z}\hat{I}_{3z}} \cos(\pi J_{23} t)\cos(\pi J_{12} t)\,\hat{I}_{2y} - \sin(\pi J_{23} t)\cos(\pi J_{12} t)\,2\hat{I}_{2x}\hat{I}_{3z}.$$

For the $-\sin(\pi J_{12} t)\,2\hat{I}_{1z}\hat{I}_{2x}$ term, the factor $-\sin(\pi J_{12} t)\,2\hat{I}_{1z}$ is unaffected by the evolution of the 2–3 coupling: writing this factor as A we have

$$A\,\hat{I}_{2x} \xrightarrow{2\pi J_{23} t \hat{I}_{2z}\hat{I}_{3z}} A\,\cos(\pi J_{23} t)\,\hat{I}_{2x} + A\,\sin(\pi J_{23} t)\,2\hat{I}_{2y}\hat{I}_{3z}.$$

Reinserting the factor A gives

$$-\cos(\pi J_{23} t)\sin(\pi J_{12})\,2\hat{I}_{1z}\hat{I}_{2x} - \sin(\pi J_{23} t)\sin(\pi J_{12} t)\,4\hat{I}_{1z}\hat{I}_{2y}\hat{I}_{3z}.$$

The overall result of the evolution of $\hat{I}_{2y}$ under coupling is summarized in the table:

term	dependence on J_{12}	dependence on J_{23}	axis	description
$\hat{I}_{2y}$	$\cos(\pi J_{12} t)$	$\cos(\pi J_{23} t)$	y	in-phase
$-2\hat{I}_{1z}\hat{I}_{2x}$	$\sin(\pi J_{12} t)$	$\cos(\pi J_{23} t)$	$-x$	anti-phase with respect to J_{12}
$-2\hat{I}_{2x}\hat{I}_{3z}$	$\cos(\pi J_{12} t)$	$\sin(\pi J_{23} t)$	$-x$	anti-phase with respect to J_{23}
$-4\hat{I}_{1z}\hat{I}_{2y}\hat{I}_{3z}$	$\sin(\pi J_{12} t)$	$\sin(\pi J_{23} t)$	$-y$	doubly anti-phase with respect to J_{12} and J_{23}

As expected, going anti-phase with respect to the coupling between spins i and j introduces a factor $\sin(\pi J_{ij} t)$, whereas remaining in-phase with respect to this coupling introduces a factor $\cos(\pi J_{ij} t)$. The in-phase term is along y, singly anti-phase terms are along $-x$, and the doubly anti-phase term is along $-y$ i.e. they follow around in the usual sequence $x \to y \to -x \to -y$.
The corresponding tree diagram is

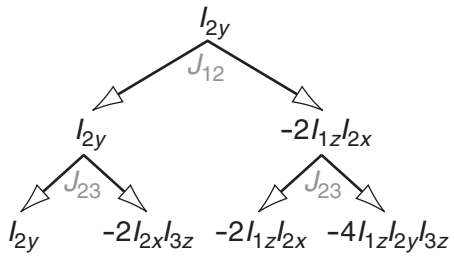

10.3

The trick to getting the signs right is just to think about the usual way in which y evolves into $-x$ and then into $-y$:

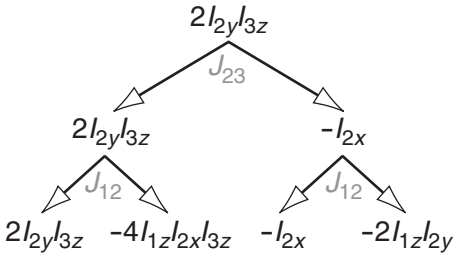

The term $4\hat{I}_{1z}\hat{I}_{2x}\hat{I}_{3z}$ arises from splitting first to the left, giving the coefficient $\cos(\pi J_{23}t)$, and second to the right, giving the coefficient $\sin(\pi J_{12}t)$. Note also that there is a minus sign introduced. So the overall factor multiplying $4\hat{I}_{1z}\hat{I}_{2x}\hat{I}_{3z}$ is $-\cos(\pi J_{23}t)\sin(\pi J_{12}t)$.

10.4

Term [1] is

$$\cos(\pi J_{13}t_1)\cos(\pi J_{12}t_1)\sin(\Omega_1 t_1)\,\hat{I}_{1x}.$$

First, let us consider the modulation in t_1. We use the identity

$$\sin A\cos B \equiv \tfrac{1}{2}\left[\sin(A+B)+\sin(A-B)\right]$$

to combine the terms $\cos(\pi J_{12}t_1)\sin(\Omega_1 t_1)$ to give

$$\tfrac{1}{2}\cos(\pi J_{13}t_1)\left[\sin(\Omega_1 t_1+\pi J_{12}t_1)+\sin(\Omega_1 t_1-\pi J_{12}t_1)\right].$$

Next we multiply out the square brace:

$$\tfrac{1}{2}\cos(\pi J_{13}t_1)\sin(\Omega_1 t_1+\pi J_{12}t_1)+\tfrac{1}{2}\cos(\pi J_{13}t_1)\sin(\Omega_1 t_1-\pi J_{12}t_1). \tag{10.1}$$

Now we combine the two terms $\cos(\pi J_{13}t_1)\sin(\Omega_1 t_1+\pi J_{12}t_1)$ to give

$$\tfrac{1}{2}\sin(\Omega_1 t_1+\pi J_{12}t_1+\pi J_{13}t_1)+\tfrac{1}{2}\sin(\Omega_1 t_1+\pi J_{12}t_1-\pi J_{13}t_1).$$

Doing the same for the two terms $\cos(\pi J_{13}t_1)\sin(\Omega_1 t_1-\pi J_{12}t_1)$ gives

$$\tfrac{1}{2}\sin(\Omega_1 t_1-\pi J_{12}t_1+\pi J_{13}t_1)+\tfrac{1}{2}\sin(\Omega_1 t_1-\pi J_{12}t_1-\pi J_{13}t_1).$$

So overall Eq. 10.1 expands to four terms

$$\begin{aligned}\tfrac{1}{4}\Big[&\sin(\Omega_1 t_1+\pi J_{12}t_1+\pi J_{13}t_1)+\sin(\Omega_1 t_1+\pi J_{12}t_1-\pi J_{13}t_1)\\&+\sin(\Omega_1 t_1-\pi J_{12}t_1+\pi J_{13}t_1)+\sin(\Omega_1 t_1-\pi J_{12}t_1-\pi J_{13}t_1)\Big].\end{aligned}$$

Therefore, what we have in ω_1 is a completely in-phase doublet of doublets on spin one.
In ω_2 the operator is $\hat{I}_{1x}$, which also gives rise to an in-phase doublet of doublets on spin one. 'Multiplying' these two multiplets together in the manner of Fig. 10.6 on p. 325 gives rise to a two-dimensional multiplet consisting of sixteen lines, all with the same sign; this is in contrast to the cross-peak multiplet, which consists of four anti-phase square arrays.
Note, too, that the magnetization which gives rise to the diagonal peak is along x in t_2 and is sine modulated in t_1. This is the complete opposite of the cross peak, which is along y in t_2 and cosine modulated. Thus, as in the COSY of the two-spin system, the diagonal and cross peaks are 90° out of phase with one another in both dimensions.
The reason why the splittings due to J_{12} and J_{13} are in-phase in the ω_1 dimension is that the modulation with respect to these couplings takes the form of a cosine: $\cos(\pi J_{ij} t_1)$.

10.5

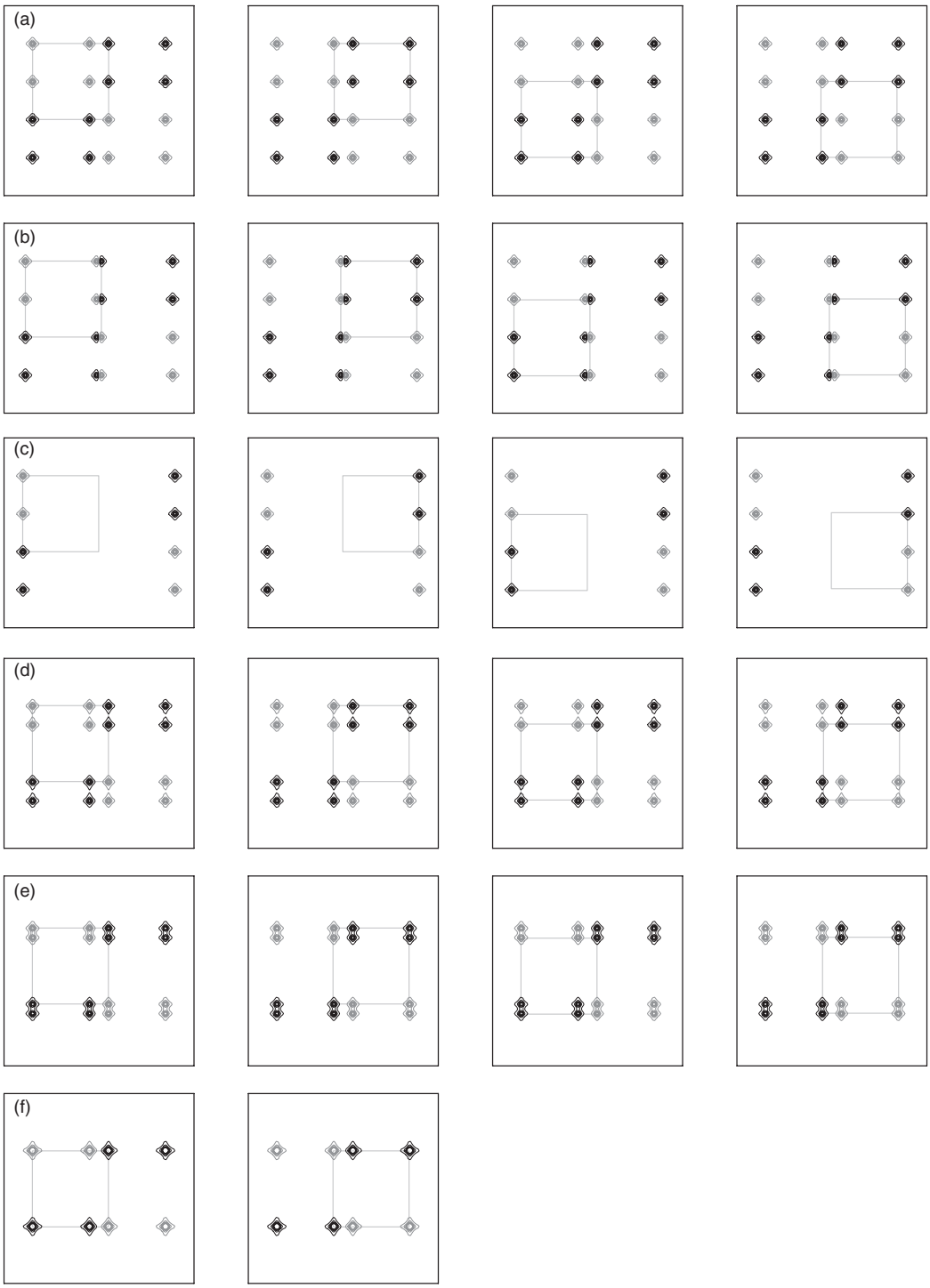

For (f) there are only two anti-phase square arrays.

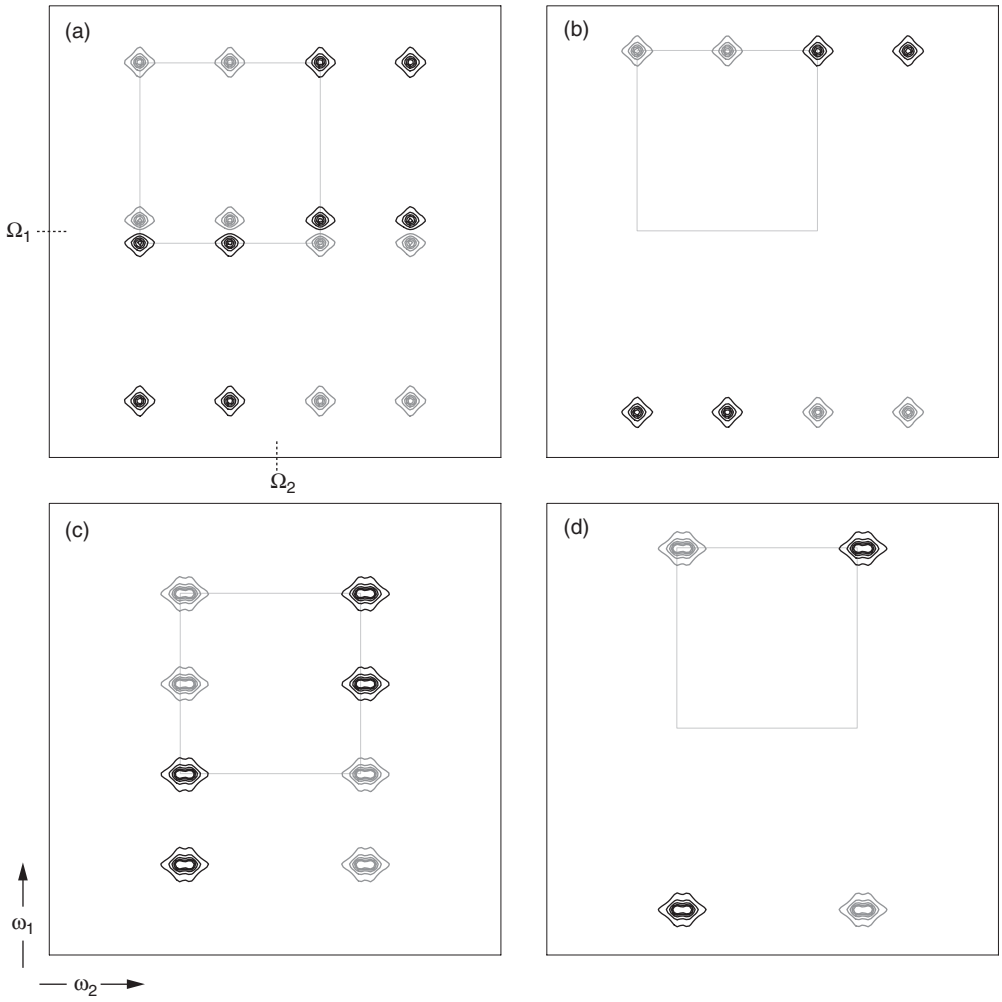

In each case, the region plotted is ±10 Hz from the centre of the cross-peak multiplet; for clarity, only one anti-phase square array is shown. The linewidth is 0.5 Hz in each dimension.

10.6

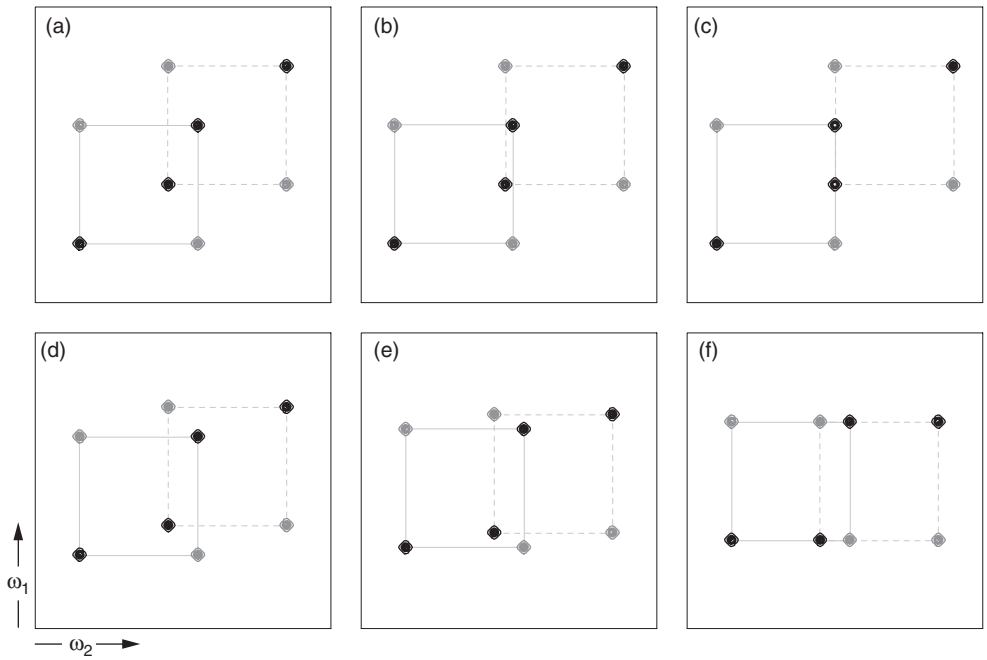

In each case ± 10 Hz is plotted from the centre of the cross-peak multiplet. Note that in (c), where $J_{12} = J_{23}$, the column of peaks down the centre of the cross peak no longer cancel one another out, as four of the peaks are missing from the reduced multiplet.
In the series (a) to (c), J_{23} is increasing, thus increasing the ω_2 separation of the two anti-phase square arrays. In the series (d) to (f), J_{13} is decreasing, thus decreasing the ω_1 separation of the two anti-phase square arrays.

10.7

It is not usually possible to measure a value for the active coupling constant since this appears as an anti-phase splitting. If the positive and negative peaks overlap significantly, the separation between the maxima and minima of the anti-phase peaks is no longer equal to the value of the active coupling constant.
See section 10.3.3 on p. 332 for a description of how, under some circumstances, the values of passive couplings may be determined from reduced multiplets.

10.8

$\hat{I}_{1\alpha}\hat{I}_{2-}\hat{I}_{3\alpha}$: observable magnetization corresponding to the line of the spin-two multiplet which is associated with spin one and spin three both being in the α state.

$\hat{I}_{1\alpha}\hat{I}_{2-}\hat{I}_{3-}$: double-quantum coherence, with $p = -2$, between spins two and three. More specifically, this operator is associated with one of the lines of the double-quantum 'doublet' – see section 3.7.3 on p. 44. This term is not observable.

$\hat{I}_{1\beta}\hat{I}_{2\beta}\hat{I}_{3\beta}$: the population of the $\beta\beta\beta$ energy level. This term is not observable.

$\hat{I}_{1\alpha}\hat{I}_{2\beta}\hat{I}_{3+}$: single-quantum coherence, with $p = +1$, corresponding to the line of the spin-three multiplet which is associated with spin one being in the α state and spin two being in the β state. Although it is single quantum, this term is not observable as only coherence order -1 is observable.

As described in section 10.4.2 on p. 336, free evolution simply gives a phase factor, with the frequency depending on the offset of the spin in question and on the spin states of the passive spins. If the passive spin is in the α state, a term $-\pi J$ is contributed to the frequency, whereas if it is in the β state, a term $+\pi J$ is contributed. The overall sense of the phase factor depends on whether the operator is $\hat{I}_+$ or $\hat{I}_-$.

$$\hat{I}_{1\alpha}\hat{I}_{2-}\hat{I}_{3\alpha} \longrightarrow \exp\left(\mathrm{i}[\Omega_2 - \pi J_{12} - \pi J_{23}]t_1\right)\hat{I}_{1\alpha}\hat{I}_{2-}\hat{I}_{3\alpha}$$

$$\hat{I}_{1\alpha}\hat{I}_{2\beta}\hat{I}_{3+} \longrightarrow \exp\left(-\mathrm{i}[\Omega_3 - \pi J_{13} + \pi J_{23}]t_1\right)\hat{I}_{1\alpha}\hat{I}_{2\beta}\hat{I}_{3+}$$

10.9

During t_1 the term $\hat{I}_{1+}\hat{I}_{2\beta}\hat{I}_{3\alpha}$ acquires a phase factor:

$$\exp\left(-\mathrm{i}[\Omega_1 + \pi J_{12} - \pi J_{13}]t_1\right)\hat{I}_{1+}\hat{I}_{2\beta}\hat{I}_{3\alpha}.$$

The small flip angle pulse causes the following transfers to observable operators on spin two (the coefficients come from Eq. 10.7 on p. 338)

$$\begin{aligned}
\hat{I}_{1+}\hat{I}_{2\beta}\hat{I}_{3\alpha} &\longrightarrow \left(+\tfrac{1}{2}\mathrm{i}\theta\right)\left(+\tfrac{1}{2}\mathrm{i}\theta\right)(1)\,\hat{I}_{1\alpha}\hat{I}_{2-}\hat{I}_{3\alpha}\\
\hat{I}_{1+}\hat{I}_{2\beta}\hat{I}_{3\alpha} &\longrightarrow \left(-\tfrac{1}{2}\mathrm{i}\theta\right)\left(+\tfrac{1}{2}\mathrm{i}\theta\right)(1)\,\hat{I}_{1\beta}\hat{I}_{2-}\hat{I}_{3\alpha}\\
\hat{I}_{1+}\hat{I}_{2\beta}\hat{I}_{3\alpha} &\longrightarrow \left(+\tfrac{1}{2}\mathrm{i}\theta\right)\left(+\tfrac{1}{2}\mathrm{i}\theta\right)\left(\tfrac{1}{4}\theta^2\right)\hat{I}_{1\alpha}\hat{I}_{2-}\hat{I}_{3\beta}\\
\hat{I}_{1+}\hat{I}_{2\beta}\hat{I}_{3\alpha} &\longrightarrow \left(-\tfrac{1}{2}\mathrm{i}\theta\right)\left(+\tfrac{1}{2}\mathrm{i}\theta\right)\left(\tfrac{1}{4}\theta^2\right)\hat{I}_{1\beta}\hat{I}_{2-}\hat{I}_{3\beta}.
\end{aligned}$$

For a small flip angle, we discard the third and fourth terms as these go as θ^4. This leaves

$$\hat{I}_{1+}\hat{I}_{2\beta}\hat{I}_{3\alpha} \longrightarrow -\tfrac{1}{4}\theta^2\,\hat{I}_{1\alpha}\hat{I}_{2-}\hat{I}_{3\alpha} \qquad \hat{I}_{1+}\hat{I}_{2\beta}\hat{I}_{3\alpha} \longrightarrow +\tfrac{1}{4}\theta^2\hat{I}_{1\beta}\hat{I}_{2-}\hat{I}_{3\alpha}. \tag{10.2}$$

These two transfers can be found in the table on p. 340.

Next we consider the behaviour of the term $\hat{I}_{1-}\hat{I}_{2\beta}\hat{I}_{3\alpha}$. For this term the sense of the phase modulation is opposite to that of $\hat{I}_{1+}\hat{I}_{2\beta}\hat{I}_{3\alpha}$:

$$\exp\left(+\mathrm{i}[\Omega_1 + \pi J_{12} - \pi J_{13}]t_1\right)\hat{I}_{1-}\hat{I}_{2\beta}\hat{I}_{3\alpha}.$$

For this term, the transfer $\hat{I}_{1-} \longrightarrow \hat{I}_{1\alpha}$ has associated with it a factor of $(-\frac{1}{2}\mathrm{i}\theta)$, which is the opposite sign to that for the transfer $\hat{I}_{1+} \longrightarrow \hat{I}_{1\alpha}$. So, the cross-peak components arising from $\hat{I}_{1+}\hat{I}_{2\beta}\hat{I}_{3\alpha}$ and $\hat{I}_{1-}\hat{I}_{2\beta}\hat{I}_{3\alpha}$ have opposite signs.

10.10

Starting with $\hat{I}_{1+}\hat{I}_{2\beta}\hat{I}_{3\alpha}$ the first small flip angle pulse creates four possible population terms, which are the ones of interest in ZCOSY, in which spin one is in the α state:

$$\begin{aligned}
\hat{I}_{1+}\hat{I}_{2\beta}\hat{I}_{3\alpha} &\longrightarrow \left(+\tfrac{1}{2}\mathrm{i}\theta\right)(1)\,(1)\,\hat{I}_{1\alpha}\hat{I}_{2\beta}\hat{I}_{3\alpha}\\
\hat{I}_{1+}\hat{I}_{2\beta}\hat{I}_{3\alpha} &\longrightarrow \left(+\tfrac{1}{2}\mathrm{i}\theta\right)\left(\tfrac{1}{4}\theta^2\right)(1)\,\hat{I}_{1\alpha}\hat{I}_{2\alpha}\hat{I}_{3\alpha}\\
\hat{I}_{1+}\hat{I}_{2\beta}\hat{I}_{3\alpha} &\longrightarrow \left(+\tfrac{1}{2}\mathrm{i}\theta\right)(1)\left(\tfrac{1}{4}\theta^2\right)\hat{I}_{1\alpha}\hat{I}_{2\beta}\hat{I}_{3\beta}\\
\hat{I}_{1+}\hat{I}_{2\beta}\hat{I}_{3\alpha} &\longrightarrow \left(+\tfrac{1}{2}\mathrm{i}\theta\right)\left(\tfrac{1}{4}\theta^2\right)\left(\tfrac{1}{4}\theta^2\right)\hat{I}_{1\alpha}\hat{I}_{2\alpha}\hat{I}_{3\beta}.
\end{aligned}$$

Of these four terms, only the first will be significant for the case of a small flip angle.
There are four additional transfers from $\hat{I}_{1+}\hat{I}_{2\beta}\hat{I}_{3\alpha}$ to operators in which spin one is in the β state, but as before only one of these is significant in the small flip angle case:

$$\hat{I}_{1+}\hat{I}_{2\beta}\hat{I}_{3\alpha} \longrightarrow \left(-\tfrac{1}{2}\mathrm{i}\theta\right)(1)\,(1)\,\hat{I}_{1\beta}\hat{I}_{2\beta}\hat{I}_{3\alpha}$$

So, we have just two population terms at this stage:

$$\left(+\tfrac{1}{2}\mathrm{i}\theta\right)\hat{I}_{1\alpha}\hat{I}_{2\beta}\hat{I}_{3\alpha} \qquad \text{and} \qquad \left(-\tfrac{1}{2}\mathrm{i}\theta\right)\hat{I}_{1\beta}\hat{I}_{2\beta}\hat{I}_{3\alpha}.$$

From all that we have done so far we can see that, for small flip angles, the significant contributions that these terms will make to the 1–2 cross peak arise from the transfer $\hat{I}_{2\beta} \longrightarrow \hat{I}_{2-}$, with both of the other operators remaining the same:

$$\begin{aligned}
\left(+\tfrac{1}{2}\mathrm{i}\theta\right)\hat{I}_{1\alpha}\hat{I}_{2\beta}\hat{I}_{3\alpha} &\longrightarrow \left(+\tfrac{1}{2}\mathrm{i}\theta\right)\left(+\tfrac{1}{2}\mathrm{i}\theta\right)\hat{I}_{1\alpha}\hat{I}_{2-}\hat{I}_{3\alpha}\\
\left(-\tfrac{1}{2}\mathrm{i}\theta\right)\hat{I}_{1\beta}\hat{I}_{2\beta}\hat{I}_{3\alpha} &\longrightarrow \left(+\tfrac{1}{2}\mathrm{i}\theta\right)\left(-\tfrac{1}{2}\mathrm{i}\theta\right)\hat{I}_{1\beta}\hat{I}_{2-}\hat{I}_{3\alpha}.
\end{aligned}$$

So the overall transfers from $\hat{I}_{1+}\hat{I}_{2\beta}\hat{I}_{3\alpha}$ caused by the two small flip angles pulses are

$$\begin{aligned}
\hat{I}_{1+}\hat{I}_{2\beta}\hat{I}_{3\alpha} &\longrightarrow -\tfrac{1}{4}\theta^2\hat{I}_{1\alpha}\hat{I}_{2-}\hat{I}_{3\alpha}\\
\hat{I}_{1+}\hat{I}_{2\beta}\hat{I}_{3\alpha} &\longrightarrow +\tfrac{1}{4}\theta^2\hat{I}_{1\beta}\hat{I}_{2-}\hat{I}_{3\alpha}.
\end{aligned}$$

These are exactly the same as found for small flip angle COSY in the previous exercise (see Eq. 10.2 on the previous page).

10.11

From section 10.8.1 on p. 352, we found that at the end of the constant time T the following operators are present:

$$\cos(\Omega_1 t_1)\cos(\pi J_{12}T)\,\hat{I}_{1y} - \sin(\Omega_1 t_1)\cos(\pi J_{12}T)\,\hat{I}_{1x}$$
$$-\cos(\Omega_1 t_1)\sin(\pi J_{12}T)\,2\hat{I}_{1x}\hat{I}_{2z} - \sin(\Omega_1 t_1)\sin(\pi J_{12}T)\,2\hat{I}_{1y}\hat{I}_{2z}.$$

The third of these is rotated by the second 90° pulse to a mixture of double- and zero-quantum coherence:

$$-\cos(\Omega_1 t_1)\sin(\pi J_{12}T)\,2\hat{I}_{1x}\hat{I}_{2z} \xrightarrow{(\pi/2)(\hat{I}_{1x}+\hat{I}_{2x})} +\cos(\Omega_1 t_1)\sin(\pi J_{12}T)\,2\hat{I}_{1x}\hat{I}_{2y}.$$

Following section 7.12.1 on p. 178, the pure double quantum part of $2\hat{I}_{1x}\hat{I}_{2y}$ is $\frac{1}{2}(2\hat{I}_{1x}\hat{I}_{2y} + 2\hat{I}_{1y}\hat{I}_{2x})$, so the double quantum term between the final two pulses is

$$\tfrac{1}{2}\cos(\Omega_1 t_1)\sin(\pi J_{12}T)\,(2\hat{I}_{1x}\hat{I}_{2y} + 2\hat{I}_{1y}\hat{I}_{2x}).$$

The final 90° pulse makes this observable:

$$\tfrac{1}{2}\cos(\Omega_1 t_1)\sin(\pi J_{12}T)\,(2\hat{I}_{1x}\hat{I}_{2y} + 2\hat{I}_{1y}\hat{I}_{2x}) \xrightarrow{(\pi/2)(\hat{I}_{1x}+\hat{I}_{2x})}$$
$$\tfrac{1}{2}\cos(\Omega_1 t_1)\sin(\pi J_{12}T)\,(2\hat{I}_{1x}\hat{I}_{2z} + 2\hat{I}_{1z}\hat{I}_{2x}).$$

The term $\cos(\Omega_1 t_1)\sin(\pi J_{12}T)\,2\hat{I}_{1x}\hat{I}_{2z}$ gives rise to a diagonal peak centred at $\{\Omega_1, \Omega_1\}$, as it is modulated in t_1 at Ω_1 and appears on spin one in t_2. There is a single modulating frequency of Ω_1 in ω_1 i.e. no splitting due to couplings, as expected. In ω_2 the multiplet is in anti-phase.
The term $\cos(\Omega_1 t_1)\sin(\pi J_{12}T)\,2\hat{I}_{1z}\hat{I}_{2x}$ gives rise to a cross peak centred at $\{\Omega_1, \Omega_2\}$, as it is modulated in t_1 at Ω_1 and appears on spin two in t_2. Like the diagonal peak, it is in anti-phase in ω_2. Furthermore, note that the terms which give rise to both the diagonal and cross peak appear along x, so they will have the same lineshape in ω_2: this contrasts with the simple constant time COSY experiment.
The intensity of *both* the diagonal and cross peaks goes as $\sin(\pi J_{12}T)$: again, this contrasts with the simple constant time COSY, where the two kinds of peaks have a different dependence on T.
The advantage of double-quantum filtration is that it results in both diagonal and cross peaks having the same lineshape in ω_2, as well as in ω_1.

10.12

Following the same kind of analysis as in section 10.8.1 on p. 352, we first let $-\hat{I}_{1y}$ evolve under the coupling for time T: a 'tree' is perhaps useful here:

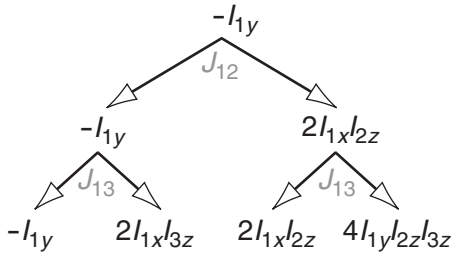

Using this, we can simply read off the four terms which arise as a result of the evolution of the coupling

$$\begin{aligned}&-\cos(\pi J_{13}T)\cos(\pi J_{12}T)\,\hat{I}_{1y}+\sin(\pi J_{13}T)\cos(\pi J_{12}T)\,2\hat{I}_{1x}\hat{I}_{3z}\\&+\cos(\pi J_{13}T)\sin(\pi J_{12}T)\,2\hat{I}_{1x}\hat{I}_{2z}+\sin(\pi J_{13}T)\sin(\pi J_{12}T)\,4\hat{I}_{1y}\hat{I}_{2z}\hat{I}_{3z}.\end{aligned}$$

The 180° pulse in the constant time period simply flips the sign of any y or z operators:

$$\begin{aligned}&+\cos(\pi J_{13}T)\cos(\pi J_{12}T)\,\hat{I}_{1y}-\sin(\pi J_{13}T)\cos(\pi J_{12}T)\,2\hat{I}_{1x}\hat{I}_{3z}\\&-\cos(\pi J_{13}T)\sin(\pi J_{12}T)\,2\hat{I}_{1x}\hat{I}_{2z}-\sin(\pi J_{13}T)\sin(\pi J_{12}T)\,4\hat{I}_{1y}\hat{I}_{2z}\hat{I}_{3z}.\end{aligned}$$

Now we have to let each of these terms evolve under the offset of spin one for time t_1. The result will be all of the above terms, multiplied by $\cos(\Omega_1 t_1)$:

$$\begin{aligned}&\cos(\Omega_1 t_1)\Big[+\cos(\pi J_{13}T)\cos(\pi J_{12}T)\,\hat{I}_{1y}-\sin(\pi J_{13}T)\cos(\pi J_{12}T)\,2\hat{I}_{1x}\hat{I}_{3z}\\&-\cos(\pi J_{13}T)\sin(\pi J_{12}T)\,2\hat{I}_{1x}\hat{I}_{2z}-\sin(\pi J_{13}T)\sin(\pi J_{12}T)\,4\hat{I}_{1y}\hat{I}_{2z}\hat{I}_{3z}\Big],\end{aligned}$$

and a related set of terms multiplied by $\sin(\Omega_1 t_1)$:

$$\begin{aligned}&\sin(\Omega_1 t_1)\Big[-\cos(\pi J_{13}T)\cos(\pi J_{12}T)\,\hat{I}_{1x}-\sin(\pi J_{13}T)\cos(\pi J_{12}T)\,2\hat{I}_{1y}\hat{I}_{3z}\\&-\cos(\pi J_{13}T)\sin(\pi J_{12}T)\,2\hat{I}_{1y}\hat{I}_{2z}+\sin(\pi J_{13}T)\sin(\pi J_{12}T)\,4\hat{I}_{1x}\hat{I}_{2z}\hat{I}_{3z}\Big].\end{aligned}$$

After the final 90° pulse the first set of terms become

$$\begin{aligned}&\cos(\Omega_1 t_1)\Big[+\cos(\pi J_{13}T)\cos(\pi J_{12}T)\,\hat{I}_{1z}+\sin(\pi J_{13}T)\cos(\pi J_{12}T)\,2\hat{I}_{1x}\hat{I}_{3y}\\&+\cos(\pi J_{13}T)\sin(\pi J_{12}T)\,2\hat{I}_{1x}\hat{I}_{2y}-\sin(\pi J_{13}T)\sin(\pi J_{12}T)\,4\hat{I}_{1z}\hat{I}_{2y}\hat{I}_{3y}\Big],\end{aligned}$$

none of which are observable.
The second set of terms, those multiplied by $\sin(\Omega_1 t_1)$, become

$$\begin{aligned}&\sin(\Omega_1 t_1)\Big[-\cos(\pi J_{13}T)\cos(\pi J_{12}T)\,\hat{I}_{1x}+\sin(\pi J_{13}T)\cos(\pi J_{12}T)\,2\hat{I}_{1z}\hat{I}_{3y}\\&+\cos(\pi J_{13}T)\sin(\pi J_{12}T)\,2\hat{I}_{1z}\hat{I}_{2y}+\sin(\pi J_{13}T)\sin(\pi J_{12}T)\,4\hat{I}_{1x}\hat{I}_{2y}\hat{I}_{3y}\Big].\end{aligned}$$

The term in $\hat{I}_{1x}$ is the diagonal peak: in ω_2 it will appear as the in-phase doublet of doublets of spin one, and as the t_1 modulation is simply $\sin(\Omega_1 t_1)$, there will be a single frequency in ω_1 i.e. no splitting due to couplings, as expected.
The term in $2\hat{I}_{1z}\hat{I}_{2y}$ is the 1–2 cross peak: in ω_2 it will appear as the doublet of doublets of spin two, anti-phase with respect to the 1–2 coupling, but in-phase with respect to the 2–3 coupling. In ω_1 there is a single modulating frequency of Ω_1, just as for the diagonal peak.
The cross- and diagonal-peak terms have the same modulation in t_1, and so will have the same lineshape is this dimension. However, in t_2 the magnetization which gives rise to the diagonal peak appears along x, whereas that which gives rise to the cross peak appears along y. So, as for the two-spin case, in ω_2 the cross and diagonal peaks will have different lineshapes.
The intensities of the two type of peaks show a different dependence on the couplings:

$$\text{spin-one diagonal peak}: \cos(\pi J_{13}T)\cos(\pi J_{12}T) \qquad \text{1–2 cross peak}: \cos(\pi J_{13}T)\sin(\pi J_{12}T).$$

As for the two-spin case, the cross-peak goes as $\sin(\pi J_{\text{active}}T)$, whereas the diagonal peak goes as $\cos(\pi J_{\text{active}}T)$: here the active coupling is J_{12}. The two kinds of peaks have a common dependence on the passive coupling J_{13}, going as the cosine: $\cos(\pi J_{13}T)$. In words, to give rise to the 1–2 cross peak, the magnetization needs to be anti-phase with respect to the 1–2 coupling, and in-phase with respect to the 1–3 coupling, hence the sine dependence on J_{12} and the cosine dependence on J_{13}.
For the cross peak to have a maximum intensity $\pi J_{12}T$ must be an odd multiple of $\pi/2$, whereas $\pi J_{13}T$ must be an even multiple of $\pi/2$. It might be difficult to satisfy this requirement exactly.
This analysis reveals the main problem with constant time experiments, which is the complex dependence of the cross-peak intensity on the couplings in the system, and the value of the fixed delay T.

10.13

Following section 8.8 on p. 214, we found for a two-spin system the following S spin operator after the first S spin 90° pulse:

$$-\sin(2\pi J_{IS}\tau_1)\,2\hat{I}_z\hat{S}_y.$$

We need to adapt this for the more complex spin system we are dealing with here. Firstly, the S spin has to become the spin S_1, and the coupling becomes that between I and S_1, J_{IS_1}:

$$-\sin(2\pi J_{IS_1}\tau_1)\,2\hat{I}_z\hat{S}_{1y}.$$

If $\tau_1 = 1/(4J_{IS_1})$, then the sine term goes to 1 and so we just have $-2\hat{I}_z\hat{S}_{1y}$ at the start of t_1.
Just as before, we now allow the homonuclear coupling, which in this case is between S_1 and S_2, to evolve for the whole time T, giving

$$-\cos(\pi J_{12}T)\,2\hat{I}_z\hat{S}_{1y} + \sin(\pi J_{12}T)\,4\hat{I}_z\hat{S}_{1x}\hat{S}_{2z},$$

where J_{12} is the coupling between the two S spins. Note the generation of anti-phase magnetization with respect to this coupling. We also need to take account of the S spin 180° pulse which inverts the operators $\hat{S}_{1y}$ and $\hat{S}_{1z}$ to give

$$+\cos(\pi J_{12}T)\,2\hat{I}_z\hat{S}_{1y} - \sin(\pi J_{12}T)\,4\hat{I}_z\hat{S}_{1x}\hat{S}_{2z}.$$

We now allow the S spin offset terms to act for time t_1; only the offset of S_1 has an effect, giving

$$\cos(\Omega_{S_1} t_1)\cos(\pi J_{12} T)\, 2\hat{I}_z\hat{S}_{1y} - \cos(\Omega_{S_1} t_1)\sin(\pi J_{12} T)\, 4\hat{I}_z\hat{S}_{1x}\hat{S}_{2z}$$
$$-\sin(\Omega_{S_1} t_1)\cos(\pi J_{12} T)\, 2\hat{I}_z\hat{S}_{1x} - \sin(\Omega_{S_1} t_1)\sin(\pi J_{12} T)\, 4\hat{I}_z\hat{S}_{1y}\hat{S}_{2z}.$$

Finally, we need to take account of the I spin 180° pulse, which inverts all of the terms, as they all contain $\hat{I}_z$:

$$-\cos(\Omega_{S_1} t_1)\cos(\pi J_{12} T)\, 2\hat{I}_z\hat{S}_{1y} + \cos(\Omega_{S_1} t_1)\sin(\pi J_{12} T)\, 4\hat{I}_z\hat{S}_{1x}\hat{S}_{2z}$$
$$+\sin(\Omega_{S_1} t_1)\cos(\pi J_{12} T)\, 2\hat{I}_z\hat{S}_{1x} + \sin(\Omega_{S_1} t_1)\sin(\pi J_{12} T)\, 4\hat{I}_z\hat{S}_{1y}\hat{S}_{2z}.$$

Note that we do not need to worry about the evolution of the heteronuclear coupling as this is refocused by the 180° pulses in periods **A** and **B**.

Next comes the 90° pulses to the I and S spins: these have the following effect on the operators (the trigonometric terms have been left out):

$$2\hat{I}_z\hat{S}_{1y} \longrightarrow -2\hat{I}_y\hat{S}_{1z} \quad 4\hat{I}_z\hat{S}_{1x}\hat{S}_{2z} \longrightarrow 4\hat{I}_y\hat{S}_{1x}\hat{S}_{2y} \quad 2\hat{I}_z\hat{S}_{1x} \longrightarrow -2\hat{I}_y\hat{S}_{1x} \quad 4\hat{I}_z\hat{S}_{1y}\hat{S}_{2z} \longrightarrow 4\hat{I}_y\hat{S}_{1z}\hat{S}_{2y}.$$

Of these terms, only the first becomes observable on the I spin. We can see that the feature of this term is that it has remained in-phase with respect to the S_1–S_2 coupling, and is cosine modulated in t_1.

After these two 90° pulses the observable term on the I spin is

$$\cos(\Omega_{S_1} t_1)\cos(\pi J_{12} T)\, 2\hat{I}_y\hat{S}_{1z}.$$

After the following spin echo, assuming $\tau_1 = 1/(4J_{IS_1})$, this term simply becomes in-phase along $-x$:

$$-\cos(\Omega_{S_1} t_1)\cos(\pi J_{12} T)\, \hat{I}_x.$$

We then observe this term with broadband S spin decoupling, giving a single peak at $\{\Omega_{S_1}, \Omega_I\}$. As a result of using the constant time procedure, there is no splitting in ω_1 due to the coupling between the S spins.

The intensity of the peak depends on $\cos(\pi J_{12} T)$; for a maximum, $\pi J_{12} T$ must be a multiple of π, i.e. $\pi J_{12} T = n\pi$ or $T = n/J_{12} \quad n = 1, 2, \ldots$. This condition corresponds to the magnetization being in-phase with respect to the coupling between the S spins at the end of the constant time T.

In the case that the S spins are ^{13}C in a globally labelled sample, the couplings we need to worry about are the one-bond ^{13}C–^{13}C couplings, simply because these are the largest. Such couplings do not vary very much with structure, so it should be possible to find a value of T which is a reasonable compromise for all the carbons in the system.

If there are further S spins coupled to S_1, then we can see that the intensity of the cross peak will go as $\cos(\pi J_{12} T)\cos(\pi J_{13} T)\ldots$. Again, if the couplings do not cover too wide a range, we can find a value of T which will give reasonable intensity for all cross peaks.

10.14

We just use the idea that the selective 180° pulse 'drags' the curly line (the coherence) from the energy level shared by the pulse and the coherence, to the energy level at the 'other end' of the 180° pulse.

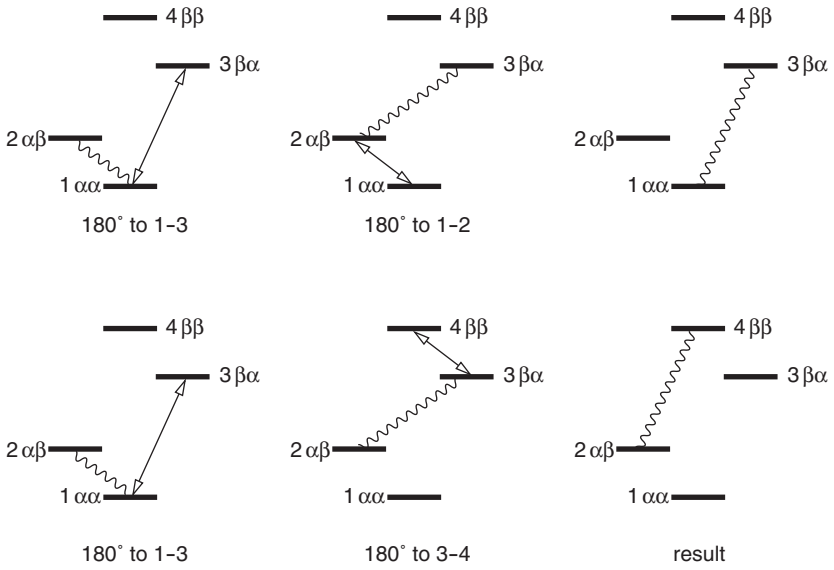

The same idea is used below. Note that the selective 180° pulse and the coherence must share an energy level for anything to happen.

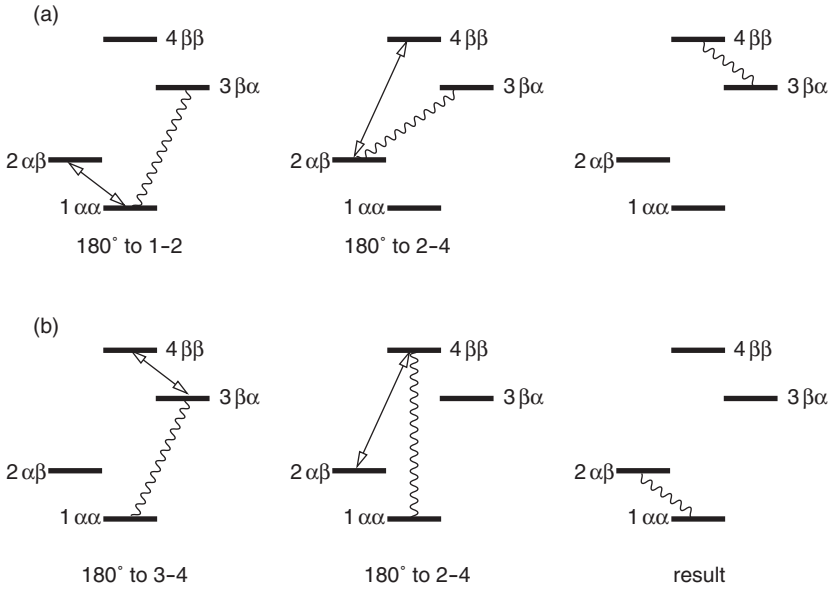

Transfer (a) can also be achieved by pulses to 3–4 and then 1–3; similarly, transfer (b) can also be achieved by pulses to 1–2 and 1–3.

10.15

After the 90°(y) pulse to the I spin and the first 90° pulse to the S spin, and assuming that $\tau = 1/(4J_{IS})$, we have already worked out that the state of the system is $-2\hat{I}_z\hat{S}_y$ (see section 8.8 on p. 214). It is then just a question of following the evolution of this term under the influence of the S spin offset and the I–S coupling.

The final stage is to use the trigonometric identities (given in the appendix). For example, the term $\hat{S}_x$ is multiplied by the trigonometric term $\cos(\Omega_S t_1)\sin(\pi J_{IS} t_1)$. Applying the identity

$$\cos A \sin B \equiv \tfrac{1}{2}\left[\sin(A+B) - \sin(A-B)\right]$$

gives

$$\cos(\Omega_S t_1)\sin(\pi J_{IS} t_1) \equiv \tfrac{1}{2}\left[\sin(\Omega_S t_1 + \pi J_{IS} t_1) - \sin(\Omega_S t_1 - \pi J_{IS} t_1)\right].$$

This is indeed $\frac{1}{2}(s_+ - s_-)$, as stated.

We now follow through the fate of the term $\hat{S}_x$ for the rest of the sequence (Fig. 10.33 on p. 362). The I spin 90° pulse at the start of period **A** has no effect, and there then follows a spin echo of total duration $1/(2J_{IS})$ during which the in-phase term is completely transferred to anti-phase, giving $2\hat{I}_z\hat{S}_y$. We need to take account of the two 180° pulses which invert both $\hat{I}_z$ and $\hat{S}_y$, leaving the term overall unaffected. The 90°(y) pulse to the I spin transforms this term to $2\hat{I}_x\hat{S}_y$; this brings us to the end of period **A**.

The 90° pulse to the S spin which starts period **B** rotates the operator to $2\hat{I}_x\hat{S}_z$, and this anti-phase term evolves completely into in-phase during the subsequent spin echo, giving $\hat{I}_y$. We need to take account of the two 180° pulses in the spin echo, which invert this term to give $-\hat{I}_y$. This term is unaffected by the final 90° pulse to the S spin, so the observable term arising from $\hat{S}_x$ is

$$-\tfrac{1}{2}(s_+ - s_-)\,\hat{I}_y.$$

This term can be found on the first line of the table on p. 363.

10.16

The combinations S_3 and S_4 are:

$$S_3 = \tfrac{1}{2}\left[(\mathrm{a}) + (\mathrm{d})\right] \qquad S_4 = \tfrac{1}{2}\left[(\mathrm{a}) - (\mathrm{d})\right],$$

where (a) and (d) are given in the table on p. 363:

			observable operator at $t_2 = 0$			
expt	ϕ_I	ϕ_S	$\hat{I}_x$	$\hat{I}_y$	$2\hat{I}_x\hat{S}_z$	$2\hat{I}_y\hat{S}_z$
(a)	y	y	$(-c_+ - c_-)$	$(-s_+ + s_-)$	$(c_+ - c_-)$	$(s_+ + s_-)$
(b)	$-y$	y	$(-c_+ - c_-)$	$(s_+ - s_-)$	$(-c_+ + c_-)$	$(s_+ + s_-)$
(c)	y	$-y$	$(-c_+ - c_-)$	$(-s_+ + s_-)$	$(-c_+ + c_-)$	$(-s_+ - s_-)$
(d)	$-y$	$-y$	$(-c_+ - c_-)$	$(s_+ - s_-)$	$(c_+ - c_-)$	$(-s_+ - s_-)$

Forming these combinations we have

$$\begin{aligned} S_3 &= \tfrac{1}{2}\left[(\mathrm{a}) + (\mathrm{d})\right] \\ &= \underbrace{(-c_+ - c_-)\,\hat{I}_x}_{E} + \underbrace{(c_+ - c_-)\,2\hat{I}_x\hat{S}_z}_{F} \\ S_4 &= \tfrac{1}{2}\left[(\mathrm{a}) - (\mathrm{d})\right] \\ &= \underbrace{(-s_+ + s_-)\,\hat{I}_y}_{G} + \underbrace{(s_+ + s_-)\,2\hat{I}_y\hat{S}_z}_{H}. \end{aligned}$$

As before, we have a clean separation of x- and y-magnetization. If the two combinations are processed separately, and a 90° phase correction applied to one combination in both dimensions, we will have two spectra in which all peaks are in the absorption mode.
Term E is in-phase in ω_2 and also in-phase in ω_1, so all four peaks of the multiplet have the same sign, which is this case is negative. The multiplet is the same as from term A given in Eq. 10.12 on p. 363. Term F is anti-phase in each dimension, so gives rise to an anti-phase square array. Note, however, that the overall sign is opposite to that of term B given in Eq. 10.12.
Term G is in-phase in ω_2 and anti-phase in ω_1, and is again opposite in overall sign to term C in Eq. 10.13 on p. 363. Finally, term H is anti-phase in ω_2, but in-phase in ω_1: it is identical to term D in Eq. 10.13.
The multiplets from the four terms, along with the way they combine to give S_3 and S_4, are shown in the diagram below, which should be compared to Fig. 10.34 on p. 364.

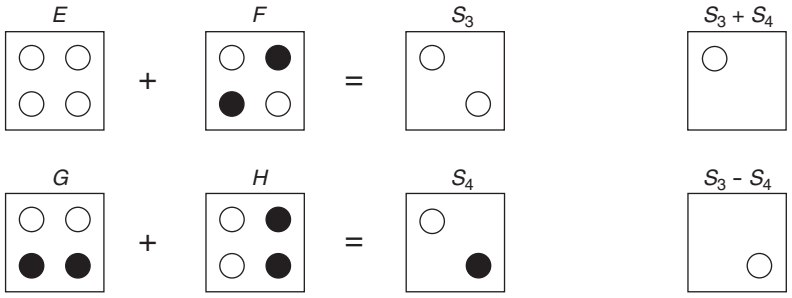

We see from the digram that by combining the spectra S_3 and S_4, either as $(S_3 + S_4)$ or $(S_3 - S_4)$, we are left with just one line of the multiplet, either top left, or bottom right.

10.17

Aside from the extra complication of the pulse sequence and data processing, probably the only significant difficulty is that the peak does not appear at $\{\Omega_S, \Omega_I\}$, but offset from this by $\frac{1}{2}J_{IS}$ in each dimension. Account needs to be take of this when comparing TROSY type spectra with other spectra.

Chapter 11

Coherence selection: phase cycling and field gradient pulses

11.1

$$\begin{aligned}\hat{I}_{i-} \equiv \hat{I}_{ix} - \mathrm{i}\hat{I}_{iy} \xrightarrow{\phi\hat{I}_{iz}} & \cos\phi\,\hat{I}_{ix} + \sin\phi\,\hat{I}_{iy} - \mathrm{i}\left[\cos\phi\,\hat{I}_{iy} - \sin\phi\,\hat{I}_{ix}\right] \\ &= \cos\phi\left[\hat{I}_{ix} - \mathrm{i}\,\hat{I}_{iy}\right] + \mathrm{i}\sin\phi\left[\hat{I}_{ix} - \mathrm{i}\,\hat{I}_{iy}\right] \\ &= (\cos\phi + \mathrm{i}\sin\phi)\left[\hat{I}_{ix} - \mathrm{i}\,\hat{I}_{iy}\right] \\ &= \exp(\mathrm{i}\phi)\,\hat{I}_{i-}.\end{aligned}$$

Assigning coherence orders

$$\hat{I}_{1+}\hat{I}_{2-}: \qquad p_1 = 1 \quad p_2 = -1 \quad p = p_1 + p_2 = \boxed{0}$$

$$2\hat{I}_{1+}\hat{I}_{2+}\hat{I}_{3z}: \qquad p_1 = 1 \quad p_2 = 1 \quad p_3 = 0 \quad p = p_1 + p_2 + p_3 = \boxed{2}$$

$$\hat{I}_{1x} \equiv \tfrac{1}{2}\left(\hat{I}_{1+} + \hat{I}_{1-}\right): \qquad p = \boxed{\pm 1}$$

$$\hat{I}_{2y} \equiv \tfrac{1}{2\mathrm{i}}\left(\hat{I}_{2+} - \hat{I}_{2-}\right): \qquad p = \boxed{\pm 1}$$

$$2\hat{I}_{1z}\hat{I}_{2y} \equiv 2 \times \tfrac{1}{2\mathrm{i}}\hat{I}_{1z}\left(\hat{I}_{2+} - \hat{I}_{2-}\right): \qquad p_1 = 0 \quad p_2 = \pm 1 \quad p = \boxed{\pm 1}$$

$$\begin{aligned}\left(2\hat{I}_{1x}\hat{I}_{2x} + 2\hat{I}_{1y}\hat{I}_{2y}\right) &\equiv 2\tfrac{1}{2}\tfrac{1}{2}\left(\hat{I}_{1+} + \hat{I}_{1-}\right)\left(\hat{I}_{2+} + \hat{I}_{2-}\right) + 2\tfrac{1}{2\mathrm{i}}\tfrac{1}{2\mathrm{i}}\left(\hat{I}_{1+} - \hat{I}_{1-}\right)\left(\hat{I}_{2+} - \hat{I}_{2-}\right) \\ &\equiv \tfrac{1}{2}\left[\hat{I}_{1+}\hat{I}_{2+} + \hat{I}_{1+}\hat{I}_{2-} + \hat{I}_{1-}\hat{I}_{2+} + \hat{I}_{1-}\hat{I}_{2-} - \hat{I}_{1+}\hat{I}_{2+} + \hat{I}_{1+}\hat{I}_{2-} + \hat{I}_{1-}\hat{I}_{2+} - \hat{I}_{1-}\hat{I}_{2-}\right] \\ &\equiv \hat{I}_{1+}\hat{I}_{2-} + \hat{I}_{1-}\hat{I}_{2+}\end{aligned}$$

$$\text{hence } p_1 = 1 \quad p_2 = -1 \quad \text{or} \quad p_1 = -1 \quad p_2 = 1 \qquad p = \boxed{0}$$

Heteronuclear spin system

$$\hat{I}_x \equiv \tfrac{1}{2}\left(\hat{I}_+ + \hat{I}_-\right): \qquad p_I = \boxed{\pm 1}$$

$$\hat{S}_y \equiv \tfrac{1}{2\mathrm{i}}\left(\hat{S}_+ - \hat{S}_-\right): \qquad p_S = \boxed{\pm 1}$$

$$2\hat{I}_x\hat{S}_z \equiv 2 \times \tfrac{1}{2}\left(\hat{I}_+ + \hat{I}_-\right)\hat{S}_z: \qquad p_I = \boxed{\pm 1} \quad p_S = \boxed{0}$$

$$2\hat{I}_x\hat{S}_y \equiv 2\tfrac{1}{2}\tfrac{1}{2\mathrm{i}}\left(\hat{I}_+ + \hat{I}_-\right)\left(\hat{S}_+ - \hat{S}_-\right): \qquad p_I = \boxed{\pm 1} \quad p_S = \boxed{\pm 1}$$

Following section 11.1.2 on p. 372, free evolution results in these operators acquiring a phase

$$\exp\left(-\mathrm{i}\,\Omega^{(p_1+p_2+\ldots)}t\right),$$

where $\Omega^{(p_1+p_2+\ldots)} = p_1\Omega_1 + p_2\Omega_2 + \ldots$. The table gives this phase term for each operator:

operator	p_1 or p_I	p_2 or p_S	p_3	$\Omega^{(p_1+p_2+\ldots)}$	phase term
$\hat{I}_{1+}$	$+1$			Ω_1	$\exp(-\mathrm{i}\,\Omega_1 t)$
$\hat{I}_{2-}$		-1		$-\Omega_2$	$\exp(\mathrm{i}\,\Omega_2 t)$
$\hat{I}_{1+}\hat{I}_{2+}$	$+1$	$+1$		$\Omega_1 + \Omega_2$	$\exp(-\mathrm{i}\,[\Omega_1 + \Omega_2]t)$
$\hat{I}_+\hat{S}_-$	$+1$	-1		$\Omega_I - \Omega_S$	$\exp(-\mathrm{i}\,[\Omega_I - \Omega_S]t)$
$\hat{I}_{1-}\hat{I}_{2-}\hat{I}_{3-}$	-1	-1	-1	$\Omega_1 + \Omega_2 + \Omega_3$	$\exp(\mathrm{i}\,[\Omega_1 + \Omega_2 + \Omega_3]t)$.

11.2

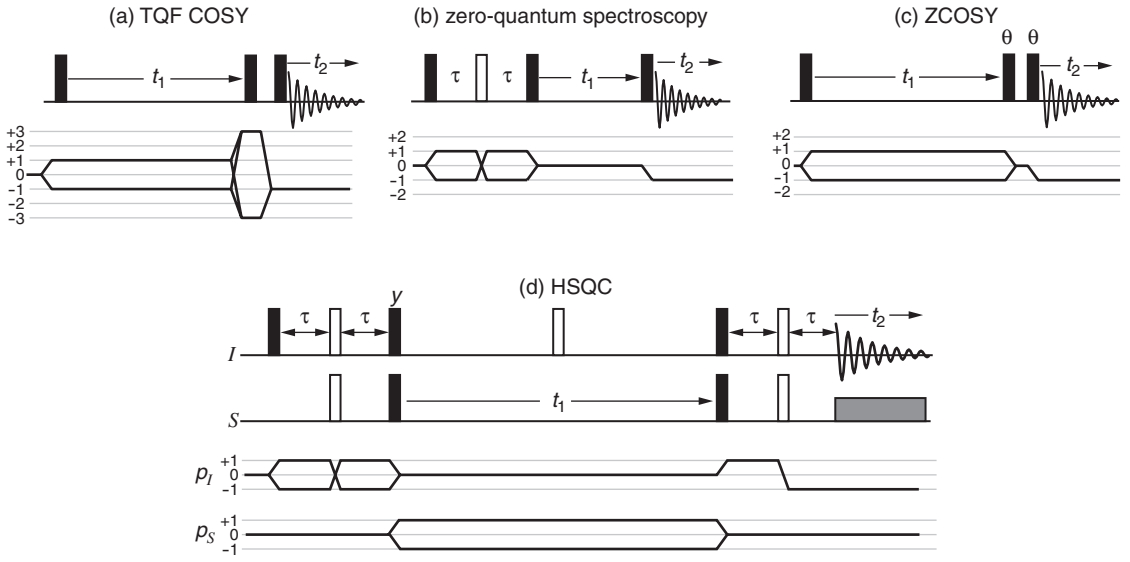

Note that in HSQC, sequence (d), we have $p_S = \pm 1$ and $p_I = 0$ during t_1 i.e. S spin single-quantum coherence, and that during t_2 we have $p_I = -1$ and $p_S = 0$, as these are the coherence orders for observable signals on the I spin.

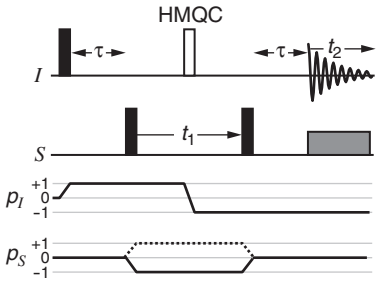

(a) As described in section 11.3 on p. 377, the P-type spectrum has the same sign of p in t_1 and t_2: this is the solid line in the CTP. The resulting spectrum will be phase modulated in t_1, and so is frequency discriminated.

(b) The N-type spectrum has the opposite sign of p in t_1 and t_2: this is the dashed line in the CTP; like the P-type spectrum, the N-type spectrum is frequency discriminated.

(c) To be able to give absorption mode lineshapes we need to retain symmetrical pathways in t_1 i.e. $p_S = \pm 1$. Thus we need to select both the solid and dashed CTP. The resulting spectrum is not frequency discriminated, but discrimination can be achieved using the SHR or TPPI methods (section 8.13 on p. 231).

11.3

By inspecting Fig. 11.5 on p. 380 we can determine the form of the signal from detectors A and B using simple trigonometry. For example in (b) it is clear that the component along A is $-\sin(\Omega t)$ whereas that along B is $\cos(\Omega t)$. The table gives these components and the required combinations for all four cases:

	A	B	combination	result
(a)	$\cos(\Omega t)$	$\sin(\Omega t)$	$A + \mathrm{i}\,B$	$\cos(\Omega t) + \mathrm{i}\,\sin(\Omega t) = \exp(\mathrm{i}\,\Omega t)$
(b)	$-\sin(\Omega t)$	$\cos(\Omega t)$	$B - \mathrm{i}\,A$	$\cos(\Omega t) - \mathrm{i}\,[-\sin(\Omega t)] = \exp(\mathrm{i}\,\Omega t)$
(c)	$-\cos(\Omega t)$	$-\sin(\Omega t)$	$-A - \mathrm{i}\,B$	$-[-\cos(\Omega t)] - \mathrm{i}\,[-\sin(\Omega t)] = \exp(\mathrm{i}\,\Omega t)$
(d)	$\sin(\Omega t)$	$-\cos(\Omega t)$	$-B + \mathrm{i}\,A$	$-[-\cos(\Omega t)] + \mathrm{i}\,\sin(\Omega t) = \exp(\mathrm{i}\,\Omega t)$

Each combination gives modulation of the form $\exp(\mathrm{i}\,\Omega t)$, which will all give the same lineshape on Fourier transformation.

Following the approach of Fig. 11.6 on p. 382, for the case where the pulse goes $[x, y, -x, -y]$ and the receiver phase goes $[-180°, -270°, 0°, -90°]$ we have

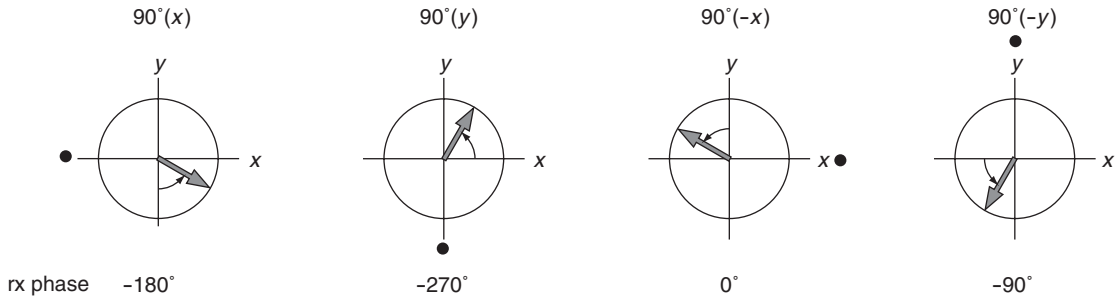

A $90°(x)$ pulse places the magnetization along $-y$ and then precession through an angle Ωt rotates the vector towards $+x$. Similarly, a $90°(y)$ pulse places the magnetization along $+x$, and then precession rotates the vector towards $+y$.
The receiver phase is measured *clockwise* from 3 o'clock, and is indicated by the bullet •. We see that in each diagram there is a *constant angle* between the position of the magnetization and the receiver phase. As a result, each combination of pulse and receiver phase will give the same lineshape, and so all four spectra will add up.

11.4

For $\Delta p = -1$ the phase shift experienced by the pathway when the pulse is shifted in phase by $\Delta\phi$ is $-\Delta p \times \Delta\phi = -(-1)\Delta\phi = \Delta\phi$. Similarly for $\Delta p = 0$ the phase shift is $-0 \times \Delta\phi = 0$, and for $\Delta p = 5$ the phase shift is $-5 \times \Delta\phi = -5\Delta\phi$. The table gives the phase shifts for each of these three pathways:

	pulse phase	$\Delta p = -1$	$\Delta p = 0$	$\Delta p = 5$	
step	$\Delta\phi$	$\Delta\phi$	0	$-5\,\Delta\phi$	equiv$(-5\,\Delta\phi)$
1	0°	0°	0°	0°	0°
2	90°	90°	0°	−450°	270°
3	180°	180°	0°	−900°	180°
4	270°	270°	0°	−1350°	90°

These phases can be represented in the manner of Fig. 11.8 on p. 386:

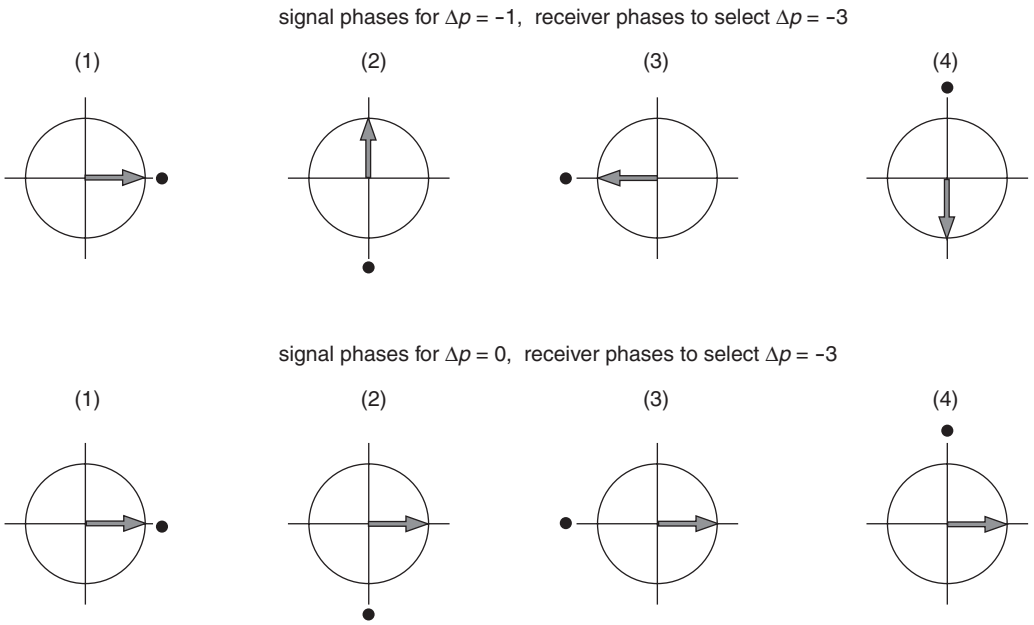

For $\Delta p = -1$, steps (1) and (3) have the signal and receiver in alignment, whereas in steps (2) and (4) the signal and the receiver are opposed. As a result steps (1) and (3) will cancel steps (2) and (4).

For $\Delta p = 0$, steps (1) and (3) will cancel as the signal and the receiver are aligned in one and opposed in the other. Similarly, steps (2) and (4) will cancel as in step (2) the signal is 90° ahead of the receiver, whereas in step (4) it is 90° behind i.e. there is an overall shift of 180°.

For $\Delta p = 5$ the signal phase shifts are exactly the same as those for $\Delta p = -3$, so both pathways are selected. This is of course exactly what is expected for a four-step cycle since $-3 + 2 \times 4 = +5$ i.e. $\Delta p = -3$ and $\Delta p = 5$ are separated by a multiple of four.

11.5

The second pulse has $\Delta p = -2$, so if the pulse phase goes [0°, 90°, 180°, 270°] the receiver phase shifts must be [0°, 180°, 0°, 180°]. The first pulse has $\Delta p = +1$, so if the pulse phase goes [0°, 90°, 180°, 270°] the receiver phase shifts must be [0°, 270°, 180°, 90°].
In the first four steps, $\Delta\phi_2$ therefore goes [0°, 90°, 180°, 270°], $\Delta\phi_1$ remains fixed, and the receiver goes [0°, 180°, 0°, 180°].
In the second group of four steps, $\Delta\phi_2$ does the same, but $\Delta\phi_1$ is now 90°, and this results in an extra 270° which must be added to the receiver phase shifts from the first group of four. The required receiver phase shifts are therefore

$$[0°+270°, 180°+270°, 0°+270°, 180°+270°] \equiv [270°, 90°, 270°, 90°].$$

In the third group of four steps $\Delta\phi_1$ is 180°, and this results in an extra 180° which must be added to the receiver phase shifts from the first group of four. Finally, for the fourth group of four steps $\Delta\phi_1$ is 270°, and 90° must be added to the receiver phase shifts. The complete sixteen-step cycle is therefore

step	$\Delta\phi_1$	$\Delta\phi_2$	ϕ_{rx}
1	0°	0°	0°
2	0°	90°	180°
3	0°	180°	0°
4	0°	270°	180°
5	90°	0°	270°
6	90°	90°	90°
7	90°	180°	270°
8	90°	270°	90°

step	$\Delta\phi_1$	$\Delta\phi_3$	ϕ_{rx}
9	180°	0°	180°
10	180°	90°	0°
11	180°	180°	180°
12	180°	270°	0°
13	270°	0°	90°
14	270°	90°	270°
15	270°	180°	90°
16	270°	270°	270°

Selection of $\Delta p = -1$ and then $\Delta p = +3$

The first pulse has $\Delta p = -1$, so if the pulse phase goes [0°, 90°, 180°, 270°] the receiver phase shifts must be [0°, 90°, 180°, 270°]. The second pulse has $\Delta p = +3$, so if the pulse phase goes [0°, 90°, 180°, 270°] the receiver phase shifts must be [0°, 90°, 180°, 270°]. For these four-step cycles the receiver phases needed to select $\Delta p = -1$ and +3 are, of course, the same.
The sixteen-step cycle is:

step	$\Delta\phi_1$	$\Delta\phi_2$	ϕ_{rx}
1	0°	0°	0°
2	90°	0°	90°
3	180°	0°	180°
4	270°	0°	270°
5	0°	90°	90°
6	90°	90°	180°
7	180°	90°	270°
8	270°	90°	0°

step	$\Delta\phi_1$	$\Delta\phi_3$	ϕ_{rx}
9	0°	180°	180°
10	90°	180°	270°
11	180°	180°	0°
12	270°	180°	90°
13	0°	270°	270°
14	90°	270°	0°
15	180°	270°	90°
16	270°	270°	180°

11.6

For $\Delta p = -2$ the phase shift experienced by the pathway when the pulse is shifted in phase by $\Delta\phi$ is $-\Delta p \times \Delta\phi = -(-2)\Delta\phi = 2\Delta\phi$. So, as the pulse goes [0°, 120°, 240°] the pathway experiences phase shifts of [0°, 240°, 480°] which are equivalent to [0°, 240°, 120°]. So, to select $\Delta p = -2$, we would use the cycle:

pulse: [0°, 120°, 240°] receiver: [0°, 240°, 120°].

On modern spectrometers, the receiver phase can be shifted by arbitrary amounts, not just multiples of 90°.
The selectivity of this three-step sequence can be represented in the manner described on p. 386:

$$\mathbf{-5} \quad (-4) \quad (-3) \quad \mathbf{-2} \quad (-1) \quad (0) \quad \mathbf{1} \quad (2) \quad (3) \quad \mathbf{4}$$

Here the boldface numbers are the values of Δp which are selected, and the numbers in brackets are the values which are rejected; these selected values are separated by three, as we are dealing with a three-step cycle.
The CTP for N-type COSY is:

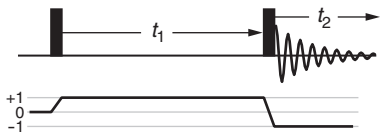

The second pulse has $\Delta p = -2$, so we can use the three-step cycle described above to select this. As the first pulse can only generate $p = \pm 1$, this three step cycle is sufficient to select the overall pathway we require. To be specific, $p = -1$ present during t_1 would only lead to observable coherence via the pathway $\Delta p = 0$ on the second pulse, which is blocked by this three-step cycle.

For P-type COSY (Fig. 11.4 (b) on p. 378), $\Delta p = 0$ on the second pulse. This is selected by the following three-step cycle of the second pulse:

pulse: [0°, 120°, 240°] receiver: [0°, 0°, 0°].

Such a cycle would be sufficient to select the wanted pathway as it would reject the $\Delta p = -2$ pathway on the second pulse.

11.7

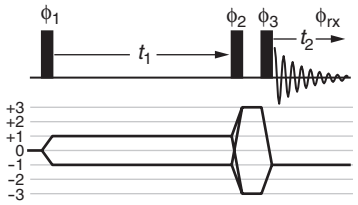

Grouping together the first two pulses means that they are required to achieve the transformation $\Delta p = \pm 3$. Concentrating for the moment on the pathways with $\Delta p = -3$, shifting the phase of the first two pulses by $\Delta\phi$ will result in a phase shift of $-\Delta p \times \Delta\phi = -(-3)\Delta\phi = 3\Delta\phi$.
If the pulse goes through the phases [0°, 60°, 120°, 180°, 240°, 300°] then the phase acquired by the pathway with $\Delta p = -3$ is [0°, 180°, 360°, 540°, 720°, 900°]. Reducing these to the range 0° to 360° gives [0°, 180°, 0°, 180°, 0°, 180°]. So the phase cycle needed is

ϕ_1 and ϕ_2: [0°, 60°, 120°, 180°, 240°, 300°] receiver: [0°, 180°, 0°, 180°, 0°, 180°].

This six-step phase cycle also selects $\Delta p = +3$.
Since $p = \pm 3$ has been selected prior to the last pulse, and as the first pulse can only generate $p = \pm 1$, no further phase cycling is needed (with the possible exception of axial peak suppression, see section 11.7 on p. 391).

Other pathways selected by this six-step cycle include $\Delta p = +3 + 6 = +9$ and $\Delta p = -3 - 6 = -9$. These involve such high orders of coherence that we can safely ignore them.

The final pulse has $\Delta p = -4$ and $\Delta p = +2$; as these are separated by 6, they will both be selected by a six-step cycle. The phase experienced by the pathway with $\Delta p = -4$ will be $4\,\Delta\phi$ so as the pulse goes [0°, 60°, 120°, 180°, 240°, 300°] then the phase acquired by the pathway will be [0°, 240°, 480°, 720°, 960°, 1200°]. Reducing these to the range 0° to 360° gives the following cycle:

ϕ_3: [0°, 60°, 120°, 180°, 240°, 300°] receiver: [0°, 240°, 120°, 0°, 240°, 120°].

11.8

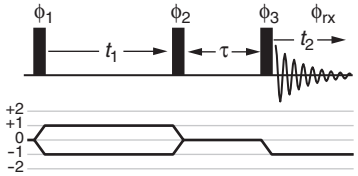

The first two pulses achieve the transformation $\Delta p = 0$, so a four-step cycle will be:

ϕ_1 and ϕ_2: [0°, 90°, 180°, 270°] receiver: [0°, 0°, 0°, 0°].

Axial peak suppression (section 11.7 on p. 391) involves shifting the phase of the first pulse [0°, 180°] and similarly for the receiver. Combining these two cycles gives eight steps:

step	1	2	3	4	5	6	7	8
ϕ_1	0°	90°	180°	270°	180°	270°	0°	90°
ϕ_2	0°	90°	180°	270°	0°	90°	180°	270°
ϕ_{rx}	0°	0°	0°	0°	180°	180°	180°	180°

The CTP for N-type NOESY is

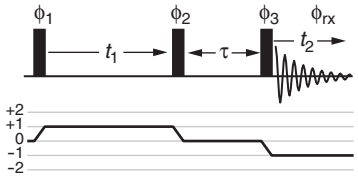

We need to select $\Delta p = -1$ on the last pulse. A suitable four-step cycle is [0°, 90°, 180°, 270°] for ϕ_3 and [0°, 90°, 180°, 270°] for the receiver.
We also need to select $\Delta p = +1$ on the first pulse. The four-step cycle [0°, 90°, 180°, 270°] for ϕ_1 and [0°, 270°, 180°, 90°] for the receiver achieves this selection.
The complete sixteen-step cycle is

step	$\Delta\phi_1$	$\Delta\phi_3$	ϕ_{rx}
1	0°	0°	0°
2	90°	0°	270°
3	180°	0°	180°
4	270°	0°	90°
5	0°	90°	90°
6	90°	90°	0°
7	180°	90°	270°
8	270°	90°	180°

step	$\Delta\phi_1$	$\Delta\phi_3$	ϕ_{rx}
9	0°	180°	180°
10	90°	180°	90°
11	180°	180°	0°
12	270°	180°	270°
13	0°	270°	270°
14	90°	270°	180°
15	180°	270°	90°
16	270°	270°	0°

It is not necessary to add explicit axial peak suppression to this cycle as we are selecting $\Delta p = +1$ on the first pulse, and so all of the peaks we see in the spectrum must derive from the first pulse.

11.9

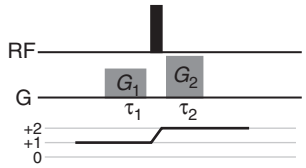

The spatially dependent phase is given by Eq. 11.8 on p. 400:

$$\phi(z) = -p \times \gamma G z t.$$

Hence the phases due to the two gradient pulses are

$$\phi_1 = -(1) \times \gamma G_1 z \tau_1 \qquad \text{and} \qquad \phi_2 = -(2) \times \gamma G_2 z \tau_2.$$

The refocusing condition is that the total phase, $\phi_1 + \phi_2$, is zero:

$$\phi_1 + \phi_2 = -\gamma G_1 z \tau_1 - 2\gamma G_2 z \tau_2 = 0.$$

The factors of z and γ cancel to give, after some rearrangement:

$$\frac{G_2 \tau_2}{G_1 \tau_1} = -\frac{1}{2}$$

(a) If the gradients have the same length, then $\boxed{G_2/G_1 = -\frac{1}{2}}$, i.e. the second gradient needs to be half the strength of the first, and applied in the opposite sense.

(b) If the gradients have the same *absolute* strength, they still have to be applied in the opposite sense i.e. $G_1 = -G_2$. Inserting this gives the refocusing condition as $(G_2\tau_2)/(-G_2\tau_1) = -\frac{1}{2}$, which means that $\boxed{\tau_2 = \frac{1}{2}\tau_1}$.

11.10

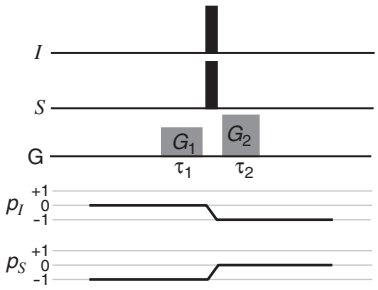

In the heteronuclear case we use Eq. 11.9 on p. 402 to find the spatially dependent phase:

$$\phi(z) = -\left(p_I\gamma_I + p_S\gamma_S\right) G\, z\, t.$$

During the first gradient $p_I = 0$ and $p_S = -1$, whereas during the second $p_I = -1$ and $p_S = 0$. So the spatially dependent phases are

$$\phi_1 = \gamma_S G_1 z \tau_1 \qquad \text{and} \qquad \phi_2 = \gamma_I G_2 z \tau_2.$$

The refocusing condition is $\phi_1 + \phi_2 = 0$, which in this case rearranges to

$$\frac{G_1\tau_1}{G_2\tau_2} = -\frac{\gamma_I}{\gamma_S}.$$

If I is ^{1}H and S is ^{15}N, then $\gamma_I/\gamma_S = 10/(-1)$ so the refocusing condition becomes

$$\frac{G_1\tau_1}{G_2\tau_2} = 10.$$

If the gradients have the same duration, $\tau_1 = \tau_2$ then $\boxed{G_1 = 10G_2}$.

Note that ratio of the gyromagnetic ratios of ^{1}H and ^{15}N is in fact $9.86 : -1$.

11.11

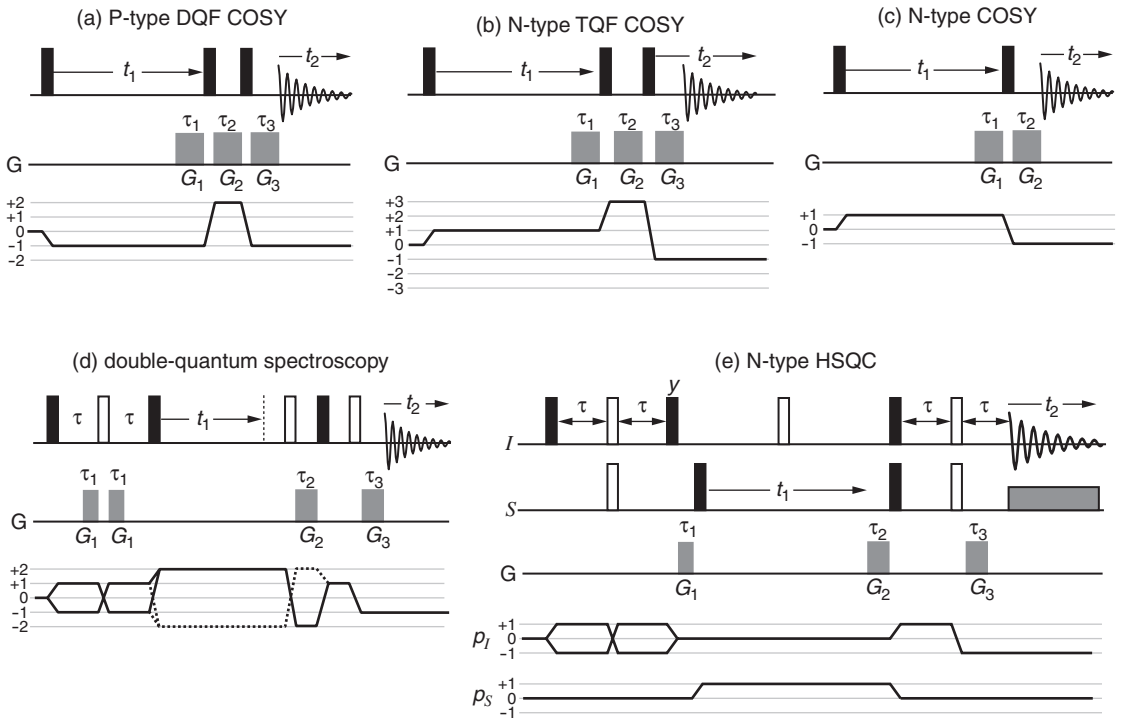

(a) *P-type DQF COSY* We have chosen $p = 2$ in the interval between the last two pulses, but it would have been just as acceptable to choose $p = -2$. The pathway will give a P-type spectrum as $p = -1$ is present during t_1. The refocusing condition is

$$G_1\tau_1 - 2\,G_2\tau_2 + G_3\tau_3 = 0.$$

If the gradients are all the same length, then one choice is for the strengths to be in the ratio

$$G_1 : G_2 : G_3 = 1 : 1 : 1.$$

(b) *N-type TQF COSY* We have chosen $p = 3$ in the interval between the last two pulses, but it would have been just as acceptable to choose $p = -3$. The pathway will give an N-type spectrum as $p = +1$ is present during t_1. The refocusing condition is

$$-G_1\tau_1 - 3\,G_2\tau_2 + G_3\tau_3 = 0.$$

If the gradients are all the same length, then one choice is for the strengths to be in the ratio

$$G_1 : G_2 : G_3 = 1 : 1 : 4.$$

(c) *N-type COSY* The pathway will give a N-type spectrum as $p = +1$ is present during t_1. The refocusing condition is

$$-G_1\tau_1 + G_2\tau_2 = 0.$$

If the gradients are all the same length, then the strengths must be in the ratio

$$G_1 : G_2 = 1 : 1$$

(d) *Double-quantum spectroscopy* The two gradients G_1 serve to 'clean up' the 180° pulse in the spin echo (see section 11.12.3 on p. 406). Double-quantum coherence is dephased by G_2 and then rephased by G_3; to control phase errors due to the underlying evolution of the offsets, both gradients are placed within spin echoes (see section 11.12.5 on p. 407). We will need to record separate P- and N-type spectra, and then recombine them in order to obtain an absorption mode spectrum (see section 11.12.2 on p. 405); the N-type pathway is given by the solid line, and the P-type by the dashed line.

The refocusing condition for the N-type pathway is

$$2\,G_2\tau_2 + G_3\tau_3 = 0.$$

If the gradients are the same length, then the strengths must be in the ratio

$$G_2 : G_3 = 1 : -2.$$

The refocusing condition for the P-type pathway is

$$-2\,G_2\tau_2 + G_3\tau_3 = 0.$$

If the gradients are the same length, then the strengths must be in the ratio

$$G_2 : G_3 = 1 : 2.$$

(e) *N-type HSQC* G_1 is a 'purge' gradient (see section 11.12.6 on p. 408). S spin magnetization is dephased by G_2 and rephased after transfer to I by G_3. The refocusing condition is

$$-\gamma_S G_2\tau_2 + \gamma_I G_3\tau_3 = 0.$$

If the gradients are both the same length, then the strengths must be in the ratio

$$G_2 : G_3 = \gamma_I : \gamma_S\,.$$

For the case where the I spin is ^{1}H and the S spin is ^{13}C, $\gamma_I : \gamma_S = 4$, and so the refocusing condition is

$$G_2 : G_3 = 4 : 1.$$

Chapter 12

How the spectrometer works

12.1

The magnetic field strength can be computed from the given Larmor frequency, f_0, and gyromagnetic ratio using $2\pi f_0 = \gamma B_0$. Hence

$$B_0 = \frac{2\pi f_0}{\gamma} = \frac{2\pi \times 180 \times 10^6}{1.08 \times 10^8} = 10.47 \text{ T}.$$

A homogeneity of one part in 10^8 means that the magnetic field varies by $\Delta B = 10^{-8} \times 10.47 = 1.047 \times 10^{-7}$ T. This translates to a variation in frequency, Δf, of

$$\Delta f = \frac{\gamma \Delta B}{2\pi} = \frac{1.08 \times 10^8 \times 1.047 \times 10^{-7}}{2\pi} = 1.8 \text{ Hz}.$$

This is significantly less than the expected linewidth of 25 Hz, so the magnet is useable.

The calculation is much simpler if we realise that a homogeneity of 1 part in 10^8 means that the Larmor frequency will vary by 10^{-8} times its nominal value i.e.

$$\Delta f = 10^{-8} \times 180 \times 10^6 = 1.8 \text{ Hz}.$$

12.2

For a 180° (or π) pulse, $\pi = \omega_1 t_{180}$, so

$$\omega_1 = \frac{\pi}{t_{180}} = \frac{\pi}{24.8 \times 10^{-6}} = 1.27 \times 10^5 \text{ rad s}^{-1}.$$

Therefore $\omega_1/(2\pi) = 20.2$ kHz.
The same result can be found more simply by noting that a 360° pulse takes $2 \times 24.8 = 49.6$ μs; this is the period of the rotation about the RF field, so the frequency is just the reciprocal of this: $\omega_1/(2\pi) = 1/(49.6 \times 10^{-6}) = 20.2$ kHz.

Using Eq. 12.2 on p. 434 we have

$$\text{attenuation} = 20 \log \frac{2}{20.2} = \boxed{-20.1 \text{ dB}}.$$

12.3

To go from a 90° pulse width of 20 μs to 7.5 μs, the RF field has to be increased by a factor of $20/7.5 = 2.67$, since the pulse width is inversely proportional to the RF field strength. As the RF field strength is proportional to the square root of the power, the power would need to increase by a factor of $(2.67)^2 = 7.11$, so the transmitter power would be $7.11 \times 100 = \boxed{711\ \text{W}}$.
This is a very large increase and, unless the probe is designed to take this much power, there would be a significant risk of probe arcing.

12.4

The output of a two-bit ADC is two binary digits which are capable of representing the numbers 00, 01, 10 and 11 i.e. just four levels.

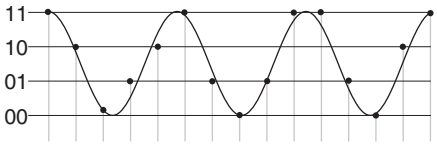

Note how the data points, because they are constrained to correspond to one of the four levels, are not a particularly good representation of the smooth curve.

Having a larger number of bits means that there are more possible output levels, and hence the digital representation of the signal will be more precise. As a result, the digitization sidebands are reduced.

12.5

15 ppm at 800 MHz is $15 \times 800 = 12\,000$ Hz. The range of frequencies, assuming that the receiver reference frequency is placed in the middle, is thus $-6\,000$ Hz to $+6\,000$ Hz. From section 12.5.2 on p. 436, the sampling interval, Δ, is given by

$$\Delta = \frac{1}{2 \times f_{\text{max}}} = \frac{1}{2 \times 6\,000} = \boxed{83.3\ \mu\text{s}}.$$